

AN ABSTRACT OF THE THESIS OF

Kaijun Lin for the degree of Master of Science in Oceanography
presented on June 12, 1986

Title: Application of Linear Free Energy Relationship in Marine
Chemistry and Analysis of the Wintertime Carbonate Data
in the Northern North Atlantic Ocean

Redacted for privacy

Abstract approved:

 Dr. Chen-Tung A. Chen 

Two topics are included in this thesis: (1) The application of linear free energy relationship (LFER) to marine chemistry is discussed and (2) winter carbonate data collected in the northern North Atlantic Ocean, mainly the Norwegian and Greenland seas, are analyzed. First, the occurrence of LFER has been confirmed by the stability constant data reported in the cited literature. Comparison of LFERs was made between the condition of zero ionic strength and that of 0.7 ionic strength which is considered similar to the condition in the marine environment. The application of LFERs yielded estimates of some undetermined stability constants, especially for carbonate and bicarbonate complexes and ion pairs, and adjustments to some data reported in the literature needed to be made. The goals achieved in the present work were: (1) to provide the evidence of LFERs in seawater in terms of the logarithms of stability constants (thermodynamic and stoichiometric at 0.7 ionic strength) at 25°C and 1

atmosphere; (2) to analyze the reason that the separate LFERs form and indicate their appearances occur only when $\log K_{MF}$ and $\log K_{MF}$ at 0.7 ionic strength are correlated with other logarithms of stability constants; (3) to suggest the separate LFERs are dependent on the type classification of metal ions according to Lewis' theory; (4) to provide the improved stability constants and compare them with the reported values from literature and to predict unknown stability constants, mainly for carbonate and bicarbonate complexes and ion pairs.

Secondly, excess CO_2 penetration in the northern North Atlantic Ocean in winter has been revealed based on carbonate data. The direct carbonate data in wintertime were collected on the HUDSON 82 cruise to the Norwegian and Greenland seas. The results indicate that the whole water column in the two seas has been contaminated by anthropogenic CO_2 , more so in the Greenland sea than in the Norwegian sea and more in the western basin than in the eastern basin. Observations of the apparent oxygen utilization and tritium data support this conclusion.

APPLICATION OF LINEAR FREE ENERGY RELATIONSHIP IN MARINE CHEMISTRY
AND ANALYSIS OF THE WINTERTIME CARBONATE DATA IN THE NORTHERN NORTH
ATLANTIC OCEAN

by
Kaijun Lin

A THESIS
submitted to
Oregon State University

in partial fulfillment of
the requirements for the
degree of
Master of Science
Completed June 12, 1986
Commencement June 1987

APPROVED:

Redacted for privacy

Associate Professor of Oceanography in Charge of Major

Redacted for privacy

Dean of the College of Oceanography

Redacted for privacy

Dean of the Graduate School

Date thesis presented June 12, 1986

Commencement June 1987

Typed by Celeste Correia for Kaijun Lin

ACKNOWLEDGMENTS

So many people deserve thanks for helping with this thesis that it would be impossible to mention all of them. First of all, my major professor, Dr. Chen-Tung A. Chen, is given my greatest thanks for his valuable support, suggestions, encouragement and patience over the two and one half years I stayed here. Without him, this work could not have been accomplished.

I am particularly indebted to Dr. Ellen T. Drake whose scientific advise and English correction throughout the thesis have been essential for the completion of this thesis.

A special note of thanks to Celeste Correia who helped put the manuscripts together and typed endlessly. Her assistance is thereby warmly appreciated.

I must also acknowledge with thanks Dr. Ricardo M. Pytkowicz, Dr. Chih-An Huh and other faculty members in the College of Oceanography for their counsel and assistance which will continue to benefit me in the future. I would like to express my appreciation of Ahmed, Yip and other fellow students with whom I shared the enjoyable life and working experience.

Thanks also to my parents, my grandmother and my fiancée, Min Wang, for their spiritual encouragement and deepest concern for my success. The Chinese government, my financial sponsor, should be specifically mentioned. Without its support, I would never have had the chance to begin my graduate study in the United States.

TABLE OF CONTENTS

	Page
I. INTRODUCTION	1
<u>Background</u>	2
<u>Linear Free Energy Relationship</u>	3
<u>Wintertime Carbonate Data in the Northern North Atlantic Ocean</u>	4
<u>References</u>	7
II. APPLICATION OF LINEAR FREE ENERGY RELATIONSHIP IN MARINE CHEMISTRY	10
<u>Abstract</u>	11
<u>Introduction</u>	12
1. Background	12
2. Thermodynamics Review	14
<u>Linear Free Energy Relationships in Seawater</u>	16
1. The Constituents and Compilation of Data	16
2. Rationalization of LFER	17
3. Classification and Cations and Ligands	19
4. Thermodynamic Constant Relationship Among MCl, MOH, MF, MNO ₃ , MHCO ₃ , MCO ₃ and MSO ₄ Aqueous Complexes and Ion Pairs at 25°C and 1 Atmosphere	20
5. Thermodynamic Constant Relationship Among NaL, KL, MgL and CaL Complexes and Ion Pairs at 25°C and 1 Atmosphere	39
6. Stoichiometric Constant Relationship Among MCl, MOH, MF, MNO ₃ , MHCO ₃ , MCO ₃ and MSO ₄ Aqueous Complexes and Ion Pairs at 25°C and 1 Atmosphere	47

<u>Application of LFER to Carbonate and Bicarbonate</u>	61
<u>Stability Constants in the Marine System</u>	
1. Prediction of Thermodynamic Stability Constants for Carbonate and Bicarbonate Complexes and Ion Pairs	62
2. Prediction of Stoichiometric Stability Constants for Carbonate and Bicarbonate Complexes and Ion Pairs	64
3. Organic Matter Complexation	66
<u>Conclusions</u>	70
<u>References</u>	74
III. ANALYSIS OF THE <u>CSS HUDSON</u> WINTERTIME CARBONATE DATA IN THE NORTHERN NORTH ATLANTIC OCEAN	82
<u>Abstract</u>	83
<u>Introduction</u>	85
<u>Source of Data</u>	87
<u>Calculating Excess CO₂</u>	91
<u>Results</u>	96
<u>Discussion</u>	114
<u>Conclusions</u>	121
<u>References</u>	122
BIBLIOGRAPHY	126
APPENDIX	138
1. Cited logarithm stability constants (thermodynamic and stoichiometric at 0.7 ionic strength) for chloride complexes and ion pairs at 25°C and 1 atmosphere.	138
2. Cited logarithm stability constants (thermodynamic and stoichiometric at 0.7 ionic strength) for fluoride complexes and ion pairs at 25°C and 1 atmosphere.	139

3.	Cited logarithm stability constants (thermodynamic and stoichiometric at 0.7 ionic strength) for hydroxide complexes at 25°C and 1 atmosphere.	141
4.	Cited logarithm stability constants (thermodynamic and stoichiometric at 0.7 ionic strength) for bicarbonate complexes at 25°C and 1 atmosphere.	142
5.	Cited logarithm stability constants (thermodynamic and stoichiometric at 0.7 ionic strength) for nitrate complexes at 25°C and 1 atmosphere.	143
6.	Cited logarithm stability constants (thermodynamic and stoichiometric at 0.7 ionic strength) for borate complexes at 25°C and 1 atmosphere.	144
7.	Cited logarithm stability constants (thermodynamic and stoichiometric at 0.7 ionic strength) for carbonate complexes at 25°C and 1 atmosphere.	145
8.	Cited logarithm stability constants (thermodynamic and stoichiometric at 0.7 ionic strength) for sulfate complexes at 25°C and 1 atmosphere.	146
9.	Cited logarithm stability constants (thermodynamic) for HSO_4^- complexes and ion pairs at 25°C and 1 atmosphere.	148
10.	Cited logarithm stability constants (thermodynamic) for H_2PO_4^- complexes and ion pairs at 25°C and 1 atmosphere.	149
11.	Cited logarithm stability constants (thermodynamic) for H_3SiO_4^- complexes and ion pairs at 25°C and 1 atmosphere.	150
12.	Cited logarithm stability constants (thermodynamic) for $\text{H}_2\text{SiO}_4^{2-}$ complexes and ion pairs at 25°C and 1 atmosphere.	151
13.	Cited logarithm stability constants (thermodynamic) for HPO_4^{2-} complexes and ion pairs at 25°C and 1 atmosphere.	152

14. Cited logarithm stability constants (thermodynamic) for PO_4^{3-} complexes and ion pairs at 25°C and 1 atmosphere. 153
15. Cited logarithm stability constants (thermodynamic) for humic acid complexes and ion pairs at 25°C and 1 atmosphere. 154

LIST OF FIGURES

Figure		Page
2.1	Correlation of $\log K_{MCl}$ with $\log K_{MOH}$ at zero ionic strength, 25°C and 1 atmosphere.	21
2.2	Correlation of $\log K_{MCl}$ with $\log K_{MF}$ at zero ionic strength, 25°C and 1 atmosphere.	25
2.3	Correlation of $\log K_{MCl}$ with $\log K_{MHCO_3}$ at zero ionic strength, 25°C and 1 atmosphere.	26
2.4	Correlation of $\log K_{MCl}$ with $\log K_{CO_3}$ at zero ionic strength, 25°C and 1 atmosphere.	29
2.5	Correlation of $\log K_{MCl}$ with $\log K_{MSO_4}$ at zero ionic strength, 25°C and 1 atmosphere.	31
2.6	Correlation of $\log K_{MF}$ with $\log K_{MOH}$ at zero ionic strength, 25°C and 1 atmosphere.	32
2.7	Correlation of $\log K_{MF}$ with $\log K_{MCO_3}$ at zero ionic strength, 25°C and 1 atmosphere.	33
2.8	Correlation of $\log K_{MHCO_3}$ with $\log K_{MOH}$ at zero ionic strength, 25°C and 1 atmosphere.	35
2.9	Correlation of $\log K_{MHCO_3}$ with $\log K_{MCO_3}$ at zero ionic strength, 25°C and 1 atmosphere.	36
2.10	Correlation of $\log K_{MSO_4}$ with $\log K_{MNO_3}$ at zero ionic strength, 25°C and 1 atmosphere.	37
2.11	Correlation of $\log K_{MSO_4}$ with $\log K_{MCO_3}$ at zero ionic strength, 25°C and 1 atmosphere.	40
2.12	Correlation of $\log K_{MCO_3}$ with $\log K_{MOH}$ at zero ionic strength, 25°C and 1 atmosphere.	41
2.13	Correlation of $\log K_{NaL}$ with $\log K_{KL}$ at zero ionic strength, 25°C and 1 atmosphere.	43

2.14	Correlation of $\log K_{\text{NaL}}$ with $\log K_{\text{MgL}}$ at zero ionic strength, 25°C and 1 atmosphere.	44
2.15	Correlation of $\log K_{\text{NaL}}$ with $\log K_{\text{CaL}}$ at zero ionic strength, 25°C and 1 atmosphere.	45
2.16	Correlation of $\log K_{\text{CaL}}$ with $\log K_{\text{KL}}$ at zero ionic strength, 25°C and 1 atmosphere.	46
2.17	Correlation of $\log K_{\text{MgL}}$ with $\log K_{\text{CaL}}$ at zero ionic strength, 25°C and 1 atmosphere.	48
2.18	Correlation of $\log K_{\text{MCl}}$ with $\log K_{\text{MOH}}$ at 0.7 ionic strength, 25°C and 1 atmosphere.	49
2.19	Correlation of $\log K_{\text{MCl}}$ with $\log K_{\text{MHCO}_3}$ at 0.7 ionic strength, 25°C and 1 atmosphere.	51
2.20	Correlation of $\log K_{\text{MCl}}$ with $\log K_{\text{MCO}_3}$ at 0.7 ionic strength, 25°C and 1 atmosphere.	52
2.21	Correlation of $\log K_{\text{MHCO}_3}$ with $\log K_{\text{MF}}$ at 0.7 ionic strength, 25°C and 1 atmosphere.	53
2.22	Correlation of $\log K_{\text{MHCO}_3}$ with $\log K_{\text{MOH}}$ at 0.7 ionic strength, 25°C and 1 atmosphere.	55
2.23	Correlation of $\log K_{\text{MHCO}_3}$ with $\log K_{\text{MCO}_3}$ at 0.7 ionic strength, 25°C and 1 atmosphere.	56
2.24	Correlation of $\log K_{\text{MHCO}_3}$ with $\log K_{\text{MSO}_4}$ at 0.7 ionic strength, 25°C and 1 atmosphere.	57
2.25	Correlation of $\log K_{\text{MCO}_3}$ with $\log K_{\text{MF}}$ at 0.7 ionic strength, 25°C and 1 atmosphere.	58
2.26	Correlation of $\log K_{\text{MCO}_3}$ with $\log K_{\text{MOH}}$ at 0.7 ionic strength, 25°C and 1 atmosphere.	60
2.27	Correlation of $\log K_{\text{MF}}$ with $\log K_{\text{MHA}}$ at zero ionic strength, 25°C and 1 atmosphere.	68

2.28	Correlation of $\log K_{\text{MSO}_4}$ with $\log K_{\text{MHA}}$ at zero ionic strength, 25°C and 1 atmosphere.	68
3.1	CSS HUDSON 82-001 Cruise station locations and cruise track.	88
3.2	Correlation of normalized surface total CO_2 with temperature.	93
3.3	Correlation of normalized surface alkalinity with temperature.	94
3.4	Vertical distribution of ΔTCO_2° for HUDSON station 20 and TTO station 152.	98
3.5	North-South cross-section of (a) potential temperature and (b) salinity. The thick line at the surface represents sea ice.	99
3.6	North-South cross-section of (a) nitrate and (b) apparent oxygen utilization. The thick line at the surface represents sea ice.	101
3.7	North-South cross-section of (a) normalized alkalinity and (b) normalized total CO_2 . The thick line at the surface represents sea ice.	102
3.8	North-South cross-section of ΔTCO_2° . The thick line at the surface represents sea ice.	103
3.9	Northern east-west cross-section of (a) potential temperature and (b) salinity. The thick line at the surface represents sea ice.	105
3.10	Northern east-west cross-section of (a) nitrate and (b) apparent oxygen utilization. The thick line at the surface represents sea ice.	106

- 3.11 Northern east-west cross-section of (a) normalized alkalinity and (b) normalized total CO_2 . The thick line at the surface represents sea ice. 107
- 3.12 Northern east-west cross-section of ΔTCO_2° . The thick line at the surface represents sea ice. 108
- 3.13 Southern east-west cross-section of (a) potential temperature and (b) salinity. The thick line at the surface represents sea ice. 109
- 3.14 Southern east-west cross-section of (a) nitrate and (b) apparent oxygen utilization. The thick line at the surface represents sea ice. 110
- 3.15 Southern east-west cross-section of (a) normalized alkalinity and (b) normalized total CO_2 . The thick line at the surface represents sea ice. 111
- 3.16 Southern east-west cross-section of ΔTCO_2° . The thick line at the surface represents sea ice. 112
- 3.17 Salinity plotted vs ΔTCO_2° for all waters below 100 m in the (a) Greenland and (b) Norwegian Seas. 115
- 3.18 Potential temperature vs ΔTCO_2° for all waters below 100 m in the (a) Greenland and (b) Norwegian Seas. 116
- 3.19 Apparent oxygen utilization plotted vs ΔTCO_2° for all waters below 100 m. 117
- 3.20 Tritium plotted vs ΔTCO_2° for all waters below 100 m. 119

LIST OF TABLES

Table		Page
2.1	The corresponding regression equation by least square method for LFERs at 25°C and 1 atmosphere.	23
2.2	The estimated stability constants (25° and 1 atmosphere) for some metal complexes and ion pairs in seawater by using LFER.	28
2.3	The estimated stability constants (25°C and 1 atmosphere) for some carbonate and bicarbonate complexes and ion pairs in seawater by using LFER.	38
3.1	Adjustments to the measured alkalinity and total CO ₂ data.	90

APPLICATION OF LINEAR FREE ENERGY RELATIONSHIP IN MARINE CHEMISTRY AND
ANALYSIS OF THE WINTERTIME CARBONATE DATE IN THE NORTHERN NORTH
ATLANTIC OCEAN

Chapter I

INTRODUCTION

Background

Prior to my arrival at the Oregon State University, I had been instructed by my mentor at the Shandong College of Oceanography to work on the thermodynamics of seawater and to return there to teach after obtaining advanced degrees. I have felt, however, as have others, that what Shandong College of Oceanography lacks dearly is the ability to analyze field data. Without such ability it is impossible to transfer the existing laboratory-confined marine sciences program to a balanced laboratory and field oceanography program (National Academy of Sciences, 1980; Chen, 1984; 1985). Consequently, I have divided my research into two topics: the Application of Linear Free Energy Relationship in Marine Chemistry, and the Analysis of Winter-time Carbonate Data in the Northern North Atlantic Ocean.

Linear Free Energy Relationship

The linear free energy relationship (LFER) has had a large variety of applications in a wide range of chemical and related sciences since it was first reported in 1924 by Bronsted and Pedersen (1924). During the last 30 years, the great interest shown by inorganic chemists in the thermodynamics of metal ion complexation and metal organic complexation in aqueous solutions has resulted in the compilation of a massive amount of stability constants for these complex formations. Analysis of these constants has led to the development of the fundamental concept and a more quantitative understanding of the linear free energy relationship.

Since the proposal of the Hammett equation (1937), which was supposed to be the most developed empirical equation for LFER at that time, much effort has been made to develop the concept of linear free energy relationship and enlarge its application. Its most valuable use is as a tool to predict unknown thermodynamic properties (such as the stability constants of complex formations) and to appraise published results. LFER is not only focused upon the correlation of stability constants, but also the correlation of the magnitude of the stability constants with other thermodynamic properties, even the properties of metal ions and ligands (Chen, 1961; Nieboer and McBryde, 1970; Chapman and Shorter, 1971; Nieboer and McBryde, 1973; Hancock *et al.*, 1974; Tardy and Garrels, 1976; 1977; Tardy and Gartner, 1977; Tardy and Vieillard, 1977; Hancock and Marsicano, 1978; Marsicano and Hancock, 1978; Langmuir, 1979; Hancock and Nakai, 1984). Such relationships between stability constants and other thermodynamic properties are reported in various fields, but are not often reported

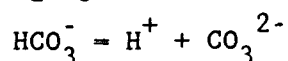
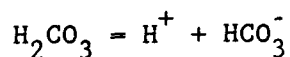
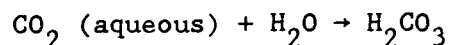
in the marine chemistry literature. It is reasonable for us to assume that many fundamental chemical properties of the marine environment including the stability constants can also be correlated linearly.

Furthermore, with the application of this relationship many thermodynamic properties not determined directly can be estimated and appraised. In this thesis, we have focused our attention on the existence of the linear free energy relationship by applying it to the evaluation of stability constants of complexes covering more than 40 cations and 15 anions in seawater at 25°C and 1 atmosphere, and using it to predict some undetermined stability constants of carbonate and bicarbonate complexes and ion pairs in seawater.

Carbonate and bicarbonate complexes and ion pairs are the most important species in the study of carbonate chemistry and the CO₂ system in the world oceans.

Wintertime Carbonate Data in the Northern North Atlantic Ocean

The CO₂-carbonate system is considered one of the most difficult problems in chemical oceanography. CO₂ hydrates rapidly with water to form carbonic acid and then it is involved in a series of proton transfer steps as follows:



All the steps involve the carbonate and bicarbonate ions. To study the carbonate system one must study the CO_2 system in seawater and vice versa. In Chapter 3, we examine the problem of excess CO_2 (human-made carbon dioxide) in the northern North Atlantic Ocean, mainly in the Norwegian and Greenland seas, widely considered as the main formation region of the deep water masses in the North Atlantic Deep Water (Wüst, 1935; Stefansson, 1968; Worthington, 1970; Reid and Lynn, 1971; Worthington, 1976; Swift et al., 1980; Swift and Aagaard, 1981; Worthington, 1981; Swift, 1982; Livingston et al., 1985). Since the industrial revolution around 1850 more and more industrial CO_2 (excess CO_2) has been released into the atmosphere from the burning of fossil fuels and from large-scale deforestation. As early as 1896, the distinguished Swedish chemist, S. Arrhenius, predicted that the increase in CO_2 in the atmosphere would warm the earth and in 1899 the American scientist, T.C. Chamberlin, proposed similar ideas (Chen and Drake, 1986). Since then much research has been done to evaluate the problem, especially in the last 15 years. Deep concern over the warming of the earth by increased CO_2 , known as the Greenhouse effect, has been shown by the scientific community. As we know, the world oceans play a very important role in taking up the excess CO_2 . It is generally believed that the amount of dissolved carbon in the oceans is sixty times higher than that in the atmosphere and oceans have acted as a major sink for excess CO_2 (Chen and Drake, 1986) and in some deep water formation areas, for example the northern North Atlantic, the entire water column is contaminated by excess CO_2 (Chen, 1982). The mechanism of transporting the excess CO_2 from the atmosphere to the oceans, then sinking into the deep ocean, however, is as yet not very clear because we do not have adequate wintertime

carbonate data in the deep-water formation regions. In this chapter, we will try to analyze the direct carbonate data, mainly as total carbon dioxide (TCO_2) and titration alkalinity (TA), collected in winter from the CSS HUDSON 1982 cruise in the Norwegian and Greenland seas and evaluate the penetration of excess CO_2 in that area. These data represent the first comprehensive winter carbonate data ever collected in this region. We have also used the tritium data collected from CSS HUDSON to support the excess CO_2 study based on direct observation of carbonate data. The penetration of excess CO_2 in wintertime in the northern North Atlantic is plotted in a number of cross sections.

References

- Brønsted, L.N. and K.P. Pedersen (1924). The catalytic decomposition of nitramide and its physico-chemical applications. Z. Physik. Chem. (Leipzig) 108, 185-235.
- Chen, C.T. (1982). On the distribution of anthropogenic CO₂ in the Atlantic and Southern Oceans. Deep-Sea Research 29, 563-580.
- Chen, C.T. (1984). Marine chemistry in the People's Republic of China. Office of Naval Research (U.S. Government Printing Office, 1984 454 158 19338), 948 pp.
- Chen, C.T. (1985). Some personal observations on the status of marine sciences in the People's Republic of China. EOS Oceanographic Report, 66, 52.
- Chen, C.T. and E.T. Drake (1986). Carbon dioxide increase in the atmosphere and oceans and possible effects on climate. Annual Review of Earth and Planetary Sciences 14, 201-235.
- Chen, Y.T. (1961). Linear free energy relationship from stability of complex compounds and acid and base strength of ligands. Z. Physik. Chem. (Leipzig) 220, 231-239.
- Hammett, L.P. (1937). Solutions of electrolytes, with particular application to qualitative analysis. Journal of the American Chemical Society 59, 96-103.
- Livingston, H.D., J.H. Swift and H.G. Ostlund (1985). Artificial radionuclide tracer supply to the Denmark Strait overflow between 1972 and 1981. Journal of Geophysical Research 90, 6971-6982.
- National Academy of Sciences (1980). Oceanography in China. CSC PRC report 9, 106 pp.

- Reid, J.H. and R. Lynn (1971). On the influence of the Norwegian-Greenland and Weddell seas upon the bottom waters of Indian and Pacific Oceans. Deep-Sea Research 18, 1063-1088.
- Stefanssen, U. (1968). Dissolved nutrients, oxygen and water masses in the North Irminger Sea. Deep-Sea Research 15, 541-545.
- Swift, J.H. (1982). The circulation of the Denmark Strait and Iceland-Scotland overflow waters on the North Atlantic. Deep-Sea Research 29, 563-580.
- Swift, J.H. and K. Aagaard (1981). Seasonal transitions and water mass formation in the Iceland and Greenland seas. Deep-Sea Research 28, 1107-1129.
- Swift, J.H., K. Aagaard and S.-A. Malmberg (1980). The contribution of the Denmark Strait overflow to the deep North Atlantic. Deep-Sea Research 27, 29-42.
- Tardy, Y. and R.M Garrels (1976). Prediction of Gibbs energies of formation, Part I: Relationships among Gibbs energies of formation of hydroxides, oxides and aqueous ions. Geochimica et Cosmochimica Acta 40, 1051-1056.
- Tardy, Y. and P. Vieillard (1977). Relationship among Gibbs free energies and enthalpies of formation of phosphates, oxides and aqueous ions. Contribution to Mineralogy and Petrology 63, 75-88.
- Tardy, Y. and L. Gartner (1977). Relationship among Gibbs free energies of formation of sulphate, nitrates, carbonates, oxides and aqueous ions. Contribution to Mineralogy and Petrology 63, 89-102.

- Tardy, Y. and R.M. Garrels (1977). Prediction of Gibbs energies of formation, Part I. Relationships among Gibbs energies of silicates, oxides, and aqueous ions. Geochimica et Cosmochimica Acta 41, 87-92.
- Worthington, L.V. (1970). The Norwegian Sea as a Mediterranean basin. Deep-Sea Research 17, 77-84.
- Worthington, L.V. (1976). On the North Atlantic circulation. The Johns Hopkins Oceanographic Studies 6, 110 pp.
- Worthington, L.V. (1981). The water masses in the World Ocean: Some results of a fine-scale census, in Evaluation of Physical Oceanography, B.A. Warren and C. Wunsch, eds., MIT Press, Cambridge, MA, pp. 6-41.
- Wust, G. (1935). The stratosphere of the Atlantic Ocean, translated by W.J. Emery, American Publishing Co., New Dehli, 1978, 112 pp.

CHAPTER II

APPLICATION OF LINEAR FREE ENERGY RELATIONSHIP
IN THE MARINE CHEMISTRY

Abstract

Linear free energy relationships (LFER) among the stability constants of major complexes and ion pairs in seawater at 25°C and 1 atmosphere are discussed. The correlations between the logarithms of the stability constants show the occurrence of LFER in seawater. The corresponding numerical equations are derived. The significance of linear free energy relationships lies in its ability to predict undetermined stability constants of complexes and ion pairs in seawater and to appraise data published in the literature. Specifically, an attempt is made to apply the concept of LFER to carbonate and bicarbonate complexes and ion pairs. By making use of this method, we hope to develop reliability in its prediction of stability constants and to establish the complete data set for the carbonate and bicarbonate system. The discussion only covers 1:1 complexes and ion pairs and so all of the stability constants in this work are first-step constants. It seems that the classification of ligands does not affect the linear free energy relationship with the exception of fluoride ligands whose behavior is anomalous.

Introduction

1. Background

One of the most important topics today in marine physical chemistry is the speciation and distribution of elements in seawater. The metal ions of geochemical and oceanographical interest exist in seawater in the form of free ions and complexes. Generally, the complexes are classified into two main groups: ion pairs and complexes with both organic and inorganic ligands. However, there are so far no criteria to distinguish ion pairs from the complexes (Langumir, 1979). For the examination of the stability of ion pair or complexes in electrolyte solution, stability constants must be available in the study of ion speciation at a certain temperature, ionic strength, and pressure. Unfortunately, many such stability constants are lacking, especially stoichiometric stability constants at seawater ionic strength ($I = 0.7$; Pytkowicz, 1983) for seawater at most salinity because it is extremely difficult to measure the stoichiometric constants with good precision in seawater. Although there are many more thermodynamic stability constants for the corresponding ion pairs and complexes, chemical oceanographers still prefer the stoichiometric constants in practical work because these constants can provide directly the concentration quantities in the Mass Action Law.

In this work, we intend to find out the linear free energy relationship in seawater in terms of the correlation among the logarithms of stability constants (both thermodynamic and stoichiometric at ionic strength = 0.7) at 25°C and 1 atmosphere. Using the plot and the regression equation, we try to predict some

undetermined stability constants for carbonate and bicarbonate species and appraise some data published in the literature in order to add to the compilation of stability constants for carbonate and bicarbonate metal complex in seawater. As is well known, seawater is a complex, multielectrolyte solution with high ionic strength, therefore, it is essentially unavoidable to produce errors when we deal with stoichiometric constants on the basis of 0.7 ionic strength ignoring other factors. Also, the large scattering of data, even for one salt, makes linear correlation problematical.

In this work, almost all the cations common in seawater are included and the anions include Cl^- , F^- , OH^- , HCO_3^- , HSO_4^- , H_3SiO_4^- , $\text{B}(\text{OH})_4^-$, NO_3^- , H_2PO_4^- , SO_4^{2-} , CO_3^{2-} , $\text{H}_2\text{SiO}_4^{2-}$, HPO_4^{2-} , PO_4^{3-} and humic acid (HA). So the obtained linear free energy relationship between stability constants of complexes or ion pairs with the same ligands, or with the same metal ions will cover most of the inorganic components in the marine environment. The data for stoichiometric stability constants at seawater ionic strength are fewer than thermodynamic ones, making the correlations for stoichiometric constants less reliable than those for thermodynamic ones. The ion pairs are all electrostatically bonded and generally at a long range. We have limited our complex formations to the 1:1 step. In other words, all the stability constants involved in this work are the first formation constants for a complex. One can obtain a better understanding of the linear free energy relationship in seawater through the 1:1 ion association.

2. Thermodynamics Review

The general expressions for the formation of a complex under certain conditions is as follows:



Where M denotes the metal ions and L denotes ligands of the complex. Z and j here are the number of positive and negative electrical charges respectively. Also n represents the number of the ligands in the complexation. In the case of 1:1 ion association, n will reduce to 1 and the above equation will be simplified to:



In accordance with the Mass Action Law, the formation constant K for this complex, $ML^{(z-j)+}$, is expressed thermodynamically by the activity quantities of all species.

$$K = \frac{a_{ML^{(z-j)+}}}{a_M^{z+} \cdot a_L^{j-}} \quad (3)$$

Where K is defined as the thermodynamic stability constant for complex $ML^{(z-j)+}$.

In practice, geochemists and chemical oceanographers prefer stoichiometric constants instead of thermodynamic ones because they can be directly related to concentrations of the involved species. Equation (3a) gives the expression of stoichiometric constants.

$$K^* = \frac{[ML^{(z-j)+}]}{[M^{z+}][L^{j-}]} \quad (3a)$$

Here the asterisk indicates the stoichiometric constant at certain ionic strength condition. The relationship between the concentration of a species and activity has been reported previously and the activity coefficient, which relates concentration and activity is well known as the function of ionic strength. So thermodynamic constants do not show any significance in the determination of species concentration unless the activity coefficient at that ionic strength is determined. However, the thermodynamic constant is still of great value for studies of physico-chemical properties of a system, therefore, we have first evaluated the linear free energy relationship for thermodynamic constants in the marine environment.

Linear Free Energy Relationships in Seawater

1. The Constituents and Compilation of Data

Ocean itself is a multicomponent system composed mainly of major ions such as Na^+ , K^+ , Ca^{2+} , Mg^{2+} , Cl^- , F^- , OH^- , HCO_3^- , NO_3^- , CO_3^{2-} , SO_4^{2-} , and minor trace metal ions such as Li^+ , Cs^+ , Rb^+ , Ag^+ , Cd^{2+} , Sr^{2+} , Cu^{2+} , Fe^{2+} , Mn^{2+} , Hg^{2+} , Ni^{2+} , Co^{2+} , Zn^{2+} , Be^{2+} , Fe^{3+} , Cr^{3+} (Grasshoff, 1983). Besides those above mentioned ions, there are also other ions, e.g. the cations such as Tl^+ , UO_2^{2+} , Ba^{2+} , Pb^{2+} , Tl^{3+} , Sc^{3+} , Y^{3+} , In^{3+} , Nb^{3+} , Zr^{3+} , La^{3+} , Dy^{3+} , Er^{3+} , Eu^{3+} , Lu^{3+} , Ng^{3+} , Pr^{3+} , Sm^{3+} , Tm^{3+} , Yb^{3+} , Tb^{3+} , Ho^{3+} , Gd^{3+} , Ce^{3+} , Nd^{3+} , Pa^{4+} , Np^{4+} , Th^{4+} , Hf^{4+} , Pu^{4+} and anions such as $\text{B}(\text{OH})_4^-$, HSO_4^- , H_2PO_4^- , H_3SiO_4^- , HPO_4^{2-} , $\text{H}_2\text{SiO}_4^{2-}$ and PO_4^{3-} . Seawater also contains much organic matter, and the typical ones are humic and fulvic acids. The complexation between metal cations and organic matter is also of paramount importance in the study of metal ion speciation of chemicals and the effect on metal inorganic ligand complexation in seawater (Mantoura *et al.*, 1978; Hirata, 1981).

In order to develop the concept of linear free energy relationships in seawater, we focus upon the compilation of stability constant data for complexations of the most geochemical and oceanographic interest. Most of the stability constants were reported at the temperature 25°C and 1 atm pressure. For the establishment of LFER in seawater the following information is provided:

- (1) a list of constituents of our interest
 - (2) thermodynamic stability constants (at zero ionic strength)
- for most of the above 1:1 complexes and ion pairs

(3) stoichiometric stability constants at 0.7 ionic strength.

All of the stability constants data collected for the 1:1 complexes and ion pairs in seawater from a survey of the literature are shown in the Appendices. Usually, different data sources provide different stability constants for a certain complex at the same conditions on the basis of their own observation. Therefore, we have to give the range of the data and assess their reliability.

2. Rationalization of LFER

For the 1:1 complexation of M and L, Pearson (1967, 1968) proposed that the stability constant can be expressed as the four-parameter equation:

$$\log K_{ML} = E_A E_B + C_A C_B \quad (5)$$

where E and C represent respectively the strength factor and softness factor and subscript A and B refer respectively to Lewis acid and base. For the complex of identical metal cation with different ligands, L1 and L2, we specify:

$$\log K_{ML1} = E_M E_{L1} + C_M C_{L1} \quad (6)$$

$$\log K_{ML2} = E_M E_{L2} + C_M C_{L2} \quad (7)$$

Subtracting (7) from (6),

$$\log K_{ML1} = (E_{L1}/E_{L2}) \log K_{ML2} + C_M [C_{L1} - (C_{L2} E_{L1}/E_{L2})] \quad (8)$$

At a given temperature, E and C are all constants respectively for the given metal cation and two different ligands (Chang *et al.*, 1983).

Similarly, E_{L1}/E_{L2} should be constant and thus the last term of the right-hand side of equation (8) should accordingly remain constant.

Thus, equation (8) can be expressed simply:

$$\log K_{ML1} = s \log K_{ML2} + b \quad (9)$$

So the plot of $\log K_{ML1}$ vs $\log K_{ML2}$ has the slope of s and the intercept of b , in which b and s are respectively combined by the parameters, strength and softness of ions.

Conversely, for the complex of the identical ligands with different metal ions, equations (6) and (7) will have the following form:

$$\log K_{M1L} = E_L E_{M1} + C_L C_{M1}$$

$$\log K_{M2L} = E_L E_{M2} + C_L C_{M2}$$

By similar means,

$$\log K_{M1L} = s^* \log K_{M2L} + b^* \quad (10)$$

Where s^* and b^* represent the slope and intercept of the correlation between $\log K_{M1L}$ and $\log K_{M2L}$.

Theoretically, the linear relationship between stability constants occurs here, and by making use of equations (9) and (10), the undetermined stability constants of a certain complex could be estimated if the related stability constants and the corresponding parameters were available under the same conditions.

3. Classification of Cations and Ligands

Since the logarithm of a stability constant is the function of four parameters, it depends on the softness and hardness factors of Lewis acid and base which could form the complex. The tendency of cations to form covalent bonds may be related to the concept of classification of metal ions and anions introduced by Schwarzenbach (1961), Pearson (1968) and Ahrland (1973), which is equivalent to the concept of hard and soft ions in an aqueous system. The cations with a rare gas configuration (d^0 cations) in our work, i.e. K^+ , Li^+ , Na^+ , Be^{2+} , Mg^{2+} , Ca^{2+} , Sr^{2+} , Ba^{2+} , Cs^{2+} , UO_2^{2+} , Sc^{3+} , Y^{3+} and Zr^{4+} , Hf^{4+} , Th^{4+} and lanthanides³⁺, constitute a related group from the point of view of stability constants of complexes and will be treated as A-type metal ions. Also, cations with an outer shell of 18 electrons (d^{10}) will be referred to as B-type metal ions. They are Ag^+ , Hg^{2+} , In^{3+} , Bi^{3+} and Tl^{3+} in our work. The rest of the metal ions belong to intermediate-type such as Co^{2+} , Cu^{2+} , Cd^{2+} , Fe^{2+} , Mn^{2+} , Ni^{2+} , Pb^{2+} , Zn^{2+} , Fe^{3+} , Cr^{3+} (Pearson, 1968).

In the classification of anions the following anions OH^- , F^- , NO_3^- , SO_4^{2-} , CO_3^{2-} , PO_4^{3-} involved in our work are classified as hard, and Cl^- is a soft base (Pearson, 1968). According to Lewis' concept, the most stable complex should be a hard acid, A-type metal ions coordinating with a hard base, or soft acid, B type metal ions

coordinating with a soft base. Because of the different stabilities among the complexes and ion pairs involved in our work, separate linear free energy relationships probably exist depending on A, B, or intermediate classifications.

4. Thermodynamic Constant Relationship Among MCl , MOH , MF , MNO_3 , $MHCO_3$, MCO_3 and MSO_4 Aqueous Complexes and Ion Pairs at $25^\circ C$ and 1 Atmosphere.

As mentioned previously, LFERs among the thermodynamic stability constants are significant theoretically even though geochemists and chemical oceanographers prefer stoichiometric ones for the marine environment. With the available data of thermodynamic stability constants at $25^\circ C$ and 1 atmosphere, logarithms of these constants of complexes with identical ligands are plotted against those constants of complexes with other identical ligands in this section.

First of all, the correlation of $\log K_{MCl}$ with $\log K_{MOH}$ at $25^\circ C$ and 1 atmosphere is demonstrated in Fig. 2.1. It covers 27 pairs of chlorides and hydroxides. Apparently, Ag^+ , Hg^{2+} , Tl^{3+} and In^{3+} , which belong to the B-type metal ions cannot fit the regression line composed of mostly of A and intermediate type complexes and ion pairs. Cd^{2+} and Pb^{2+} , also intermediate-type, however, are away from the line. Since most A-type and intermediate-type metal ions are included in the linear relationship, it is reasonable to suspect that the deviation of Cd^{2+} and Pb^{2+} is caused by measurement error. The corresponding regression equation and standard deviation are tabulated in Table 2.1.

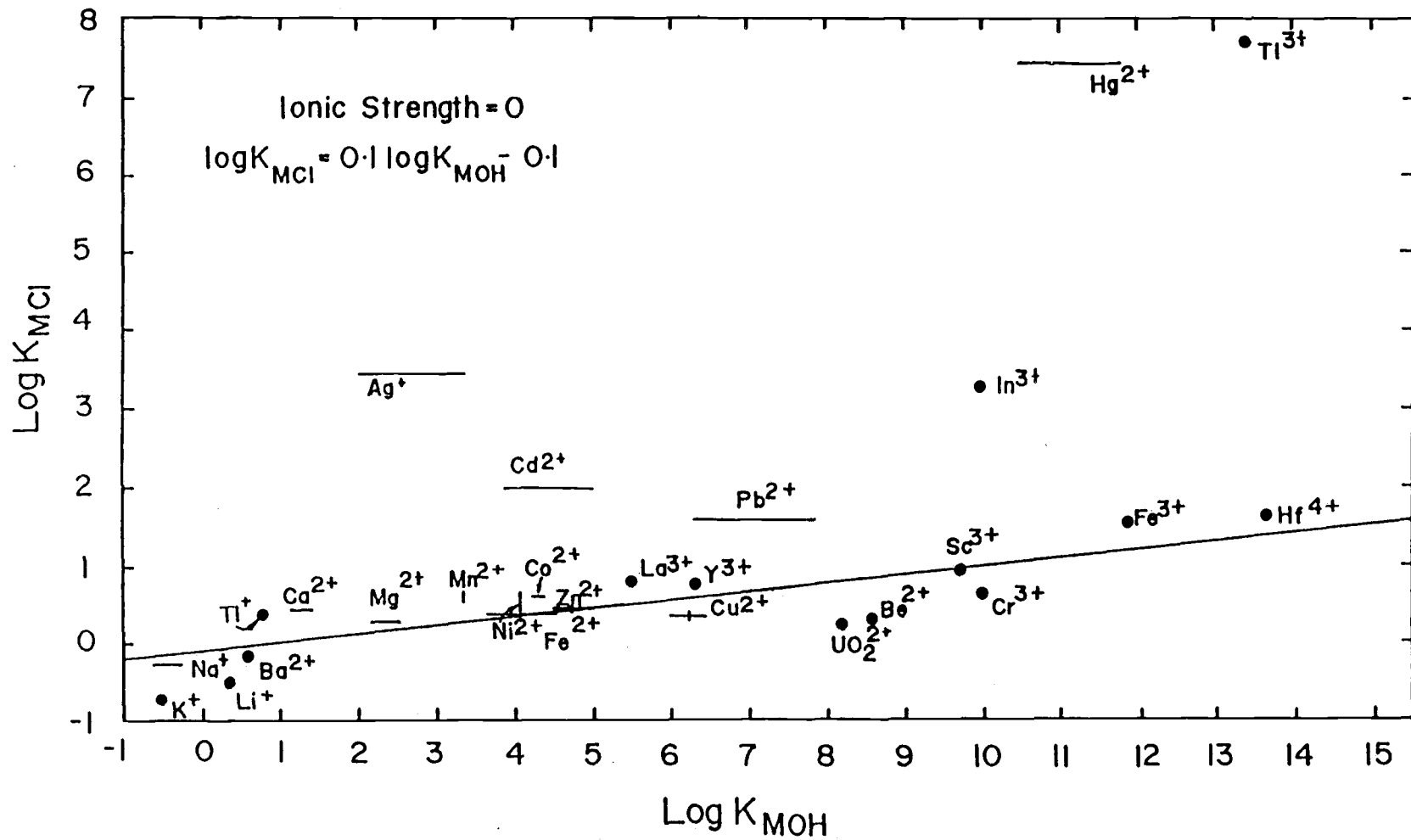


Fig. 2.1 Correlation of $\log K_{MCl}$ with $\log K_{MOH}$ at zero ionic strength, 25°C and 1 atmosphere.

Fig. 2.2 shows the correlation of $\log K_{MCl}$ with $\log K_{MF}$ including 31 pairs of chloride and fluoride constants. It seems that separate relationships occur in this case. The points for Ag^+ and In^{3+} deviate greatly from either of the regression lines, similar to Fig. 2.1. The separate lines occur depending on the types of A ($\log K_{M(A)}$) or intermediate ($\log K_{M(I)}$) metal ions. This situation occurs only when fluoride complexes and ion pairs are involved. As in Fig. 2.1, Cd^{2+} and Pb^{2+} also deviate from the line based on the type of intermediate metal ions to which they should belong. The two separate regression equations are tabulated in Table 2.1.

In Fig. 2.3, the correlation of $\log K_{MCl}$ with $\log K_{MHCO_3}$ is shown and it covers 14 pairs of chloride and bicarbonate complexes and ion pairs. In this case, we find no separate relationships based on classification of metal ions, but the regression line is not as good as the one in Figs. 2.1 and 2.2. The derivation of Cd^{2+} and Pb^{2+} is observed, which corresponds to the derivations in Figs. 2.1 and 2.2. Because the deviations happen in the plot of chloride constants vs others, it is reasonable to assume that the reported values of $CdCl^+$ and $PbCl^+$ constants may be in error and furthermore, we suggest that they need adjusting on the basis of LFERs in Figs. 2.1, 2.2 and 2.3. Thus, we suggest the value of the stability constant for $CdCl^+$ be in the range indicated by the three figures: 0.4 ± 0.3 of Fig. 2.1 on the basis of $\log K_{CdOH^+}$ value of 4.56, 0.4 ± 0.1 of Fig. 2.2 on the basis of $\log K_{CdF^+}$ value of 1.06 and 0.6 ± 0.3 of Fig. 2.3 on the basis of $\log K_{CdHCO_3^+}$ of 2.05. The value 0.1 to 0.9 for $CdCl^+$ stability constant from our estimation is, therefore, shown in Table 2.2. Similarly, the values for the $PbCl^+$ constant should be 0.7 ± 0.3 in Fig. 1, 0.6 ± 0.1 in Fig. 2 and 0.7 ± 0.3 in Fig. 3, instead of

Table 2.1. The corresponding regression equations by least squares method for LFERs at 25° and 1 atmosphere

Equations	R ²	n	Figure
$\log K_{MCl} = 0.1 \log K_{MOH} - 0.1 (\pm 0.3)$	0.65	21	2.1
$\log K_{M(A)Cl} = 0.2 \log K_{M(A)F} (\pm 0.2)$	0.74	24	2.2
$\log K_{M(I)Cl} = 0.2 \log K_{M(I)F} + 0.2 (\pm 0.1)$	0.91	7	2.2
$\log K_{MCl} = 0.3 \log K_{MHCO_3} (\pm 0.3)$	0.38	11	2.3
$\log K_{MCl} = 0.2 \log K_{MCO_3} - 0.4 (\pm 0.3)$	0.85	19	2.4
$\log K_{MCl} = 0.3 \log K_{MSO_4} - 0.4 (\pm 0.3)$	0.80	31	2.5
$\log K_{M(A)F} = 0.7 \log K_{M(A)OH} (\pm 0.4)$	0.99	11	2.6
$\log K_{M(I)F} = 0.6 \log K_{M(I)OH} - 1.3 (\pm 0.6)$	0.90	11	2.6
$\log K_{M(A)F} = 0.8 \log K_{M(A)CO_3} - 1.4 (\pm 0.5)$	0.94	16	2.7
$\log K_{M(I)F} = 0.8 \log K_{M(I)CO_3} - 2.7 (\pm 0.7)$	0.83	9	2.7
$\log K_{MHCO_3} = 0.2 \log K_{MOH} + 0.7 (\pm 0.5)$	0.60	15	2.8
$\log K_{MHCO_3} = 0.4 \log K_{MCO_3} - 0.3 (\pm 0.2)$	0.89	14	2.9
$\log K_{MSO_4} = 1.3 \log K_{MNO_3} + 1.8 (\pm 0.5)$	0.71	16	2.10
$\log K_{MSO_4} = 0.4 \log K_{MCO_3} + 0.7 (\pm 0.5)$	0.78	27	2.11
$\log K_{MCO_3} = 0.8 \log K_{MOH} + 1.8 (\pm 0.6)$	0.92	20	2.12
$\log K_{NaL} = 0.8 \log K_{KL} + 0.1 (\pm 0.4)$	0.81	6	2.13
$\log K_{NaL} = 0.4 \log K_{MgL} - 0.6 (\pm 0.4)$	0.71	11	2.14
$\log K_{NaL} = 0.4 \log K_{CaL} - 0.5 (\pm 0.3)$	0.85	12	2.15
$\log K_{CaL} = 1.4 \log K_{KL} + 1.5 (\pm 0.9)$	0.71	7	2.16
$\log K_{MgL} = 0.9 \log K_{CaL} + 0.4 (\pm 0.5)$	0.92	14	2.17
$\log K_{MCl}^* = 0.2 \log K_{MOH}^* - 0.3 (\pm 0.4)$	0.50	6	2.18
$\log K_{MCl}^* = 0.5 \log K_{MHCO_3}^* - 0.4 (\pm 0.3)$	0.78	6	2.19
$\log K_{MCl}^* = 0.2 \log K_{MCO_3}^* - 0.5 (\pm 0.3)$	0.80	7	2.20
$\log K_{M(A)HCO_3}^* = 0.4 \log K_{M(A)F}^* - 0.1 (\pm 0.2)$	0.89	3	2.21

Table 2.1 (continued)

Equations	R ²	n	Figure
$\log K_{M(I)HCO_3}^* = 1.4 \log K_{M(I)F}^* + 0.2 (\pm 0.3)$	0.89	4	2.21
$\log K_{MHCO_3}^* = 0.3 \log K_{MOH}^* - 0.2 (\pm 0.4)$	0.81	7	2.22
$\log K_{MHCO_3}^* = 0.4 \log K_{MCO_3}^* - 0.6 (\pm 0.2)$	0.94	7	2.23
$\log K_{MHCO_3}^* = 1.1 \log K_{MSO_4}^* - 0.2 (\pm 1.0)$	0.19	6	2.24
$\log K_{M(A)CO_3}^* = 0.6 \log K_{M(A)F}^* + 1.1 (\pm 0.3)$	0.92	3	2.25
$\log K_{M(I)CO_3}^* = 2.2 \log K_{M(I)F}^* + 2.6 (\pm 1.2)$	0.50	4	2.25
$\log K_{MCO_3}^* = 0.7 \log K_{MOH}^* + 0.8 (\pm 0.8)$	0.88	7	2.26

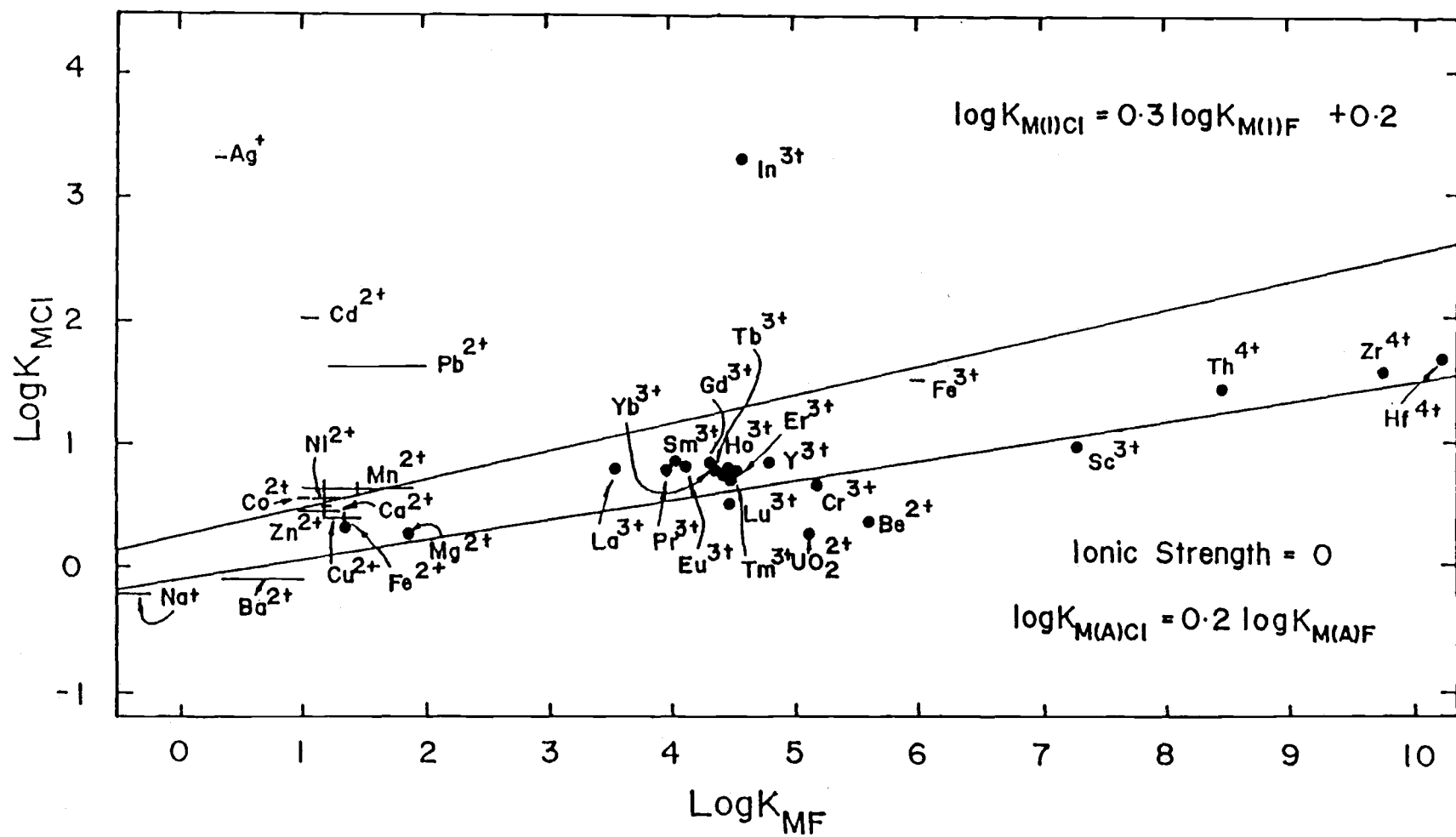


Fig. 2.2 Correlation of $\log K_{MCl}$ with $\log K_{MF}$ at zero ionic strength, 25°C and 1 atmosphere.

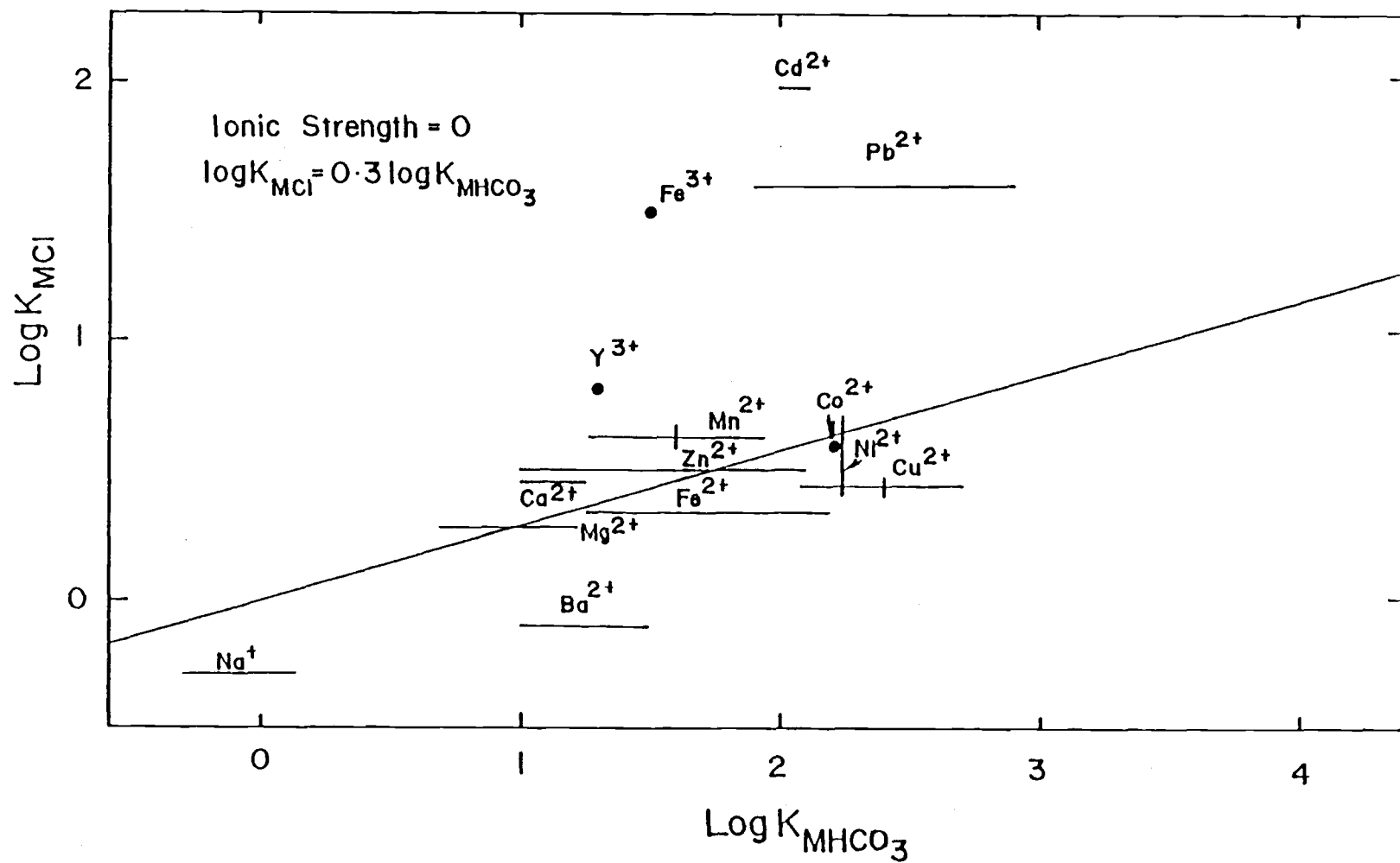


Fig. 2.3 Correlation of $\log K_{MCl}$ with $\log K_{MHCO_3}$ at zero ionic strength, 25°C and 1 atmosphere.

the reported 1.58-1.60. The possible range for the value of $\log K_{\text{PbCl}^+}$ should be most likely between 0.3 and 1.0 and this is listed in Table 2.2. The deviation of Fe^{3+} in Fig. 2.3 can be explained by either increasing the value of $\log K_{\text{FeHCO}_3^{2+}}$ or decreasing the value of $\log K_{\text{FeCl}^{2+}}$. The regression line equations are tabulated in Table 2.1.

Fig. 2.4 demonstrates the correlation between $\log K_{\text{MCl}}$ and $\log K_{\text{MCO}_3}$ for 19 pairs of mostly A and intermediate type ions. Besides the deviation of Ag^+ , which is a type-B metal ion, the deviation of CdCl^+ and PbCl^+ can be adjusted to be 0.5 ± 0.3 and 0.6 ± 0.3 respectively. These two values for CdCl^+ and PbCl^+ stability constants are in good agreement with those from Figs. 2.1-2.3. In Fig. 2.4, the larger scatter for some of the carbonate data may cause problems in the determination of LFER.

The correlation of $\log K_{\text{MCl}}$ with $\log K_{\text{MSO}_4}$ at 25°C and 1 atmosphere is given in Fig. 2.5. It covers 32 pairs of chloride and sulfate constants. The points representing Ag^+ , In^{3+} , Cd^+ and Pb^+ are far away from the regression line. The deviation of CdCl^+ can be adjusted to be 0.4 ± 0.3 , which is close to the estimated values from Figs. 2.1-2.4, and the estimated value for $\log K_{\text{PbCl}^+}$ is only 0.5 ± 0.3 , which is not in agreement with the results of Figs. 2.1-2.4. The regression equation for Fig. 2.5 is listed in Table 2.1 with its standard deviation.

Type-A and intermediate type ions show distinct LFERs when fluoride ions are involved. In Fig. 2.6, the correlation between $\log K_{\text{MF}}$ and $\log K_{\text{MOH}}$ is demonstrated, which covers 22 pairs of fluorides and hydroxides together. Separate LFERs are apparently obtained on the basis of different metal ion classification. It has been observed

Table 2.2 The estimated stability constants (25°C and 1 atmosphere) for some metal complexes and ion pairs in seawater by using LFER.

Species	log K (I=0)	Figure Source	Literature Value
CdCl^+	0.1-0.9	2.1;2.2;2.3;2.4;2.5	1.97-1.98
PbCl^+	0.3-1.0	2.1;2.2;2.3;2.4;2.5	1.58-1.6
AgNO_3°	-0.29	2.10	-0.29-2.0
KB(OH)_4°	-0.6-0.6	2.13;2.16	-
KF°	-1.3-0.4	2.6;2.7;2.13;2.16	-
KHSO_4°	-1.4--0.2	2.13;2.16	-
$\text{NaH}_3\text{SiO}_4^\circ$	-0.5-0.3	2.14;2.15	-
$\text{NaH}_2\text{SiO}_4^-$	0.9-2.0	2.14;2.15	-

Species	log K* (I=0.7)	Figure Source	Literature Value
CdCl^+	-0.3-0.7	2.18;2.19;2.20	1.36-1.60
CdSO_4°	-0.0-1.8	2.24	2.30-2.46

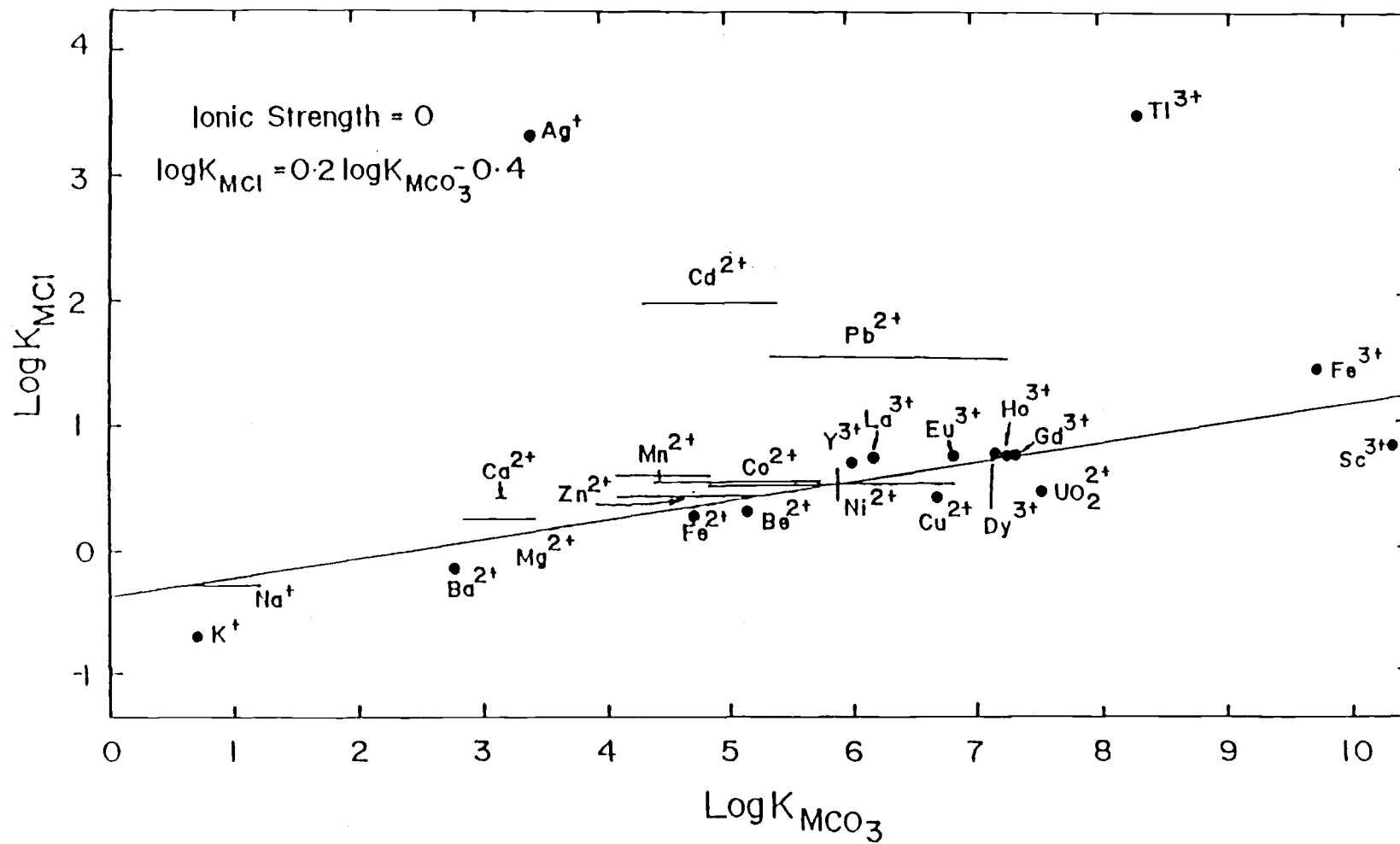


Fig. 2.4 Correlation of $\log K_{MCl}$ with $\log K_{MCO_3}$ at zero ionic strength, 25°C and 1 atmosphere.

that a single straight line contains all of the A-type metal ions, whereas the intermediate-type metal ions belong to the other bottom line. As for the B-type, only data for Ag^+ , In^{3+} and Hg^+ are available so that we could not determine the line representing the B-type metal ions. Another significant feature is that the relative stability, which can be presented as $\log K_{\text{MF}}/\log K_{\text{MOH}}$, is higher for the fluoride species of type-A metal ions than those of the intermediate-type metal ions. This higher relative stability is also reflected in Fig. 2.2 of $\log K_{\text{MCl}}$ vs $\log K_{\text{MF}}$. The two regression equations are listed in Table 2.1 with their respective standard deviations.

Fig. 2.7 gives the correlation between $\log K_{\text{MF}}$ and $\log K_{\text{MCO}_3}$, which covers 25 pairs of fluorides and carbonates together and two separate relationships are observed on the basis of type-A and type-intermediate metal ions. The existence of the separate LFERs, similar to what was found in in Figs. 2.3 and 2.6 leads to the same conclusion that fluoride, a hard base, is different from other bases. The hard base forms more stable complexes (higher K values) with hard acids (type-A ions) than with intermediate acids (intermediate type ions). The only difference is that the two LFERs in this figure are almost parallel without any indication of passing through the origin. The point representing the stability constants of BeF^+ and BeCO_3° deviates from the line representing type-A metal ions. According to the estimation from LFER, the value for $\log K_{\text{BeCO}_3^\circ}$ should be 8.4 ± 0.3 because there is no anomaly appearing for $\log K_{\text{BeF}^+}$ on Fig. 2.6.

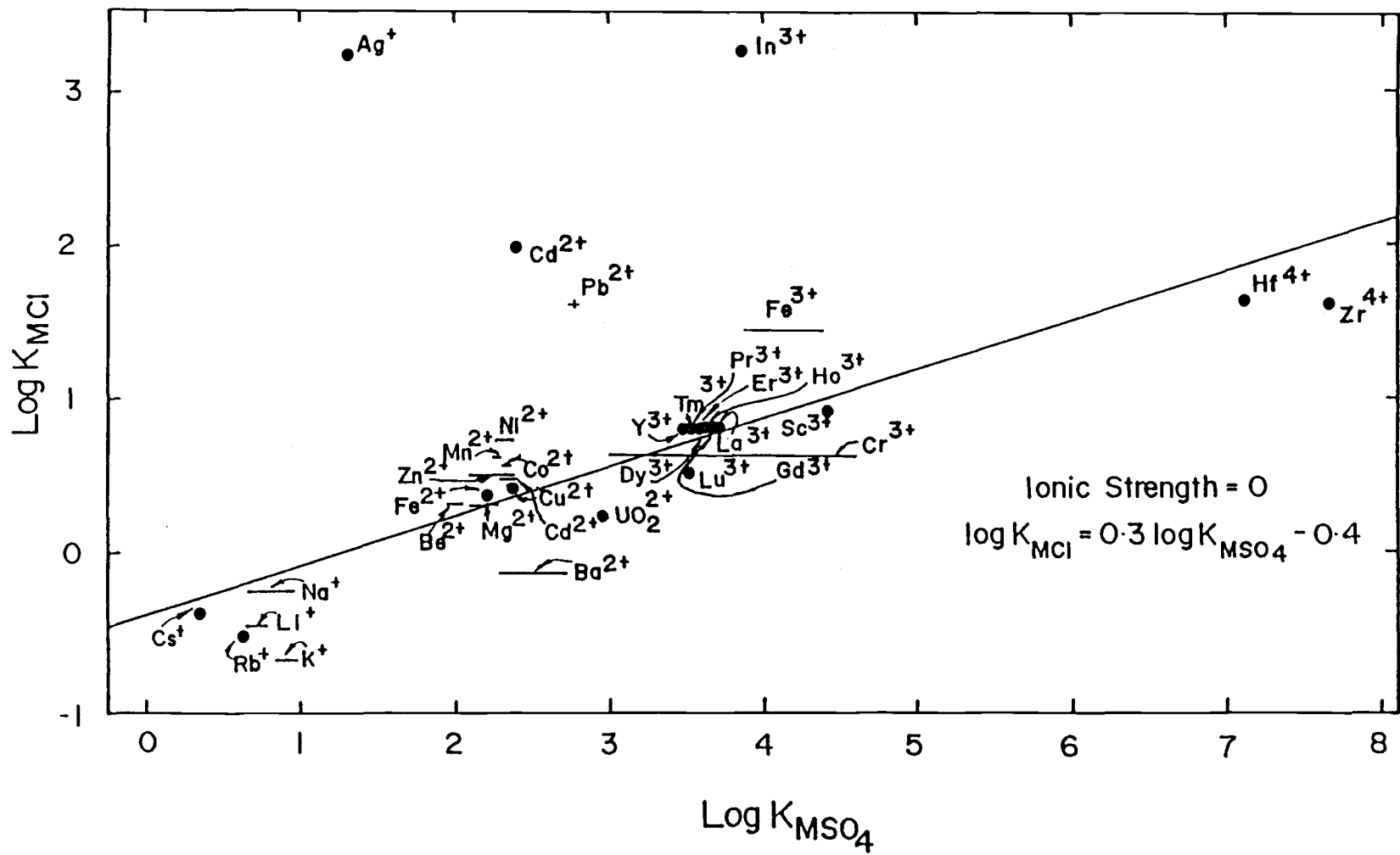


Fig. 2.5 Correlation of $\log K_{MCl}$ with $\log K_{MSO_4}$ at zero ionic strength, 25°C and 1 atmosphere.

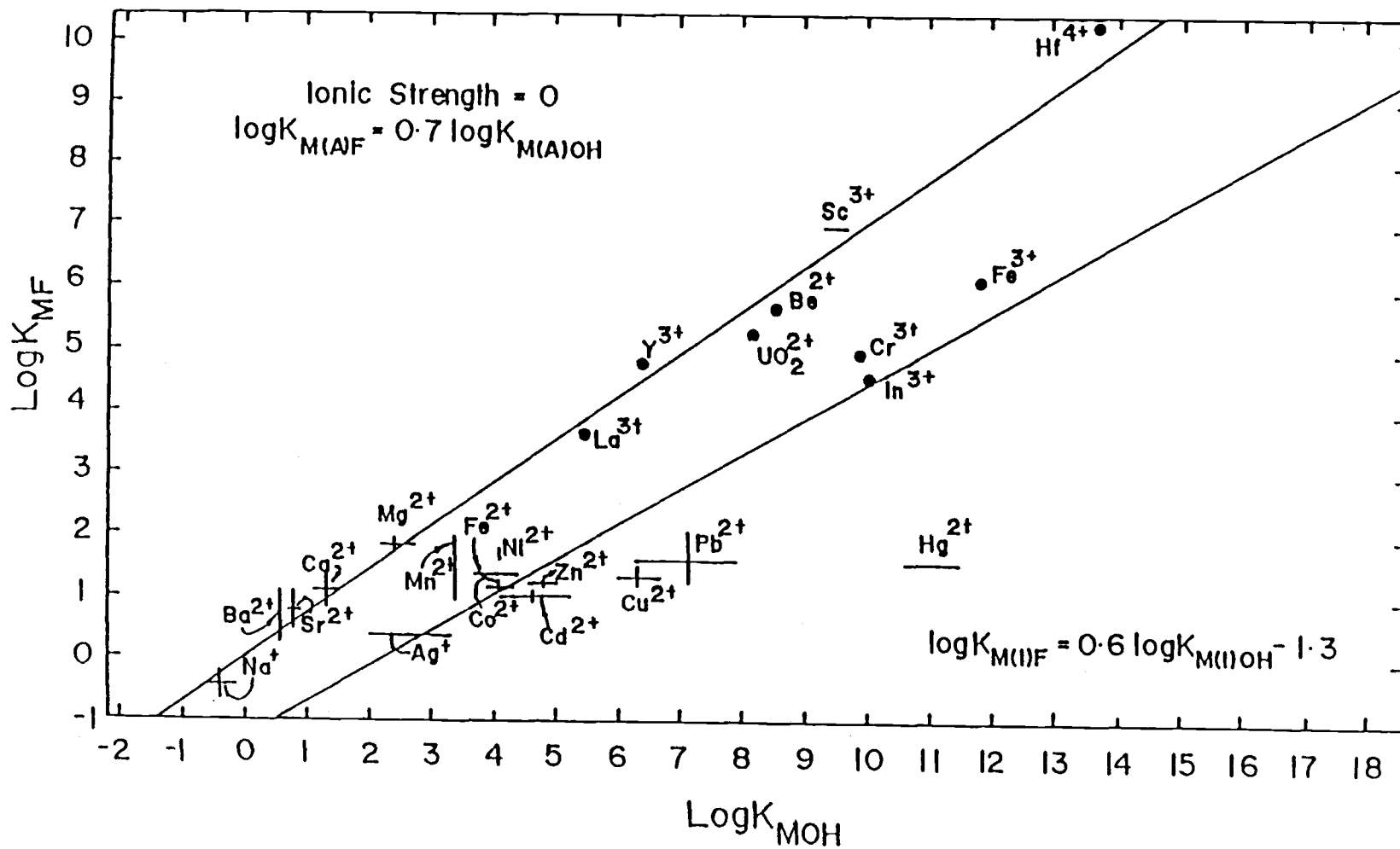


Fig. 2.6 Correlation of $\log K_{MF}$ with $\log K_{MOH}$ at zero ionic strength, 25°C and 1 atmosphere.

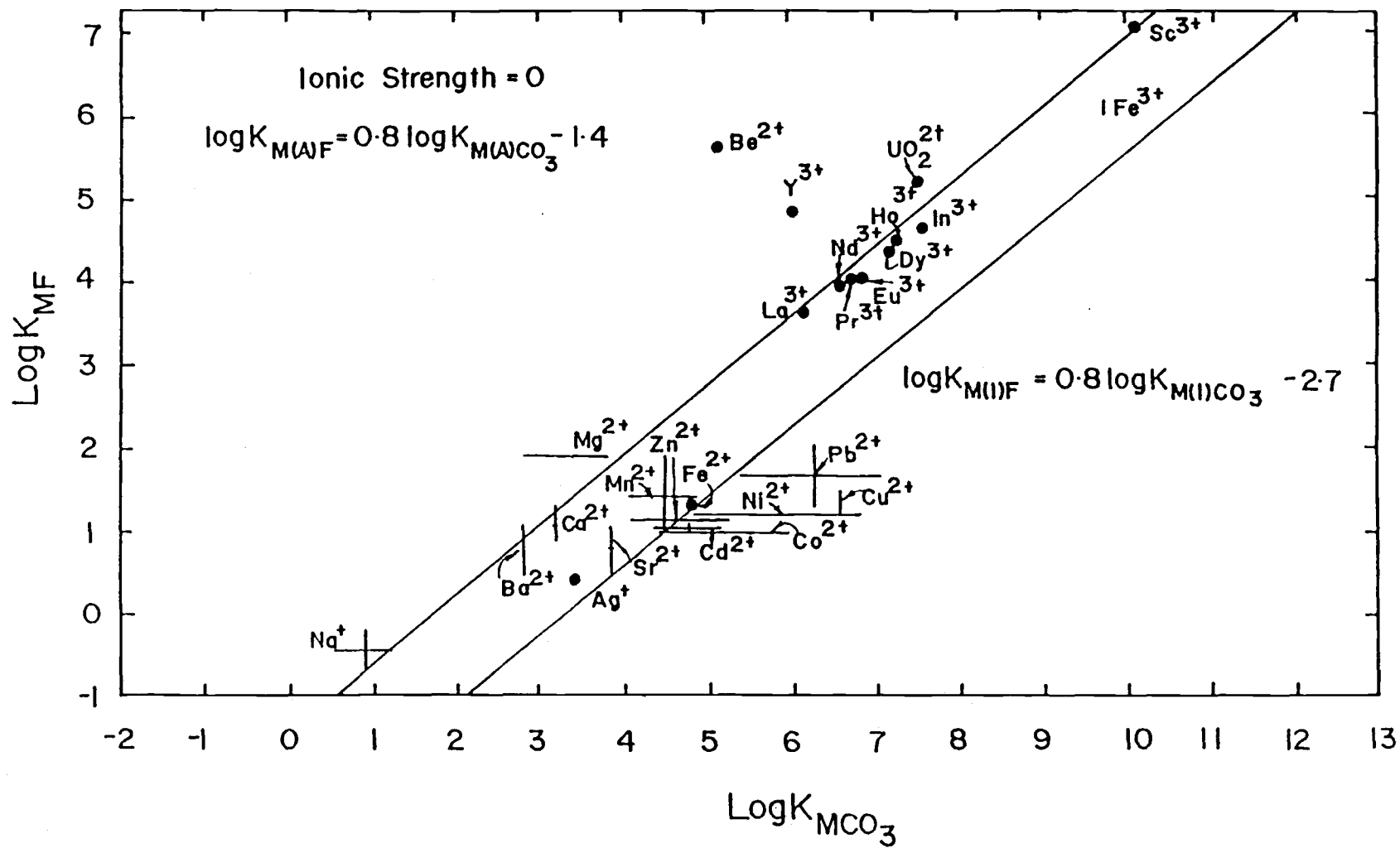


Fig. 2.7 Correlation of $\log K_{MF}$ with $\log K_{MCO_3}$ at zero ionic strength, 25°C and 1 atmosphere.

In Fig. 2.8, 15 pairs of bicarbonate and hydroxide stability constants are correlated. Only one LFER in this case is observed except for the deviation of the point for FeHCO_3^{2+} and FeOH^{2+} . As mentioned in discussion of Fig. 2.3, I assume that the reported value of $\log K_{\text{FeHCO}_3^{2+}}$ should be adjusted. It is proposed that it should be 3.3 ± 0.5 instead of 1.5 as reported in the literature. The regression equation is listed in Table 2.1 with its standard deviation.

Fig. 2.9 presents the correlation of $\log K_{\text{MHCO}_3}$ with $\log K_{\text{MCO}_3}$. It covers 14 carbonate and bicarbonate constants given. The regression equation is shown in Table 2.1. The deviation of the point representing FeHCO_3^{2+} and FeCO_3^+ constants is noted. The logarithm constant for FeHCO_3^{2+} should be adjusted to 3.8 ± 0.2 , which is in good agreement with the estimated result from Fig. 2.8. The range for $\log K_{\text{FeHCO}_3^{2+}}$ should be 2.8 to 4.0 in value and as listed in Table 2.3.

In Fig. 2.10, the correlation between $\log K_{\text{MSO}_4}$ and $\log K_{\text{MNO}_3}$ is shown and the corresponding regression equation is in Table 2.1. In this correlation, 16 sulfate and nitrate constants are included. The values of $\log K_{\text{AgNO}_3}^\circ$ are reported respectively as -0.29 (Ball *et al.*, 1981) and 2.0 (Smith and Martell, 1981). Apparently, the later datum does not fit the regression line, so I prefer employing -0.29 in the regression in this work. The adjusted value for $\log K_{\text{AgNO}_3}^\circ$ is shown in Table 2.2.

Fig. 2.11 presents the correlation between $\log K_{\text{MSO}_4}$ and $\log K_{\text{MCO}_3}$ and it covers 27 chloride and carbonate constants. The point for $\log K_{\text{BeSO}_4}^\circ$ and $\log K_{\text{BeCO}_3}^\circ$ will not be close to the regression line if we apply the adjusted value for $\log K_{\text{BeCO}_3}^\circ$ (8.4 ± 0.3 based on Fig.

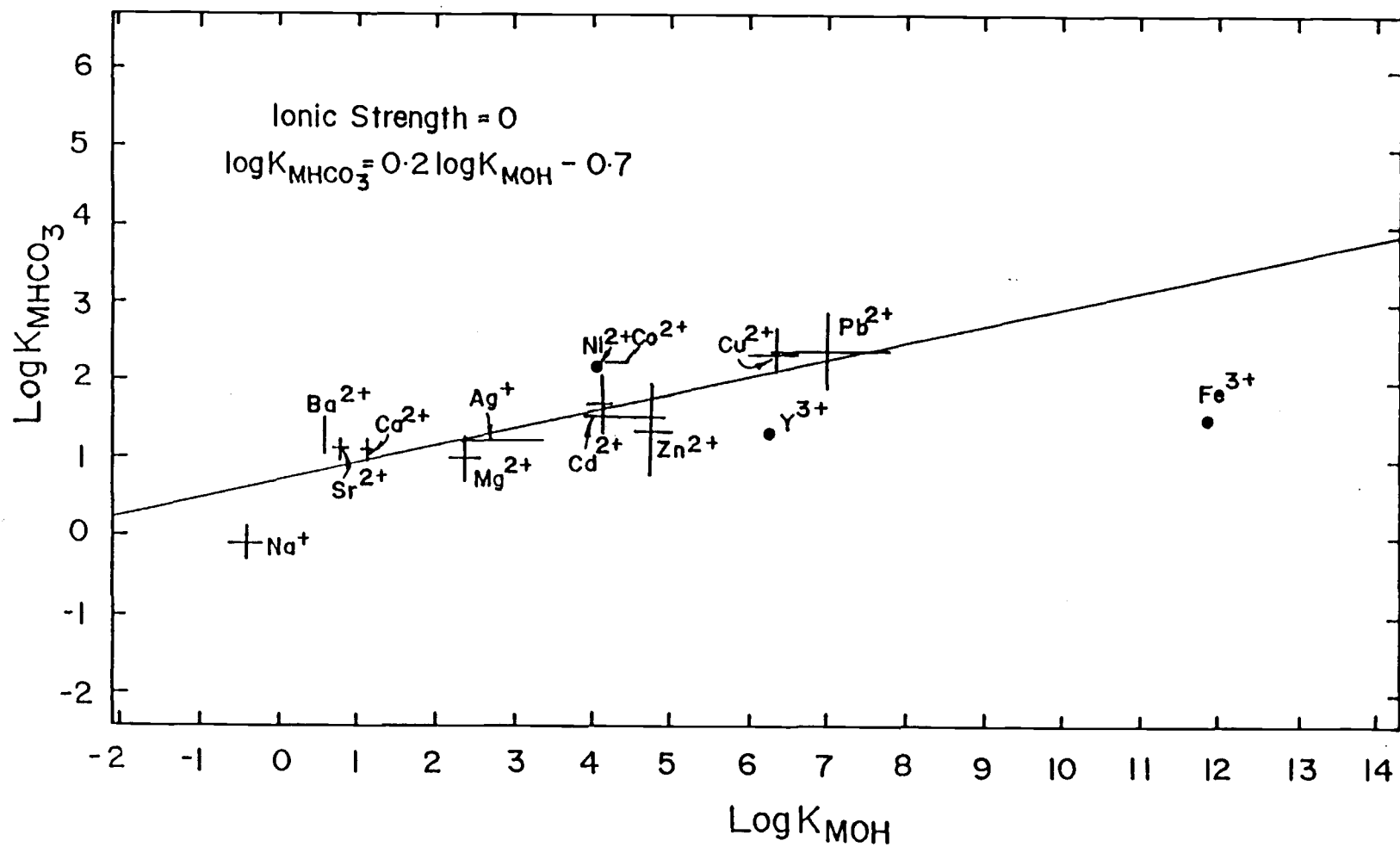


Fig. 2.8 Correlation of $\log K_{\text{MHCO}_3}$ with $\log K_{\text{MOH}}$ at zero ionic strength, 25°C and 1 atmosphere.

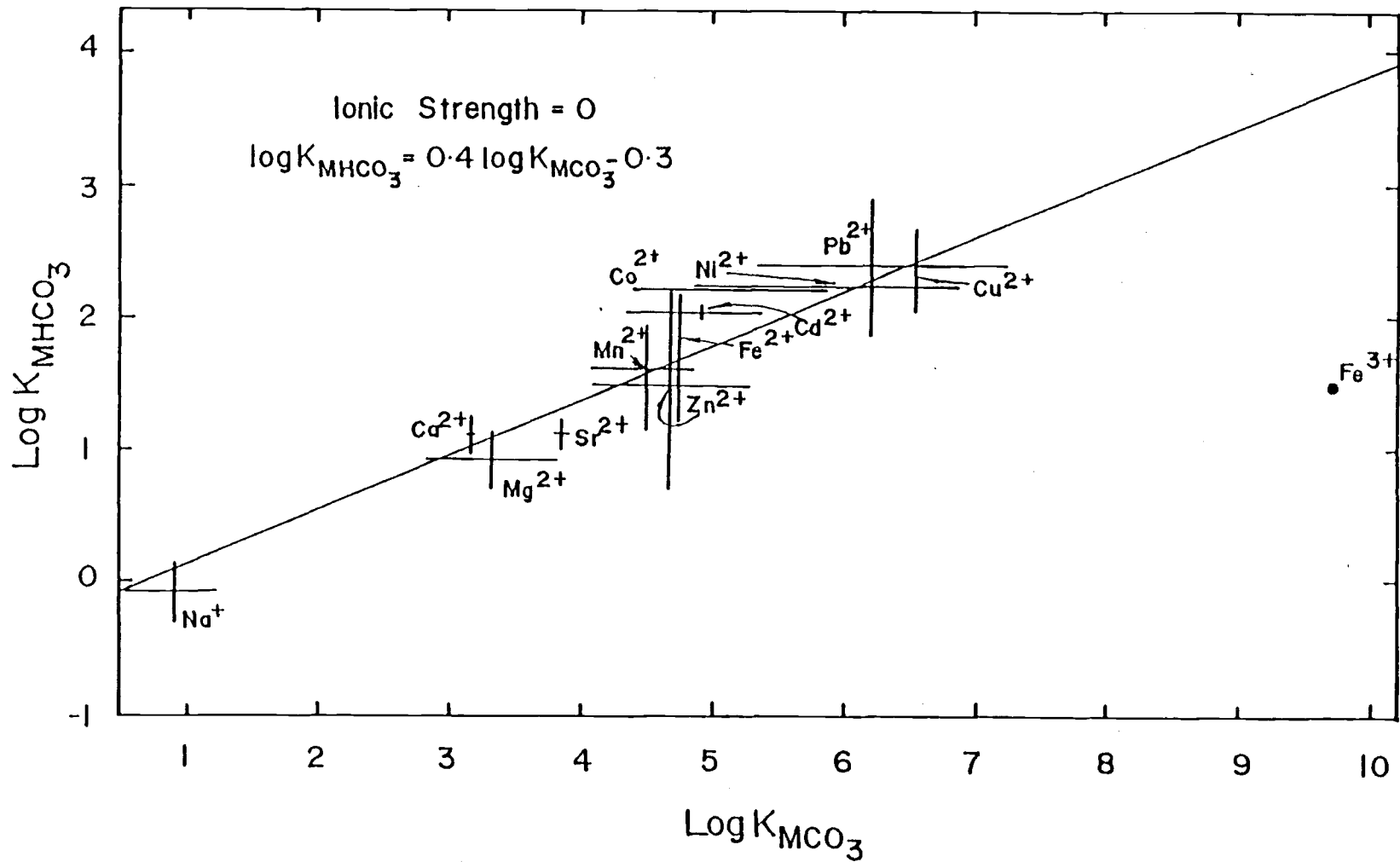


Fig. 2.9 Correlation of $\log K_{\text{MHCO}_3}$ with $\log K_{\text{MCO}_3}$ at zero ionic strength, 25°C and 1 atmosphere.

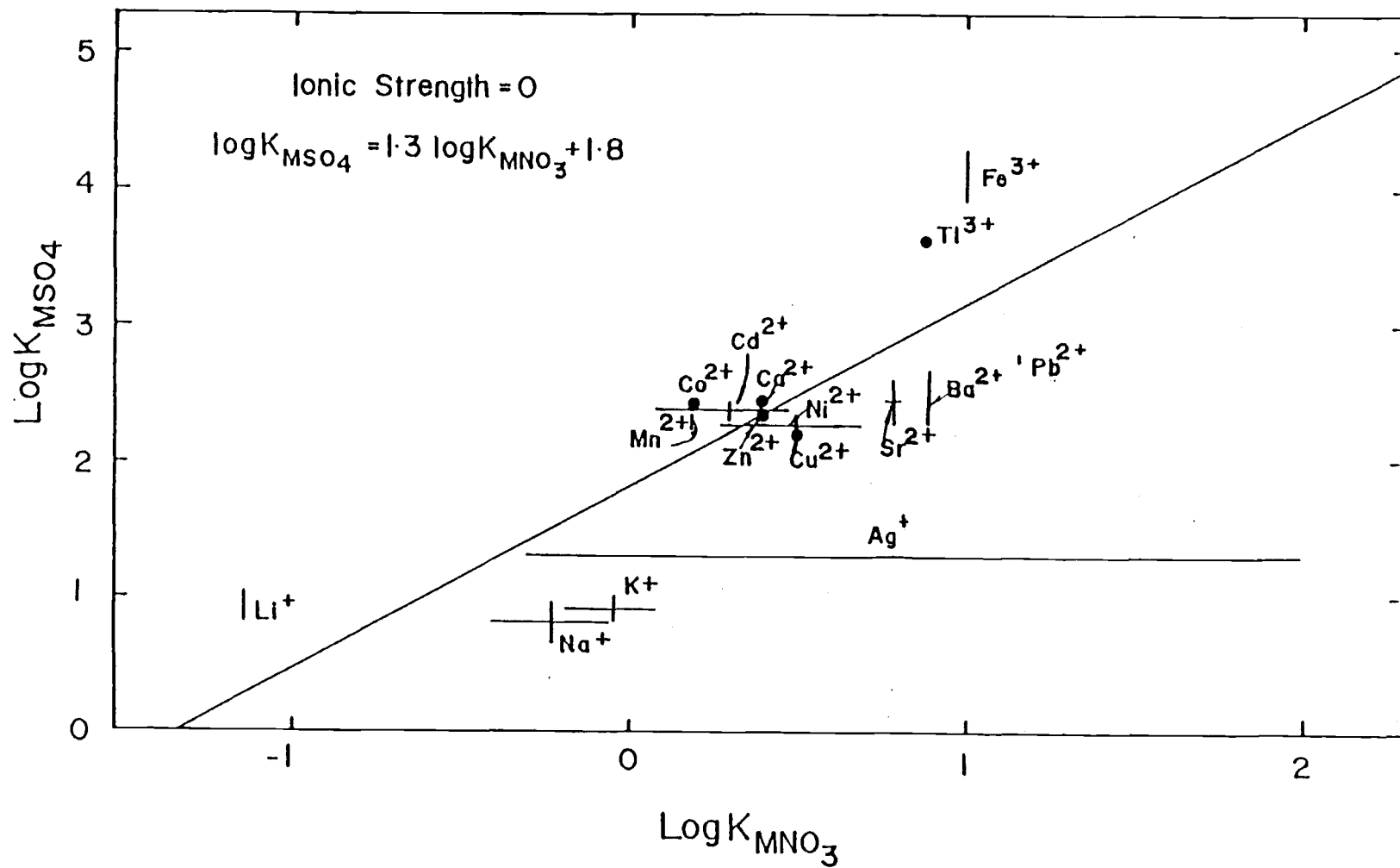


Fig. 2.10 Correlation of $\log K_{\text{MSO}_4}$ with $\log K_{\text{MNO}_3}$ at zero ionic strength, 25°C and 1 atmosphere.

Table 2.3 The estimated stability constants (25°C and 1 atmosphere) for some carbonate and bicarbonate complexes and ion pairs in seawater by using LFER.

Species	log K (I=0)	Figure Source	Literature Value
BeCO_3°	7.8-9.1	2.7;2.12	5.13
FeHCO_3^{2+}	2.8-4.0	2.8;2.9	1.5
KHCO_3°	-0.8-1.0	2.8;2.9;2.13;2.16	-
CrHCO_3^{2+}	1.5-3.4	2.3;2.8	-
LiCO_3^-	0.9-2.1	2.4;2.11;2.12	-
CrCO_3^+	8.9-10.1	2.7;2.12	-
BeHCO_3^+	2.1-3.5	2.3;2.8;2.9	-

Species	log K* (I=0.7)	Figure Source	Literature Value
SrHCO_3^+	-0.5-0.3	2.21;2.22	-
BaHCO_3^+	-0.6-0.2	2.21;2.22	-
FeHCO_3^{2+}	(1.9±0.3)	2.21	-
CrHCO_3^{2+}	(6.1±0.3)	2.21	-
MnHCO_3^+	(1.3±0.3)	2.21	-
NiHCO_3^+	(1.0±0.3)	2.21	-
CoHCO_3^+	(0.9±0.3)	2.21	-
FeCO_3^+	(5.3±1.2)	2.25	-
CrCO_3^+	(11.8±1.2)	2.25	-
NiCO_3°	(3.9±1.2)	2.25	-
CoCO_3°	(3.7±1.2)	2.25	-
MnCO_3°	(4.4±1.2)	2.25	-
SrCO_3°	0.2-1.7	2.25;2.26	-
BaCO_3°	0.1-1.6	2.25;2.26	-

2.7) either because the value of $\log K_{\text{BeSO}_4}^\circ$ needs adjusting or the reported value for $\log K_{\text{BeCO}_3}^\circ$ is correct. The correlation of $\log K_{\text{MCO}_3}$ with $\log K_{\text{MOH}}$ covering 20 pairs of carbonate and hydroxide constants is demonstrated in Fig. 2.12. The deviation of the point from LFER representing $\log K_{\text{BeCO}_3}^\circ$ and $\log K_{\text{BeOH}^+}$ is noted. As in Fig. 2.7, I can readjust the value of $\log K_{\text{BeCO}_3}^\circ$ to 8.4 ± 0.6 . The conclusion from two LFERs also indicates that the estimated value of $\log K_{\text{BeCO}_3}^\circ$ is most likely correct and that the reported values of $\log K_{\text{BeSO}_4}^\circ$ could be problematical (1.95-2.04). The point for $\log K_{\text{SrCO}_3}^\circ$ and $\log K_{\text{SrOH}^+}$ also deviates slightly from the regression line, but the deviation is not so great as to necessitate correction.

5. Thermodynamic Constant Relationship Among NaL, KL, MgL and CaL Complexes and Ion Pairs at 25°C and 1 Atmosphere.

After discussing the LFERs among aqueous complexes and ion pairs with the major anions in seawater, we focus in this section upon the occurrence of LFER among complexes and ion pairs with the four major cations. The four most important metal ions in the marine environment are Na^+ , K^+ , Mg^{2+} and Ca^{2+} . The ligands which complex with them include Cl^- , OH^- , F^- , NO_3^- , HSO_4^- , H_2PO_4^- , H_3SiO_4^- , $\text{B}(\text{OH})_4^-$, SO_4^{2-} , CO_3^{2-} , HPO_4^{2-} , $\text{H}_2\text{SiO}_4^{2-}$, $\text{C}_2\text{O}_4^{2-}$ and PO_4^{3-} . These metal ions and anions are studied frequently and well understood.

Fig. 2.13 shows the correlation between $\log K_{\text{NaL}}$ and $\log K_{\text{KL}}$ and only 12 of NaL and KL complexes and ion pairs are discussed. The regression equation for LFER is listed in Table 2.1. The value for $\log K_{\text{KB}(\text{OH})_4}^\circ$ can be estimated to be 0.0 ± 0.4 from the $\log K_{\text{NaB}(\text{OH})_4}^\circ$ value of 0.10, and the value for $\log K_{\text{KF}}^\circ$ is -0.7 ± 0.4 estimated from the $\log K_{\text{NaF}}^\circ$ value of -0.35. From Fig. 2.6, the value for $\log K_{\text{KF}}^\circ$

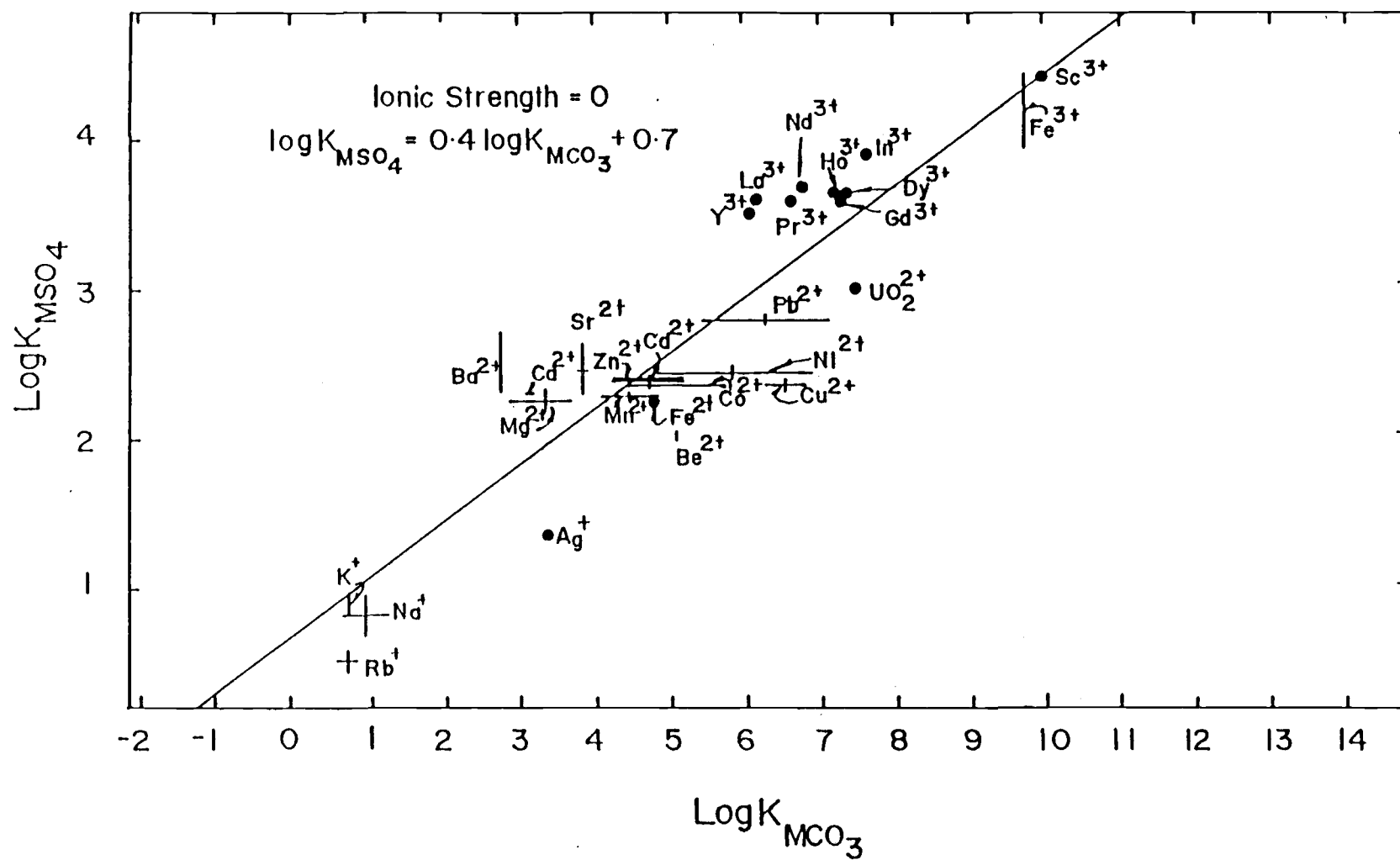


Fig. 2.11 Correlation of $\log K_{\text{MSO}_4}$ with $\log K_{\text{MCO}_3}$ at zero ionic strength, 25°C and 1 atmosphere.

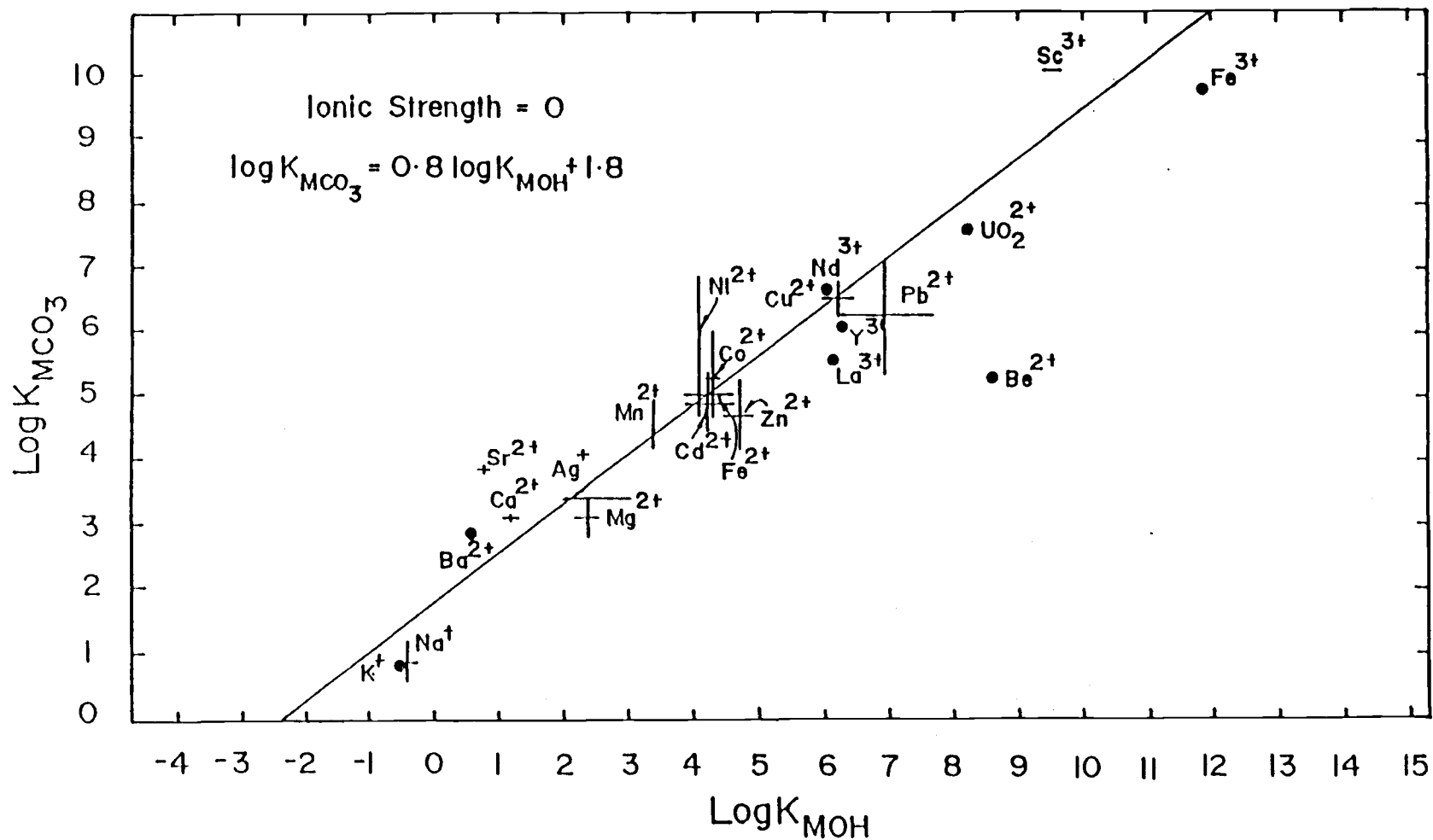


Fig. 2.12 Correlation of $\log K_{\text{MCO}_3}$ with $\log K_{\text{MOH}}$ at zero ionic strength, 25°C and 1 atmosphere.

should be -0.3 ± 0.4 and from Fig. 2.7, the value is adjusted to -0.8 ± 0.5 . The value for $\log K_{\text{KHSO}_4}^\circ$ is -1.0 ± 0.4 and for $\log K_{\text{KHCO}_3}^\circ$ -0.2 ± 0.4 from Fig. 2.13.

In Fig. 2.14, the correlation between $\log K_{\text{NaL}}$ and $\log K_{\text{MgL}}$ including 11 pairs of NaL and MgL constants is presented. From this correlation, we can estimate $\log K_{\text{NaH}_3\text{SiO}_4}^\circ$ and $\log K_{\text{NaH}_2\text{SiO}_4}^-$ to be -0.1 ± 0.4 and 1.6 ± 0.4 from $\log K_{\text{MgH}_3\text{SiO}_4}^+$ value of 1.26 and $\log K_{\text{MgH}_2\text{SiO}_4}^\circ$ value of 5.67 respectively. Similarly, the correlation of $\log K_{\text{NaL}}$ with $\log K_{\text{CaL}}$ shown in Fig. 2.15 can support these two estimates. The value of $\log K_{\text{NaH}_3\text{SiO}_4}^\circ$ is -0.1 ± 0.3 and $\log K_{\text{NaH}_2\text{SiO}_4}^-$ is 1.2 ± 0.3 . It is reasonable to conclude from Fig. 2.14 and 2.15 that the range of $\log K_{\text{NaH}_3\text{SiO}_4}^\circ$ is between -0.5 and 0.3 and of $\log K_{\text{NaH}_2\text{SiO}_4}^-$ is between 0.9 and 2.0 . The estimated results are shown in Table 2.2.

In Fig. 2.16, the correlation of $\log K_{\text{CaL}}$ with $\log K_{\text{KL}}$ is demonstrated, covering 7 pairs of CaL and KaL constants. From LFER, the value of $\log K_{\text{KF}}^\circ$ can be estimated as -0.2 ± 0.6 , which is in fair agreement with the results in Figs. 2.6, 2.7 and 2.13. Therefore, the range for $\log K_{\text{KF}}^\circ$ in accordance with those results, is between -1.3 and 0.4 , as shown in Table 2.2. Also, from LFER in this figure, the value of $\log K_{\text{KHCO}_3}^\circ$ can be assumed accordingly to be -0.2 ± 0.6 . Thus, the range for $\log K_{\text{KHCO}_3}^\circ$ is -0.8 to 0.4 , in this case. The values of $\log K_{\text{KB(OH)}_4}^\circ$ and $\log K_{\text{KHSO}_4}^\circ$ can be estimated by using this method. They are 0.0 ± 0.6 and -0.8 ± 0.6 respectively. The range for $\log K_{\text{KB(OH)}_4}^\circ$, considering the results from Fig. 2.13, is -0.6 to 0.6 and for $\log K_{\text{KHSO}_4}^\circ$ is -1.4 to -0.2 . All of the results are shown in Table 2.2. Fig. 2.17 gives the correlation containing most of the

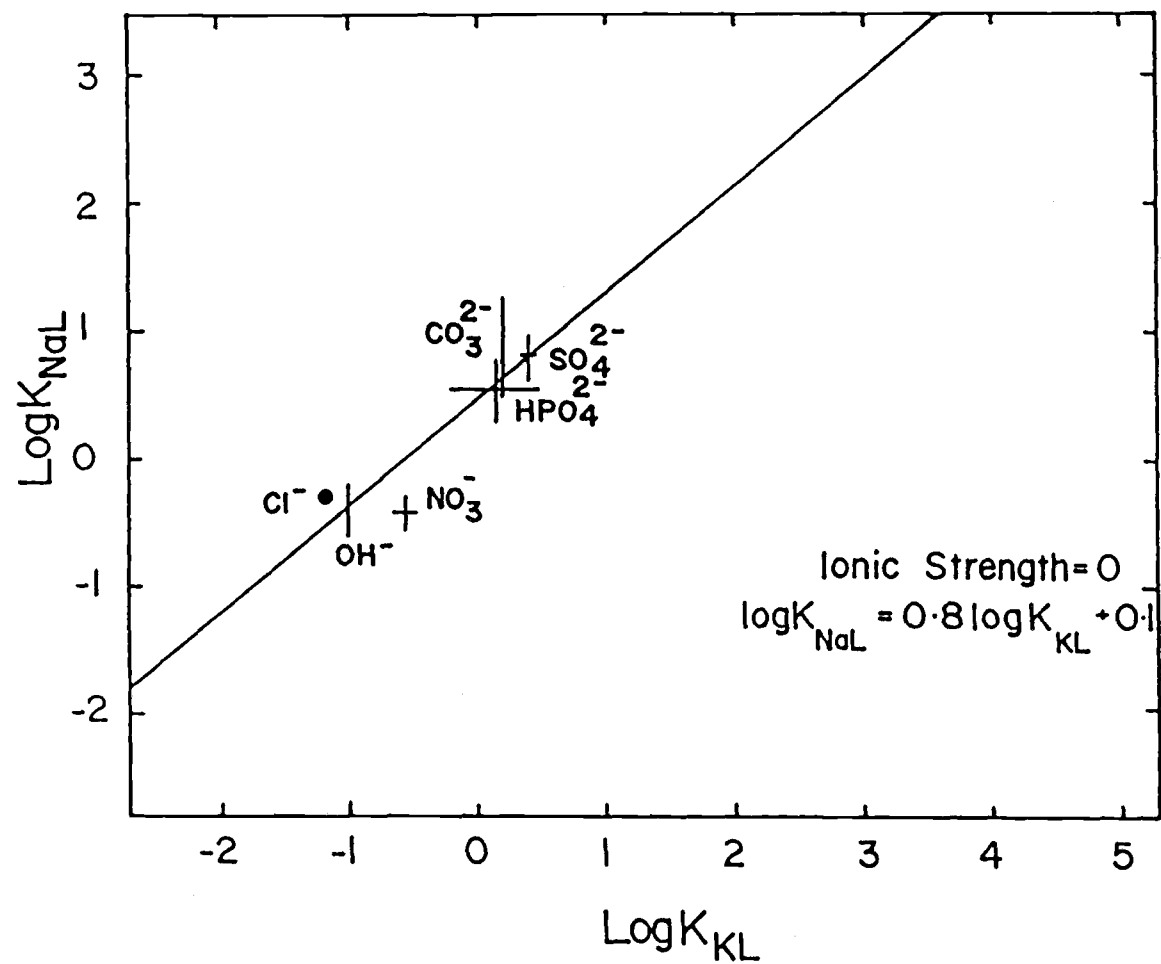


Fig. 2.13 Correlation of $\log K_{\text{NaL}}$ with $\log K_{\text{KL}}$ at zero ionic strength, 25°C and 1 atmosphere.

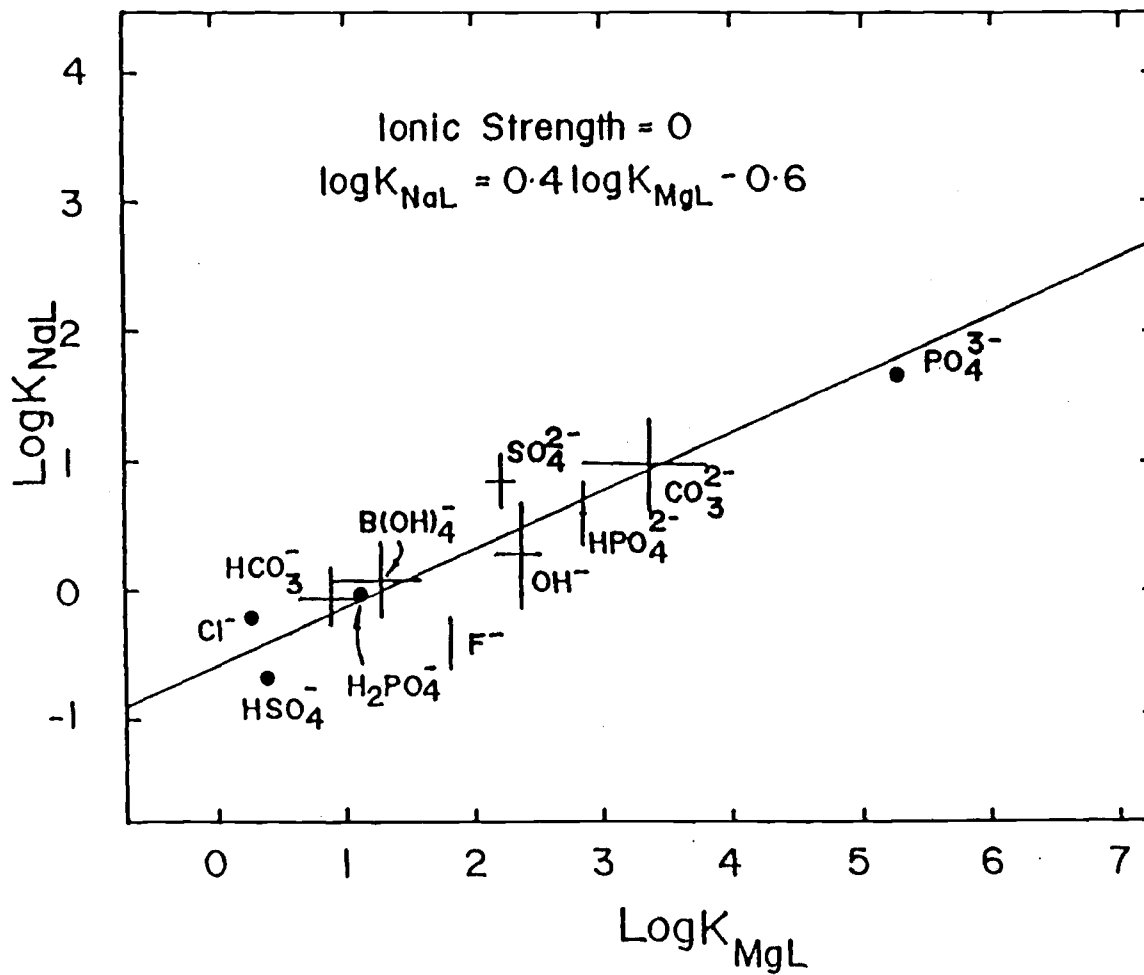


Fig. 2.14 Correlation of $\log K_{NaL}$ with $\log K_{MgL}$ at zero ionic strength, 25°C and 1 atmosphere.

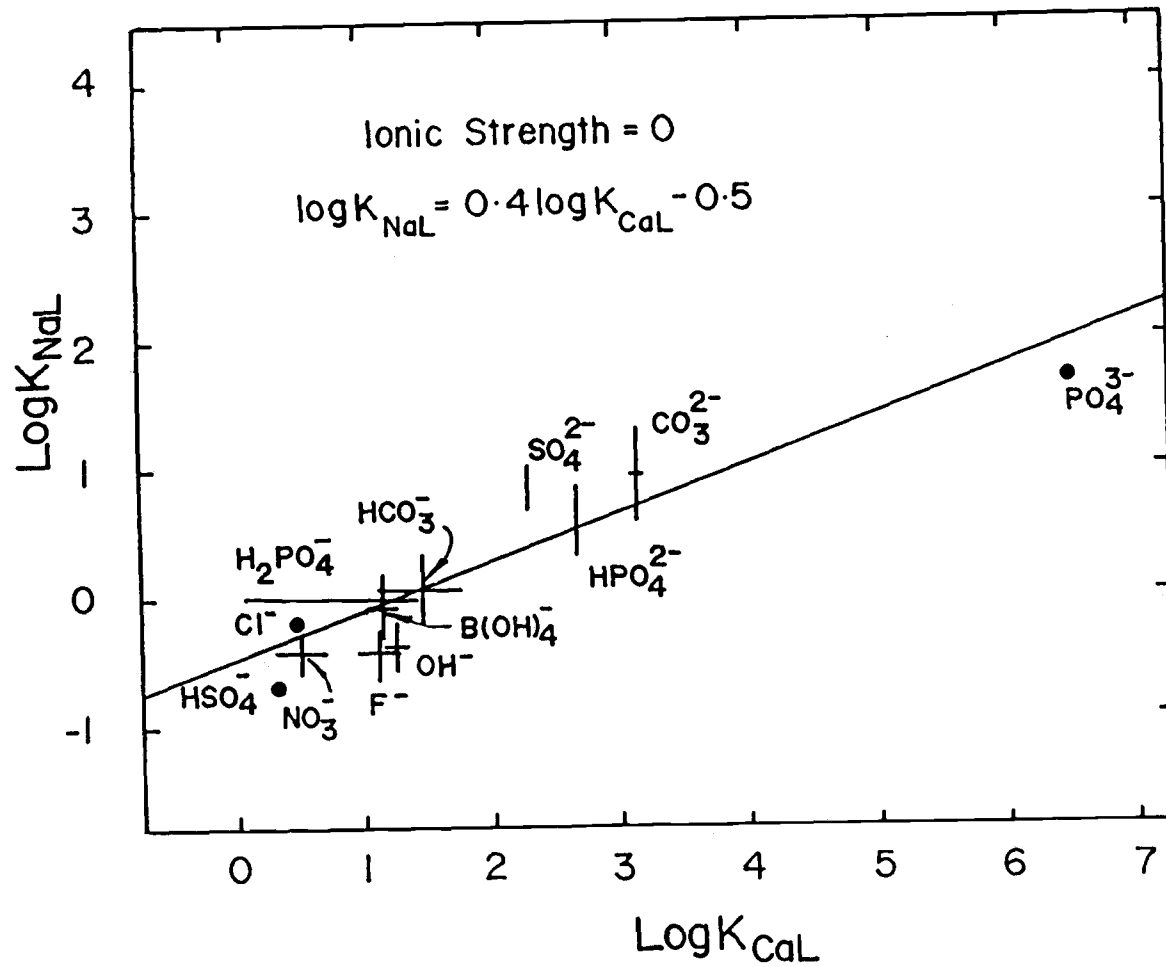


Fig. 2.15 Correlation of $\log K_{\text{NaL}}$ with $\log K_{\text{CaL}}$ at zero ionic strength, 25°C and 1 atmosphere.

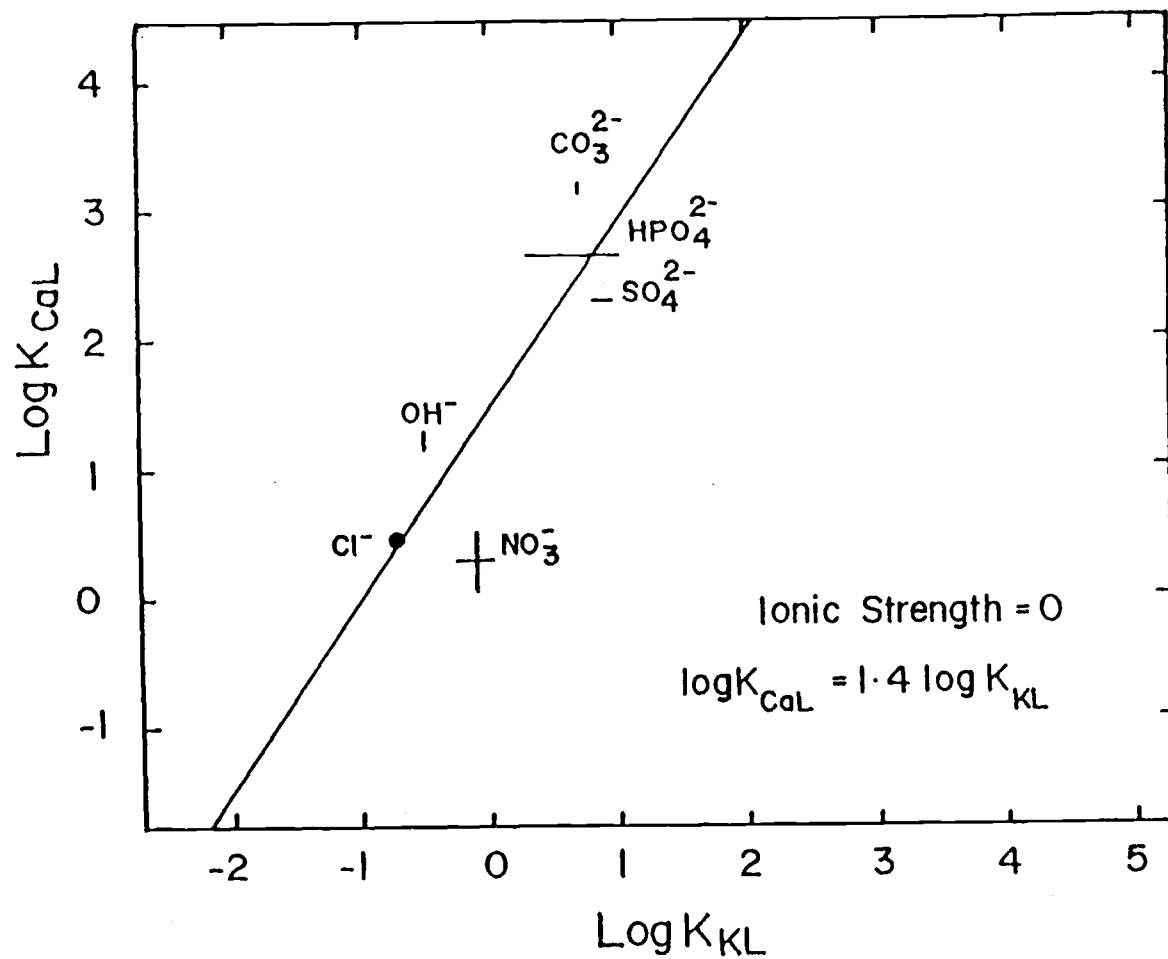


Fig. 2.16 Correlation of $\log K_{CaL}$ with $\log K_{KL}$ at zero ionic strength, 25°C and 1 atmosphere.

stability constants of the four major metal complexes so I did not use it to estimate any undetermined stability constants. The corresponding equation is given in Table 2.1.

6. Stoichiometric Constant Relationship Among MCl , MOH , MF , $MHCO_3$, MNO_3 , MCO_3 and MSO_4 Aqueous Complexes and Ion Pairs at 25°C and 1 Atmosphere.

In order to consider the practical stability constants for the above mentioned complexes and ion pairs in the marine environment, I will continue to evaluate the linear free energy relationships among these chemical species at 0.7 ionic strength. In fact, seawater contains not only the electrolytes, which will affect the ionic strength, but also organic matter. Consideration of the stability constants at 0.7 ionic strength, however, makes the complicated system simple and easy to tackle. As we mentioned in previous sections, published data on stoichiometric stability constants are not as available as those on thermodynamic ones. Evaluation of the linear free energy relationships among stoichiometric constants for the corresponding complexes and ion pairs, therefore, is not as easy as for the thermodynamic stability constants. But it is also very important to ascertain the occurrence of linear free energy relationship for stoichiometric constants at 0.7 ionic strength and to estimate some undetermined constants.

In Fig. 2.18, the correlation of $\log K_{MCl}^*$ with $\log K_{MOH}^*$ is demonstrated, which includes only 6 pairs of chloride and hydroxide stoichiometric constants. Here the asterisk denotes the stoichiometric constants at 0.7 ionic strength. Seven chloride and 7 hydroxide complexes and ion pairs are evaluated. The point

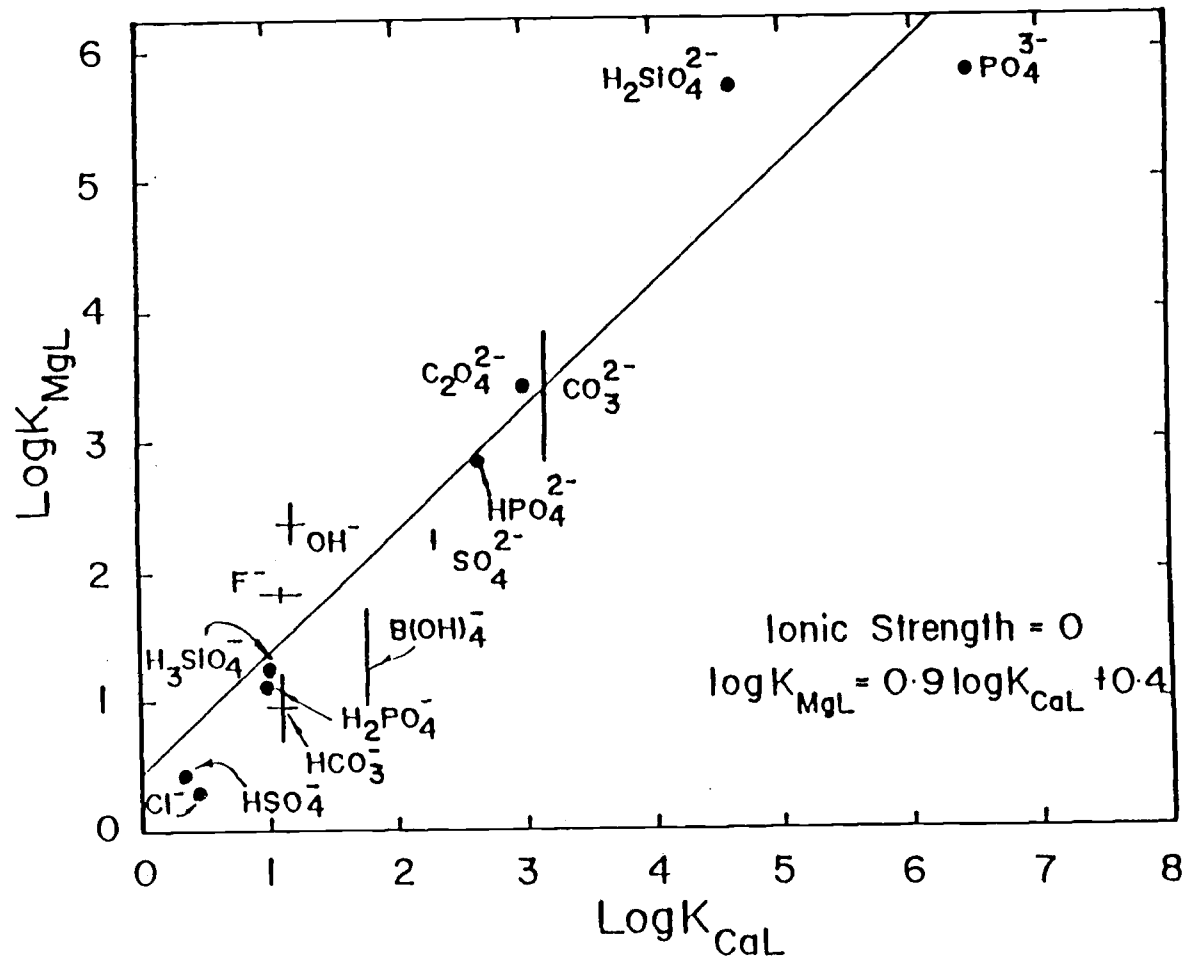


Fig. 2.17 Correlation of $\log K_{MgL}$ with $\log K_{CaL}$ at zero ionic strength, 25°C and 1 atmosphere.

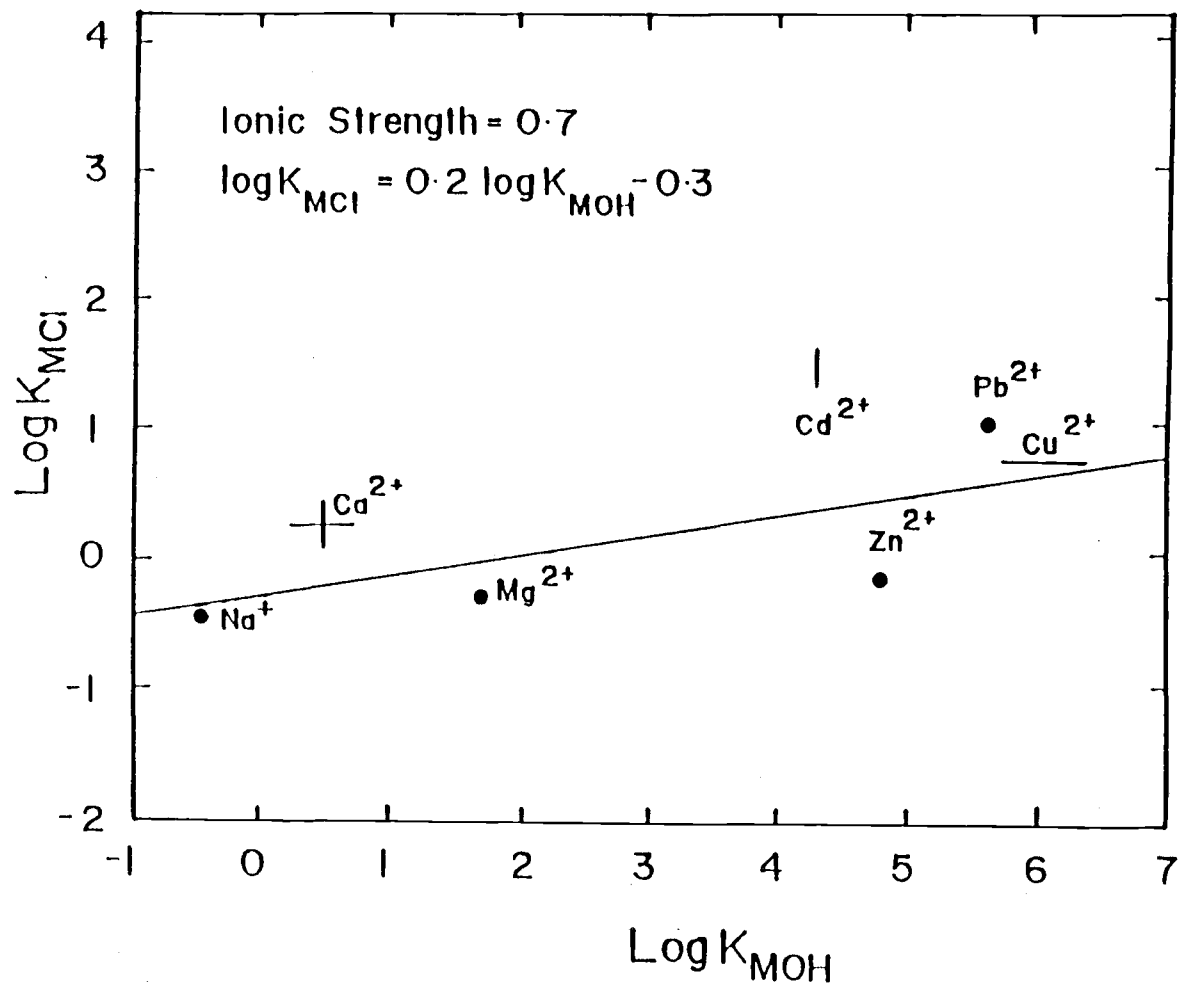


Fig. 2.18 Correlation of $\log K_{MCl}$ with $\log K_{MOH}$ at 0.7 ionic strength, 25°C and 1 atmosphere.

representing CdCl^+ and CdOH^+ constants apparently deviates from the regression line. There seems to be no separate LFER in this case. This deviation of CdCl^+ and CdHCO_3^+ constants also happens in Fig. 2.19 where the correlation between $\log K_{\text{MCl}}^*$ and $\log K_{\text{MHCO}_3}^*$ covering also 6 pairs of chloride and bicarbonate constants is shown. It appears that the value of $\log K_{\text{CdCl}^+}^*$ should be adjusted because in both cases the value is 1.0-1.3 greater than expected. The adjusted value for $\log K_{\text{CdCl}^+}^*$ is 0.4 ± 0.3 in Fig. 2.18 on the basis of $\log K_{\text{CdOH}^+}^*$ value of 4.3 and the value for $\log K_{\text{CdCl}^+}^*$ is 0.0 ± 0.3 on the basis of $\log K_{\text{CdHCO}_3^+}^*$ value of 0.75 which is the average of 0.25-1.2 in literature. Fig. 2.20 shows the correlation between $\log K_{\text{MCl}}^*$ and $\log K_{\text{MCO}_3}^*$ and covers 7 chloride and 7 carbonate stability constants. On the basis of LFER in Fig. 2.20, $\log K_{\text{CdCl}^+}^*$ should be adjusted to 0.3 ± 0.3 from the $\log K_{\text{CdCO}_3}^*$ value of 3.4 which is the average of 3.2-3.5 in literature. So the range of $\log K_{\text{CdCl}^+}^*$ should be, according to LFERs in three figures, -0.3 to 0.7, as listed in Table 2.2. The corresponding regression equations for Figs. 2.18, 2.19 and 2.20 are shown in Table 2.1 with their respective standard deviations.

Fig. 2.21 represents the correlation of $\log K_{\text{MHCO}_3}^*$ with $\log K_{\text{MF}}^*$ at 25°C and 1 atmosphere. Even though only 7 bicarbonate and 7 fluoride constants are evaluated because of the lack of available data, a separate LFER is still obvious. Similar to LFERs in Figs. 2.2, 2.6 and 2.7, the separate linear relationships occur when fluoride stability constants are considered and the separation is dependent on the type classification of metal ions. The evidence for this separate LFER is not as strong as that mentioned in the

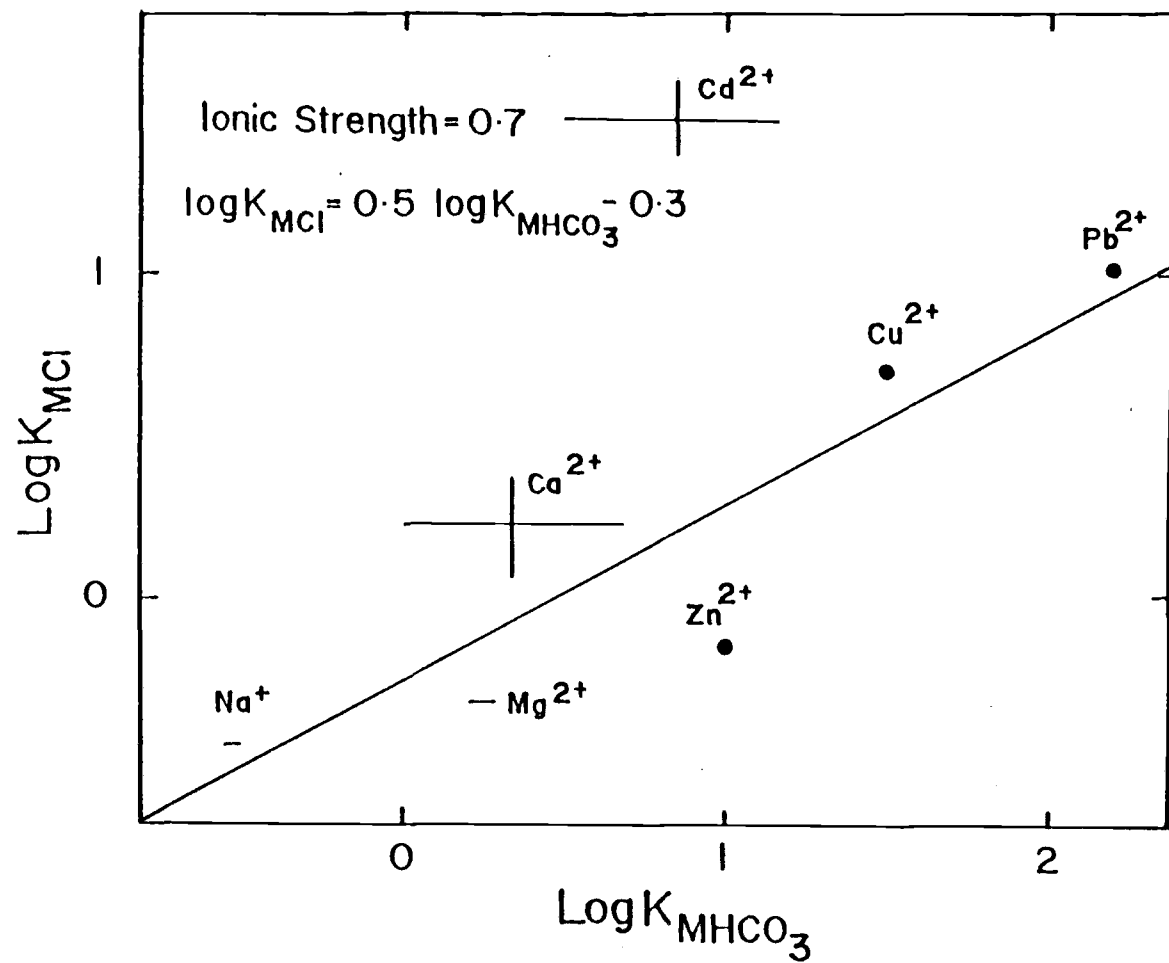


Fig. 2.19 Correlation of $\log K_{MCl}$ with $\log K_{MHCO_3}$ at 0.7 ionic strength,
 25°C and 1 atmosphere.

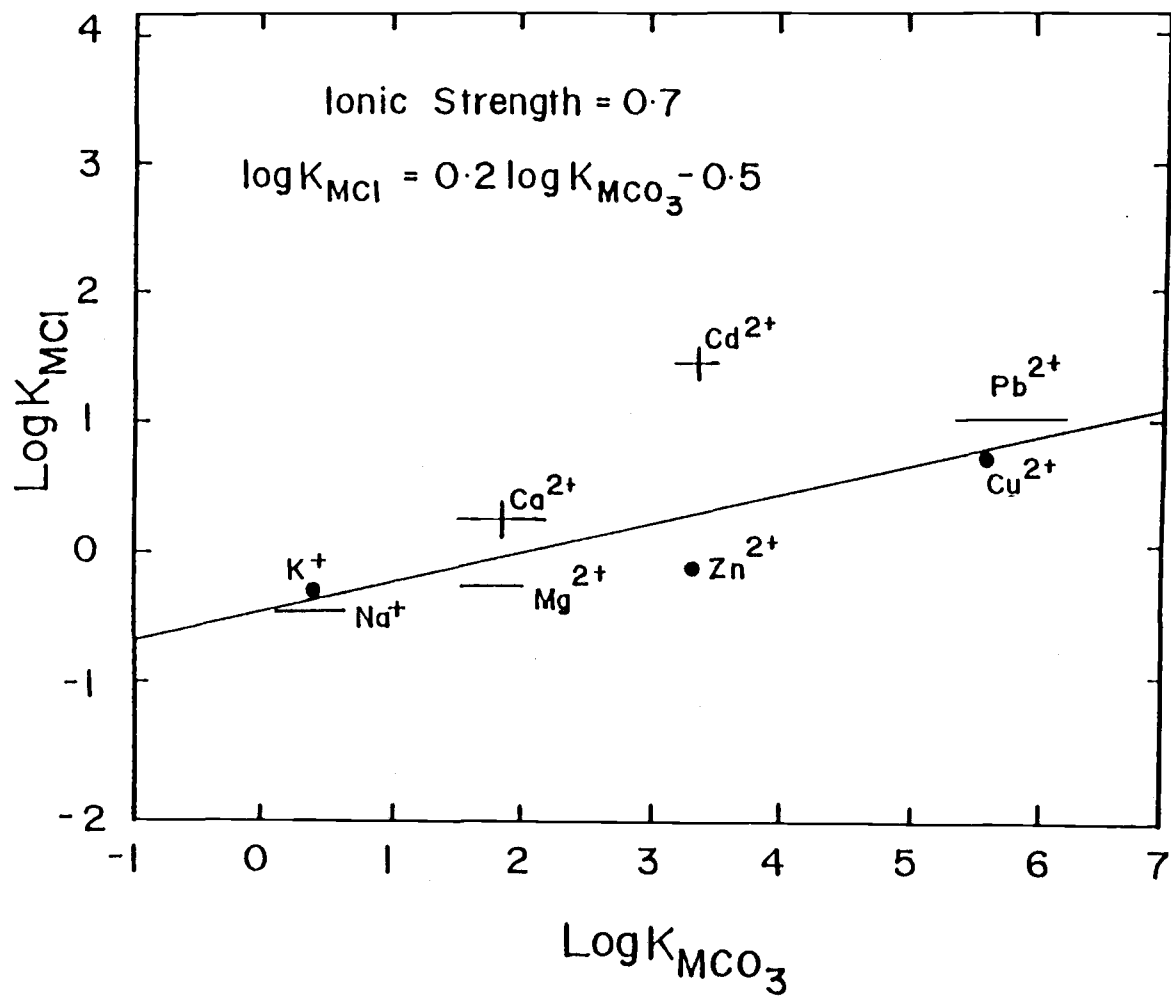


Fig. 2.20 Correlation of $\log K_{MCl}$ with $\log K_{MCO_3}$ at 0.7 ionic strength, 25°C and 1 atmosphere.

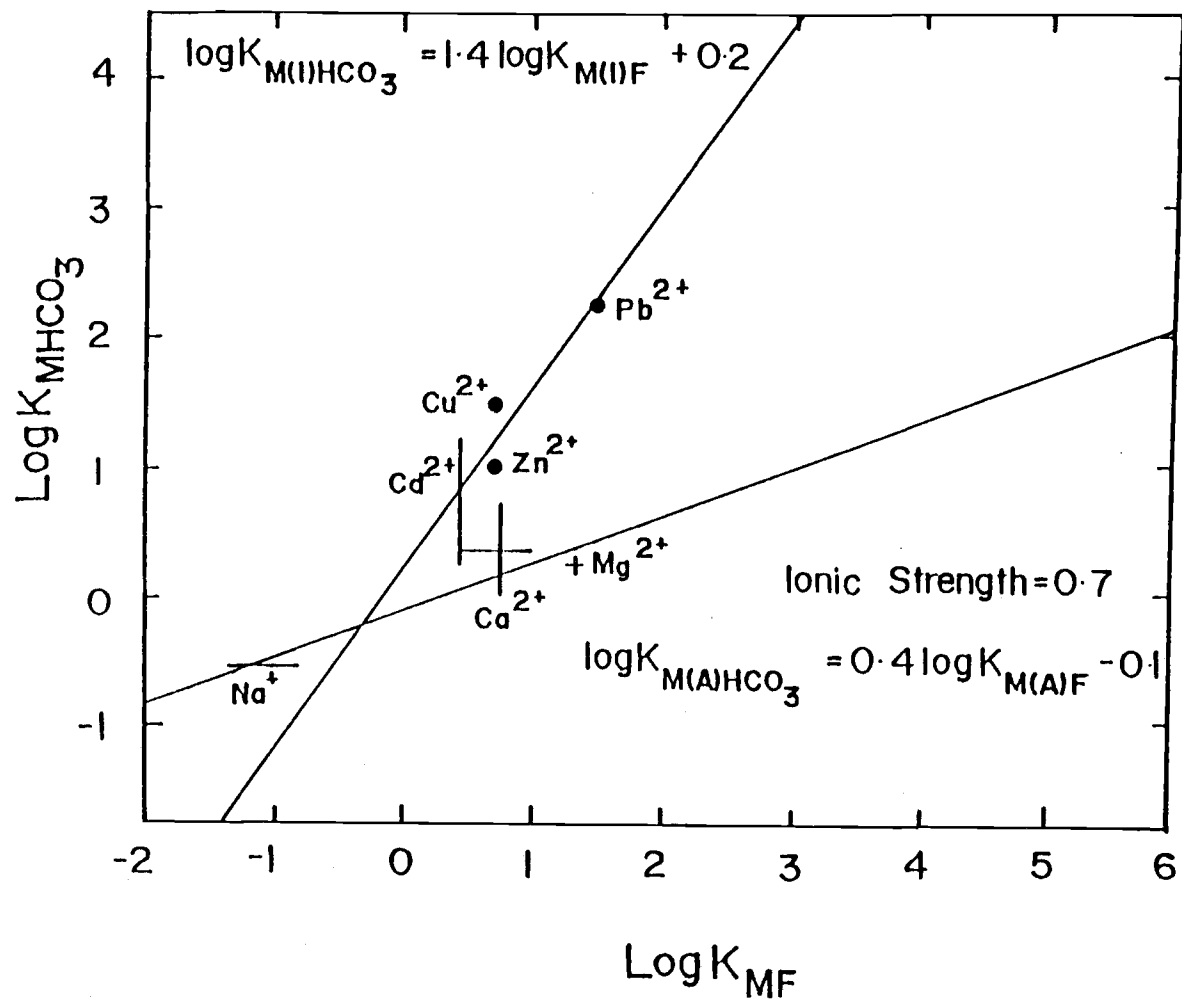


Fig. 2.21 Correlation of $\log K_{MHCO_3}$ with $\log K_{MF}$ at 0.7 ionic strength, 25°C and 1 atmosphere.

discussion of thermodynamic LFER in Section 4 because the data are lacking. The relative stability of type-A metal fluoride complexes and ion pairs is higher than that of intermediate-type metal ions.

Fig. 2.22 gives the correlation between $\log K_{\text{MHCO}_3}^*$ and $\log K_{\text{MOH}}^*$ and covers 7 pairs of bicarbonate and hydroxide constants. The regression equation is expressed in Table 2.1. No separate LFER is observed in this case.

Like Fig. 2.9, Fig. 2.23 shows a good linear relation between $\log K_{\text{MHCO}_3}^*$ and $\log K_{\text{MCO}_3}^*$. The regression equation is shown in Table 2.1 with its standard deviation. It covers 7 pairs of bicarbonate and carbonate constants.

The correlation between $\log K_{\text{MHCO}_3}^*$ and $\log K_{\text{MSO}_4}^*$ is demonstrated in Fig. 2.24 and it covers only 6 pairs of bicarbonate and sulfate constants. An apparent deviation of the point representing CdHCO_3^+ and CdSO_4° constants is observed. This point is excluded in the regression; the LFER is given and its corresponding equation is given in Table 2.1. It appears that either $\log K_{\text{CdHCO}_3^+}^*$ or $\log K_{\text{CdSO}_4^\circ}^*$ is in error, even though the points are scattered and the coefficient of determination is small. So assume the determination of $\log K_{\text{CdSO}_4^\circ}^*$ is in error since we did not find out the anomaly of $\log K_{\text{CdCO}_3^\circ}^*$ in Figs. 2.20 and 2.23. $K_{\text{CdSO}_4^\circ}^*$ should be adjusted according to the analysis of Fig. 2.24. The estimated value of $\log K_{\text{CdSO}_4^\circ}^*$ from Fig. 2.24 is 0.9 ± 0.9 .

Fig. 2.25 shows the separate correlations of $\log K_{\text{MCO}_3}^*$ with $\log K_{\text{MF}}^*$ including 7 pairs of carbonate and fluoride constants. Again, because fluoride is involved the occurrence of the separate LFERs is based upon the metal ion classification.

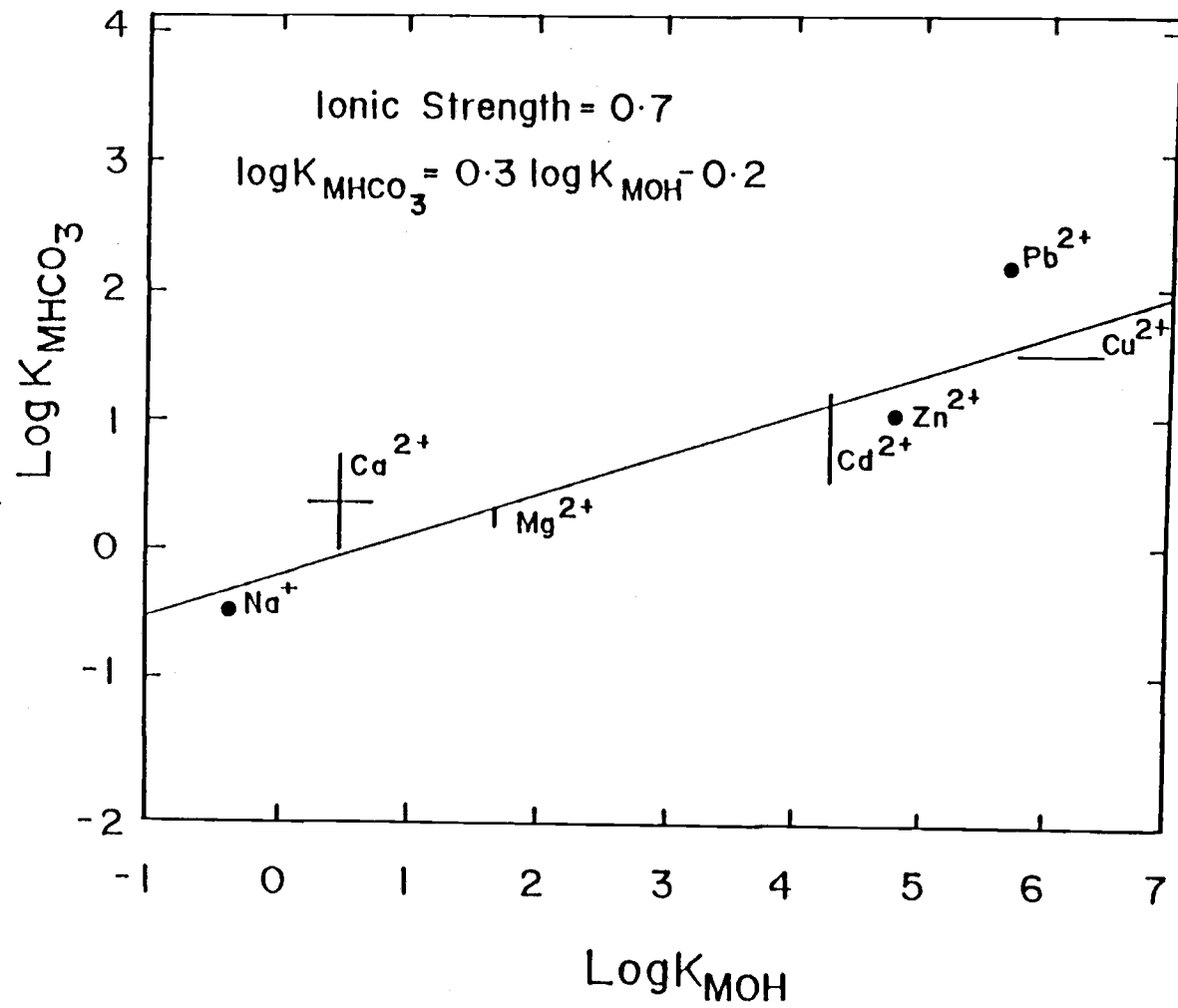


Fig. 2.22 Correlation of $\log K_{\text{MHCO}_3}$ with $\log K_{\text{MOH}}$ at 0.7 ionic strength, 25°C and 1 atmosphere.

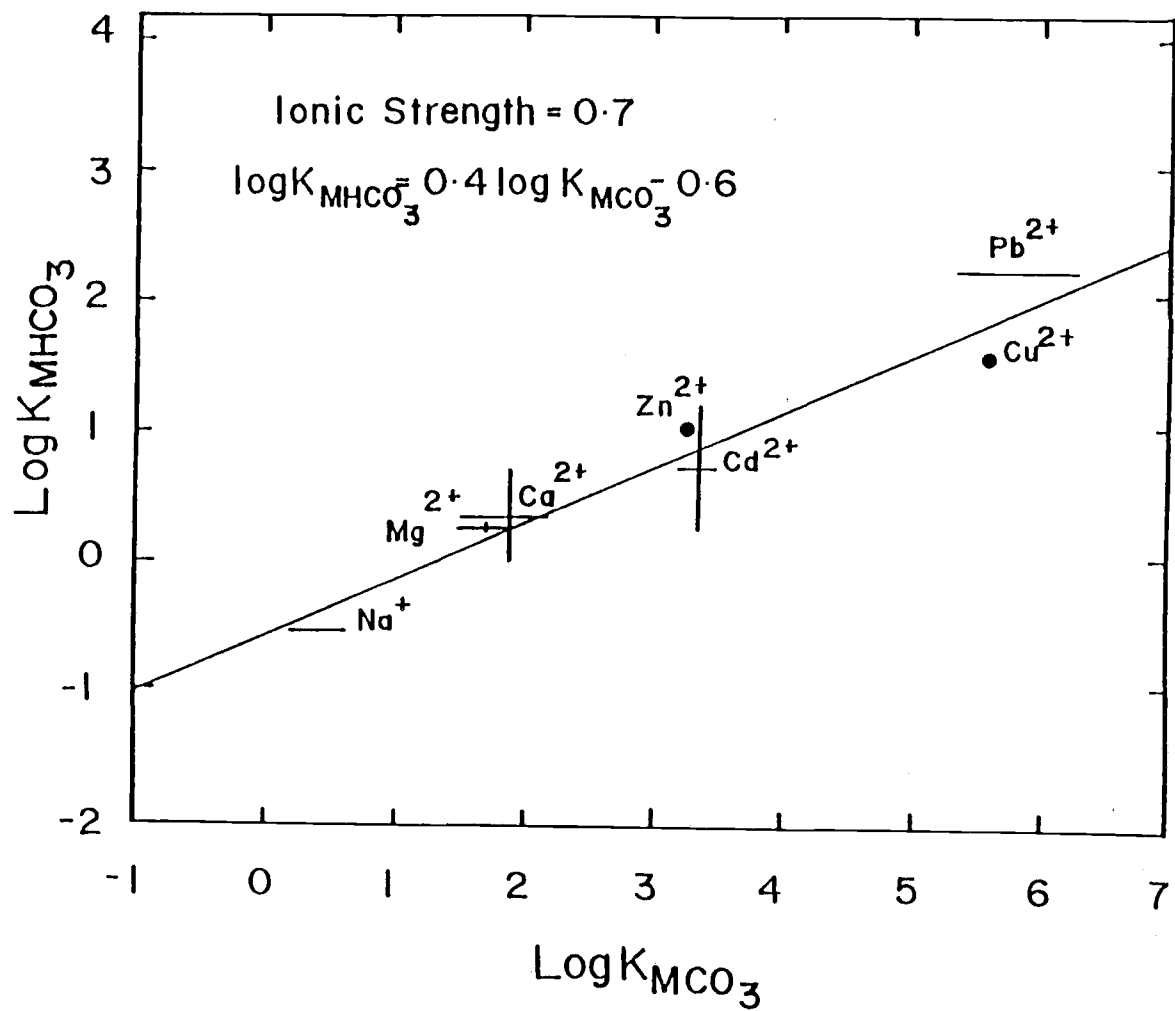


Fig. 2.23 Correlation of $\log K_{\text{MHCO}_3}$ with $\log K_{\text{MCO}_3}$ at 0.7 ionic strength, 25°C and 1 atmosphere.

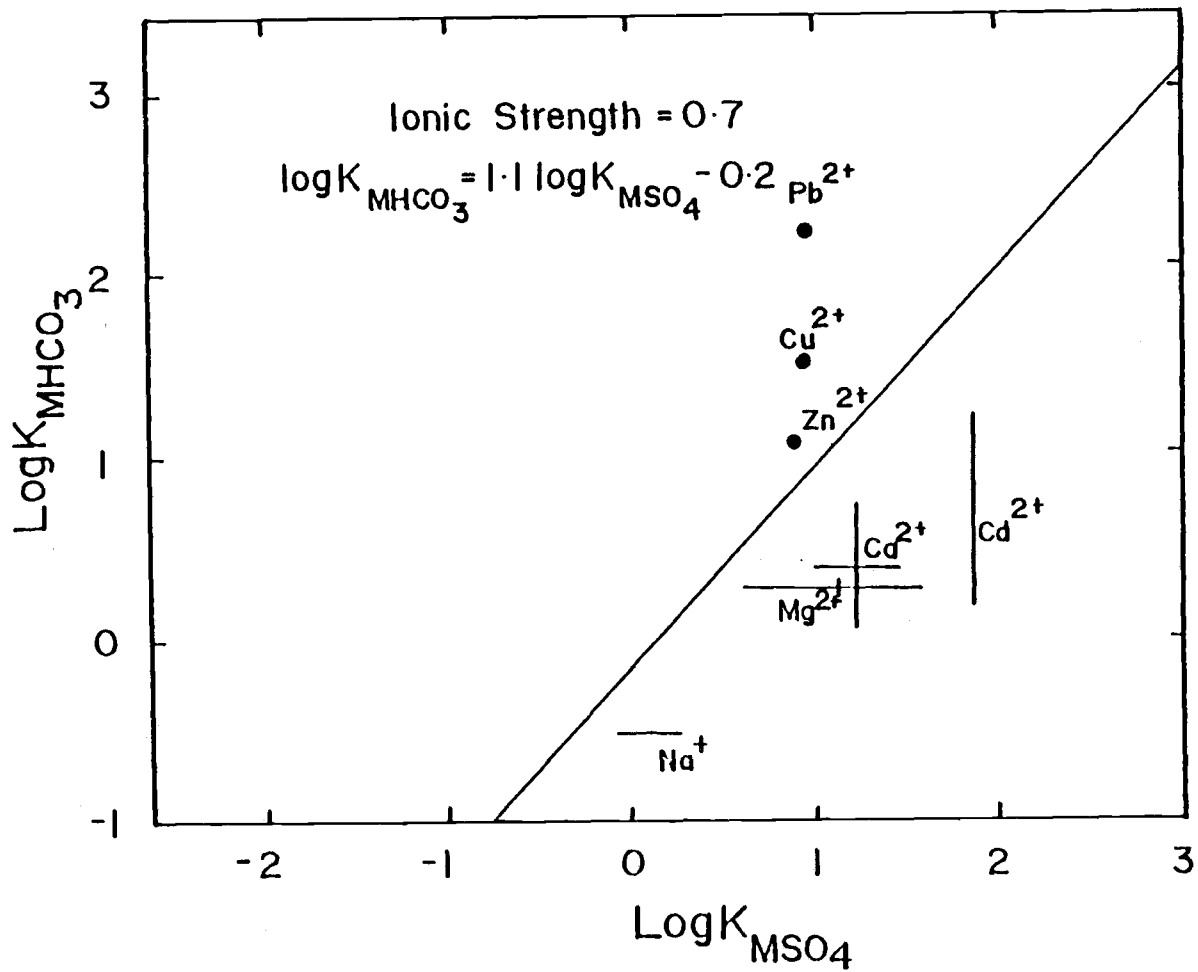


Fig. 2.24 Correlation of $\log K_{\text{MHCO}_3}$ with $\log K_{\text{MSO}_4}$ at 0.7 ionic strength, 25°C and 1 atmosphere.

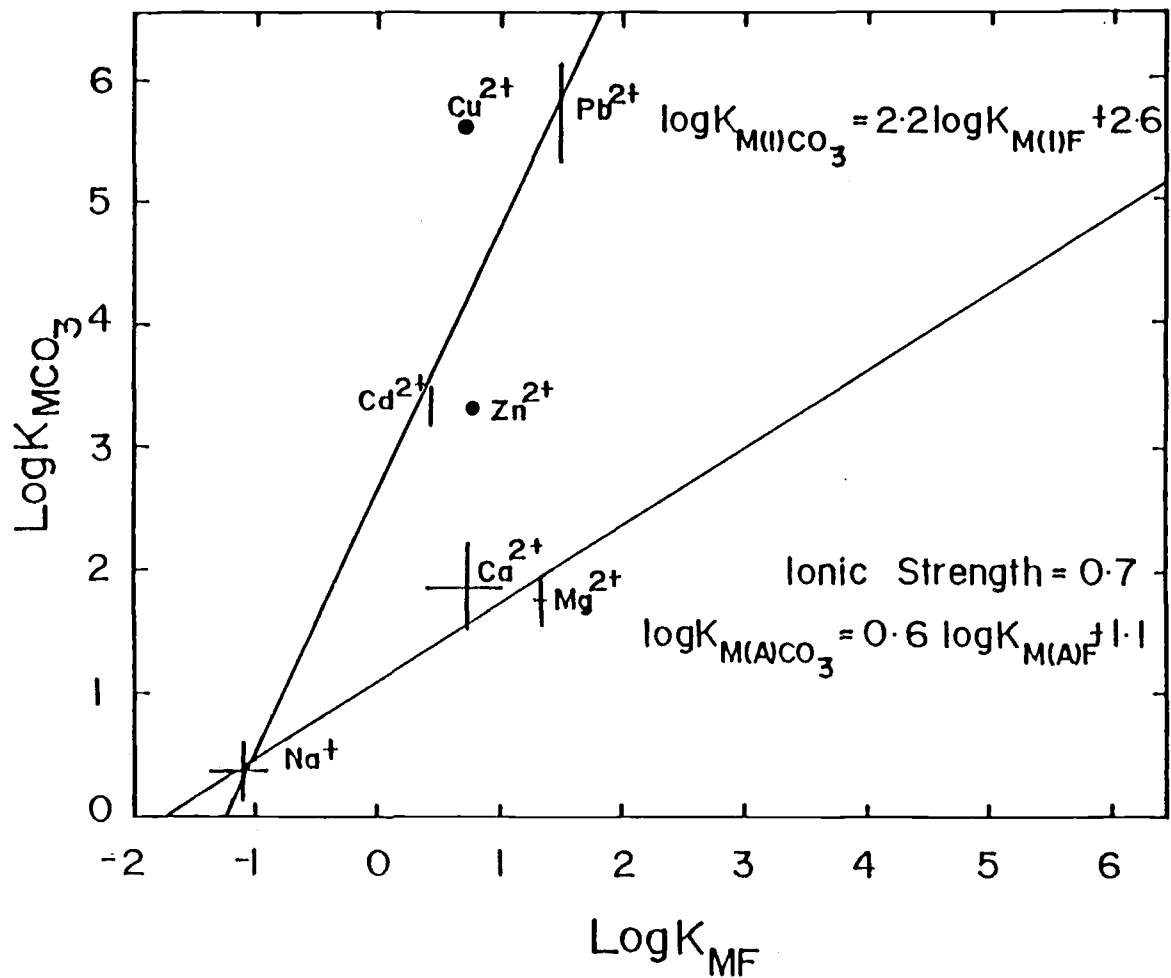


Fig. 2.25 Correlation of $\log K_{MCO_3}$ with $\log K_{MF}$ at 0.7 ionic strength, 25°C and 1 atmosphere.

Fig. 2.26 gives the correlation of $\log K_{\text{MCO}_3}^*$ with $\log K_{\text{MOH}}^*$ and it covers 7 pairs of carbonate and hydroxide constants together. Like Fig. 2.23, this correlation will be very useful for determination of stability constants of carbonate and bicarbonate complexes and ion pairs in the next section.

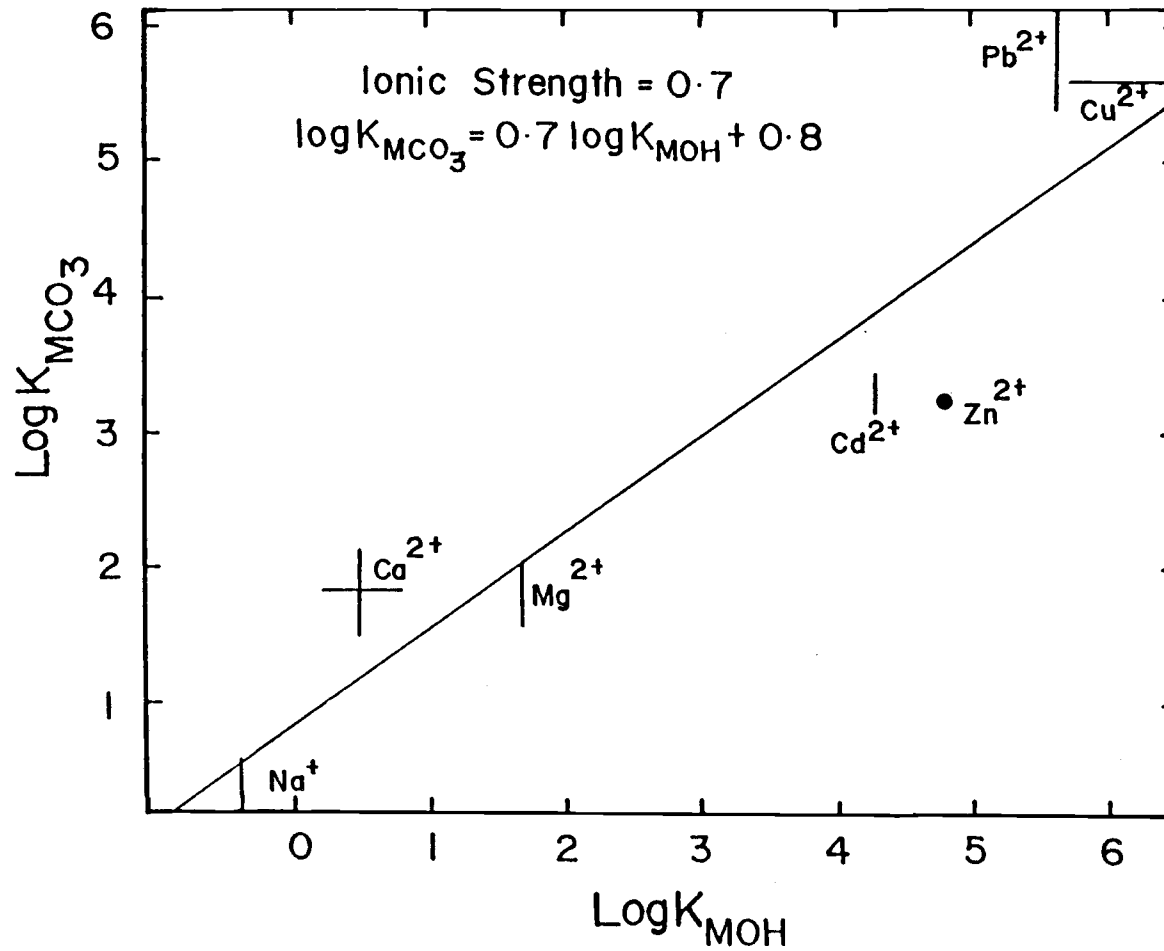


Fig. 2.26 Correlation of $\log K_{MCO_3}$ with $\log K_{MOH}$ at 0.7 ionic strength, 25°C and 1 atmosphere.

Application of LFER to Carbonate and Bicarbonate Stability Constants
in the Marine System

Analysis of the stability constants data has suggested that the thermodynamic and stoichiometric stability constants among ion pairs and metal complexes in seawater are related by linear correlations at 25°C and 1 atmosphere.

Prediction for some undetermined stability constants of ion pairs and complexes can be made by means of the linear free energy relationship. For the study of chemical speciation of seawater, one should have knowledge of the formation of ion pairs and complexes. Particular attention must be paid to the importance of the formation of metal complexation with the ligands as CO_3^{2-} and HCO_3^- because these two anions could play a major role in trace metal complexation in CO_2 -rich thermomineral waters.

As is known, the determination of the stability constants for carbonate and bicarbonate complexes and ion pairs is extremely difficult because of measurement problems. For this reason, much effort has been exerted to estimate the value of these undetermined constants (Hancock and Marcicano, 1978; Langmuir, 1979; Turner *et al.*, 1981; Fouillac and Criand, 1984; Sverjonsky, 1985). In the last section, I have appraised some reported data for stability constants at 25°C and 1 atmosphere as well as estimated some undetermined data (see Table 2.2). In this section, I will focus on the estimation of stability constants of carbonate and bicarbonate complexes and ion pairs in seawater by making use of LFERs discussed in the last section.

1. Prediction of Thermodynamic Stability Constants for Carbonate and Bicarbonate Complexes and Ion Pairs

Besides discussion on stability constants of some species such as CdCl^+ , PbCl^+ , AgNO_3° , KB(OH)_4° , KF° , KHSO_4° , $\text{NaH}_3\text{SiO}_4^\circ$, $\text{NaH}_2\text{SiO}_4^-$, CdSO_4° , I will pay more attention to the carbonate and bicarbonate complexes and ion pairs.

In Fig. 2.3, the correlation of $\log K_{\text{MCl}}$ with $\log K_{\text{MHCO}_3}$, the value of $\log K_{\text{CrHCO}_3}^{2+}$ can be predicted as 2.3 ± 0.8 if the value of $\log K_{\text{CrCl}}^{2+}$ is 0.62 as reported in the literature (see Appendix 1).

In Fig. 2.4, in which the correlation of $\log K_{\text{MCO}_3}$ with $\log K_{\text{MCl}}$ is illustrated, the value of $\log K_{\text{LiCO}_3}^-$ can be estimated by LFER as -0.8 ± 1.6 .

By using LFER in Fig. 2.7, the value of $\log K_{\text{CrCO}_3}^{2+}$ can be estimated to be on the basis of $\log K_{\text{CrF}}^{2+}$ value of 5.1 from Appendix 2.

From the obtained LFER in Fig. 2.8, in which the correlation of $\log K_{\text{MHCO}_3}$ with $\log K_{\text{MOH}}$ at 25°C and 1 atmosphere is illustrated, I can estimate $\log K_{\text{KHCO}_3}^\circ$ to be 0.6 ± 0.5 on the basis of $\log K_{\text{KOH}}^\circ$ being -0.5 (see Appendix 3). In addition, the correlation of $\log K_{\text{MHCO}_3}$ with $\log K_{\text{MCO}_3}$ in Fig. 2.9 can provide the estimated value of $\log K_{\text{KHCO}_3}^\circ$ on the basis of the reported value of $\log K_{\text{KCO}_3}^-$ being 0.7. Therefore, the value of $\log K_{\text{KHCO}_3}^\circ$ from Fig. 2.9 is predicted as 0.0 ± 0.2 , which agrees fairly well with the result from Fig. 2.8 and falls in the range that I have suggested in discussion of Figs. 2.13 and 2.16 in last section. The recommended value for $\log K_{\text{KHCO}_3}^\circ$ in this work is -0.8 to 1.0 as listed in Table 2.3. In the meantime, from LFER in Fig. 2.8 in which $\log K_{\text{MHCO}_3}$ is correlated with $\log K_{\text{MOH}}$,

the value of $\log K_{\text{CrHCO}_3^{2+}}$ can be assumed to be 2.9 ± 0.5 and value of $\log K_{\text{BeHCO}_3^+}$ to be 2.6 ± 0.5 . After the consideration of different approaches on the basis of two LFERs in Figs. 2.3 and 2.8, we estimate the range for the possible value of $\log K_{\text{CrHCO}_3^{2+}}$ at 25°C, 1 atmosphere and zero ionic strength to be 1.51-3.38, as listed in Table 2.3. In accordance with our adjusted value of $\log K_{\text{BeCO}_3^\circ}$ of 7.8 to 9.1 listed in Table 2.3, the value of $\log K_{\text{BeHCO}_3^+}$ can be estimated as 3.2 ± 0.2 on the basis of LFER in Fig. 2.9. Therefore, by considering the results from Figs. 2.8 and 2.9, it is reasonable to assume that the possible range for $\log K_{\text{BeHCO}_3^+}$ at 25°C, 1 atmosphere and zero ionic strength is between 2.1 and 3.5, as shown in Table 2.3.

The estimated value of $\log K_{\text{LiCO}_3^-}$ from LFER in Fig. 2.11, the correlation between $\log K_{\text{MSO}_4}$ and $\log K_{\text{MCO}_3}$, is 0.02 ± 1.40 . In consideration of these large variations in LFERs in both Figs. 2.4 in value of -0.8 ± 1.6 and 2.11 in value of 0.0 ± 1.4 , no estimate of undetermined stability constants of LiCO_3^+ can be made by using either of these values.

The value of $\log K_{\text{CrCO}_3^+}$ can be predicted by LFER in Fig. 2.12. If the value for $\log K_{\text{CrOH}^{2+}}$ is reported as 10.0, averaged from the literature data (see Table 2.6 in Appendices), the value of $\log K_{\text{CrCO}_3^+}$ will be 9.5 ± 0.6 . The estimate of 9.6 ± 0.7 from Fig. 2.7 strongly supports this value. So, we recommend that the range for $\log K_{\text{CrCO}_3^+}$ at 25°C, 1 atmosphere and zero ionic strength should be between 8.9 and 10.3, as shown in Table 2.3. We also can make the prediction of $\log K_{\text{LiCO}_3^-}$ in Fig. 2.12, the correlation between $\log K_{\text{MCO}_3}$ and $\log K_{\text{MOH}}$. If the value of -0.36 is used for $\log K_{\text{LiOH}^\circ}$ as reported in the literature (see Appendix 3), the value of $\log K_{\text{LiCO}_3^-}$ should be between 0.9 and 2.1, as listed in Table 2.3.

On the basis of LFERs in Figs. 2.3, 2.7, 2.8, 2.9, 2.12 and 2.16 used for the prediction of stability constants of carbonates and bicarbonate, therefore, several undetermined thermodynamic stability constants of carbonate and bicarbonate species such as CrHCO_3^{2+} , FeHCO_3^{2+} , BeCO_3° , CrCO_3^+ , KHCO_3° , BeHCO_3^+ , and LiCO_3^- have been predicted. We believe that the results represent a reasonable range.

2. Prediction of Stoichiometric Stability Constants for Carbonate and Bicarbonate Complexes and Ion Pairs

As we discussed previously in this work, researchers studying the speciation of metal ions in seawater prefer the more practical quantities of the stoichiometric constants at seawater ionic strength. However, the lack of these constants limits the development of this study. In order to overcome this difficulty in experimental work, I attempt here to predict theoretically some of the missing stoichiometric stability constants of carbonate and bicarbonate species at 0.7 ionic strength (generally considered as close to that of seawater).

The correlation between $\log K_{\text{MHCO}_3}^*$ and $\log K_{\text{MF}}^*$ (here the asterisk indicates 0.7 ionic strength) in Fig. 2.21 can supply us with two estimations of $\log K_{\text{BaHCO}_3}^+$ value and of $\log K_{\text{SrHCO}_3}^+$. From the LFER for A-type metal ions, the value of $\log K_{\text{BaHCO}_3}^+$ is assumed to be -0.2 ± 0.2 and the value of $\log K_{\text{SrHCO}_3}^+$ is -0.1 ± 0.2 , which can be strongly supported by the estimations from Fig. 2.22.

By using LFER in Fig. 2.22, in which $\log K_{\text{MHCO}_3}^*$ is correlated with $\log K_{\text{MOH}}^*$, we can estimate the value of $\log K_{\text{BaHCO}_3}^+$. The recommended value will be -0.2 ± 0.4 by estimation from LFER on the

basis of $\log K^*_{\text{BaOH}^+}$ value of 0.01. Similarly in Fig. 2.22, the value of $\log K^*_{\text{SrHCO}_3^+}$ is also estimated as -0.1 ± 0.4 by LFER on the basis of $\log K^*_{\text{SrHCO}_3^+}$ value of 0.25. So the possible range for $\log K^*_{\text{BaHCO}_3^+}$, as we recommended, is between -0.6 and 0.2. The possible range for $\log K^*_{\text{SrHCO}_3^+}$ is accordingly between -0.5 and 0.3. The two recommended values are shown in Table 2.3.

From LFER in Fig. 2.21 alone, in which $\log K^*_{\text{M(I)HCO}_3}$ is correlated with $\log K^*_{\text{M(I)F}}$ in a separate LFER for intermediate type metal ions, we obtain, by estimation, the value of $\log K^*_{\text{FeHCO}_3^{2+}}$ as 1.9 ± 0.3 , the value of $\log K^*_{\text{CrHCO}_3^{2+}}$ as 6.1 ± 0.3 and the value of $\log K^*_{\text{MnHCO}_3^+}$ as 1.3 ± 0.3 . In addition, $\log K^*_{\text{NiHCO}_3^+}$ and $\log K^*_{\text{CoHCO}_3^+}$ are also estimated from this figure to be 1.0 ± 0.3 and 0.9 ± 0.3 respectively. It is worth mentioning that the LFER is based upon only 4 bicarbonates and 4 fluorides and it is not as reliable as LFERs used previously. Similarly, we make the estimation on the basis of LFER in Fig. 2.25, in which $\log K^*_{\text{M(I)CO}_3}$ is correlated with $\log K^*_{\text{M(I)F}}$. The value of $\log K^*_{\text{FeCO}_3^+}$ is predicted to be 5.3 ± 1.2 , that of $\log K^*_{\text{CrCO}_3^+}$ as 11.8 ± 1.2 . For the divalent metal ions, the value of $\log K^*_{\text{NiCO}_3^0}$ is predicted by the same LFER as 3.9 ± 1.2 , $\log K^*_{\text{CoCO}_3^0}$ is predicted as 3.7 ± 1.2 and $\log K^*_{\text{MnCO}_3^0}$ as 4.4 ± 1.2 . All of the estimated values for stoichiometric stability constants of carbonate and bicarbonate complexes and ion pairs at 0.7 ionic strength are shown in Table 2.3 for reference. The estimations obtained from Fig. 2.21 alone for $\log K^*_{\text{FeHCO}_3^{2+}}$, $\log K^*_{\text{CrHCO}_3^{2+}}$, $\log K^*_{\text{MnHCO}_3^+}$, $\log K^*_{\text{NiHCO}_3^+}$, $\log K^*_{\text{CoHCO}_3^+}$ and from Fig. 2.25 alone for $\log K^*_{\text{FeCO}_3^+}$, $\log K^*_{\text{CrCO}_3^+}$, $\log K^*_{\text{NiCO}_3^0}$, $\log K^*_{\text{CoCO}_3^0}$ and $\log K^*_{\text{MnCO}_3^0}$ are based upon only one LFER, lacking the parallel estimation from other LFER as for a certain stability constant. Therefore, those

estimations are more likely in a longer error of determination. In the correlation of $\log K_{MCO_3}^*$ with $\log K_{MF}^*$ in Fig. 2.25, we also estimate the value of $\log K_{SrCO_3}^*$ as 1.2 ± 0.3 if $\log K_{SrF^+}^*$ is 0.1 as reported (see Appendix 2) and the LFER for A-type metal ions is utilized. In addition, this value of $\log K_{SrCO_3}^*$ is also predicted as 1.0 ± 0.8 on the basis of LFER in Fig. 2.26, which supports the estimated value of $\log K_{SrCO_3}^*$ from Fig. 2.25. Therefore, the possible range for $\log K_{SrCO_3}^*$ is between 0.2 and 1.7, as shown in Table 2.3. In the meantime, the value of $\log K_{BrCO_3}^*$ can be predicted as 1.0 ± 0.3 from Fig. 2.25 and as 0.8 ± 0.8 from Fig. 2.26. Thus, the possible range for $\log K_{BaCO_3}^*$ at 25°C and 1 atmosphere as shown in Table 2.3 is 0.1 to 1.6.

The stability constants of species of divalent metal ions, mainly those of the intermediate-type, complexing with common ligands other than carbonate and bicarbonate anions are lacking. Although LFERs are set up on the basis of A-type metal ions, the estimation from LFER in two correlations are extremely difficult. However, since the stoichiometric stability constants for carbonate and bicarbonate are in use, we here estimate some of them by a single correlation. Of course, the estimation of one LFER alone is not very reliable, but this work could be helpful in the determination of the ranges and useful as a reference for future experimental determinations.

3. Organic Matter Complexation

Besides the main inorganic ligands, seawater contains other potential ligands of which the most important is natural organic matter. In seawater and other natural water systems biodegradation of

organic matter can release carboxylic acid with intermediate molecular weight, and may form complexes with intermediate-type metal cations. Sometimes humic and fulvic acids are the important organic components in seawater and act as a chelating ligand binding mainly with phenolate and carboxylate groups (Reuter and Perdue, 1977). The stabilities of complexation of metal ions with humic and fulvic acids have been reported recently (Stevenson, 1976; Hirata, 1981). The correlation of the logarithm of the thermodynamic stability constants for humic and fulvic acid complexes with the corresponding carbonate and hydroxide stability constants have been evaluated by Turner *et al.* (1981), and the obtained LFERs among $\log K_{\text{MHA}}$, $\log K_{\text{MCO}_3}$ and $\log K_{\text{MOH}}$ are very good. It is reasonable to assume therefore, that humic acid complexation is most likely to be significant for those cations which are complexed by carbonate and hydroxide in seawater. We have also correlated in this work $\log K_{\text{MF}}$ and $\log K_{\text{MSO}_4}$ with $\log K_{\text{MHA}}$ acid respectively and fairly good correlations are also observed (Figs. 2.27 and 2.28). It appears that competition occurs between inorganic anions and humic acid in complexation with metal ions. Humic acid complexation with metal ions in seawater play an important role in influencing the stability of metal complexes and ion pairs. The complexation of metal ions with fulvic acid (Saar and Weber, 1979) is also an important factor affecting the stability constants of metal complex and ion pair formation. Unfortunately, we have not evaluated the effect of fulvic acid on the stability of metal complexes in seawater in this work. Apparently, the stability for humic acid complex with metal ions is very high compared with that of sulfates or fluorides; it is especially high for complexes of Pb-humic acid and Cu-humic acid. From our analysis of the effect of organic humic acid

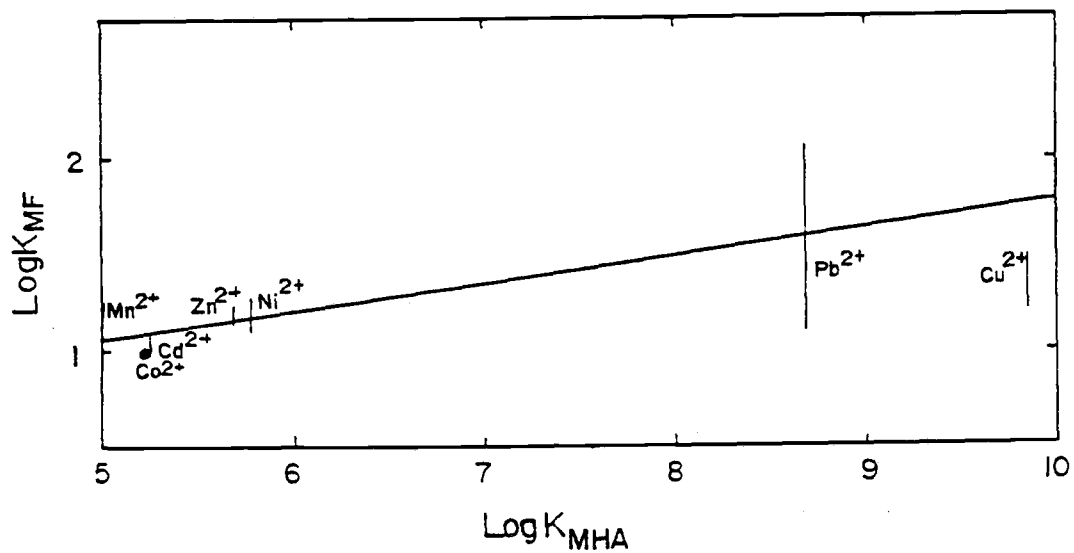


Fig. 2.27 Correlation of $\log K_{MF}$ with $\log K_{MHA}$ at zero ionic strength, 25°C and 1 atmosphere.

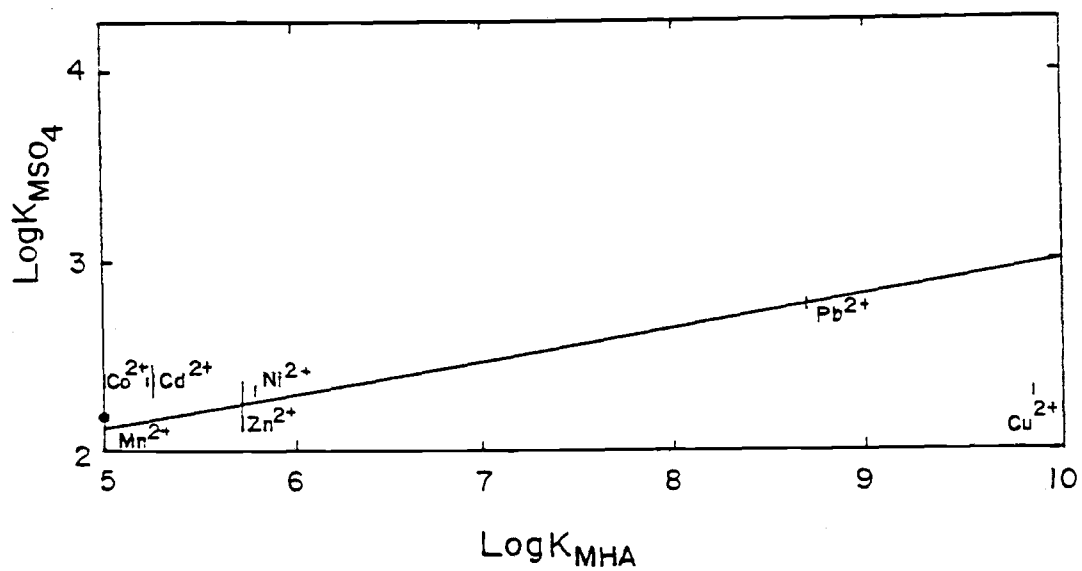


Fig. 2.28 Correlation of $\log K_{MSO_4}$ with $\log K_{MHA}$ at zero ionic strength, 25°C and 1 atmosphere.

on the stability of inorganic complexes we conclude that complexations of Pb^{2+} and Cu^{2+} with the major anions in seawater are affected by the humic acid more than other discussed metal ion complexes in seawater. A quantitative study on the effect of organic matter on the stability of aqueous complexes with inorganic ligands, and on the linear free energy relationship will be carried out in the near future.

Conclusions

The data on stability constants of aqueous complexes and ion pairs provides the basis for linear free energy relationships in seawater at 25°C and 1 atmosphere so that the existence of LFERs among most metal ions and inorganic ligands of geochemical and chemical oceanographic interest has been verified in our work. Among LFERs we discussed, only a few of them do not show the strong linear correlation, for example, the correlation of $\log K_{MCl}$ with $\log K_{MHCO_3}$ in Fig. 2.3 and the correlation of $\log K_{MHCO_3}^*$ with $\log K_{MSO_4}^*$ in Fig. 2.24. The coefficients of determination, R, for other correlations are all larger than 0.7. Although the data for stability constants at 0.7 ionic strength are relatively fewer than those at zero ionic strength, LFERs also show strong correlations. A significant feature is that the separate LFERs happen only when $\log K_{MF}$ or $\log K_{MF}^*$ is correlated with any other logarithms of stability constants. The relative stability of fluoride complexes and ion pairs with A-type metal ions is always higher than that with intermediate-type metal ions. This characteristic of fluoride complexes and ion pairs occurs in both zero ionic strength and 0.7 ionic strength conditions and could be used to exclude the random error of fluoride stability constant determination. The speciation LFER may lead to the conclusion that the bonding between A-type metal ions and fluoride is totally different from that between intermediate-type metal ions and fluoride. Therefore, the complexes and ion pairs between A-type metal ions and fluoride demonstrates the higher relative stability. The electrostatic attraction also contributes somewhat to the complexes and ion pairs so that the metal ions with lower electronic charge show

lower stability when they complex with anions. However, a separate LFER for B-type metal ions has not yet been obtained because of the lack of data at present. The few points representing B-type metal complexes usually deviate far from the regression line for A- and intermediate-type metal ions, which indicates that most likely they belong to a separate group.

The correlations among NaL, KL, CaL and MgL complexes and ion pairs at 25°C and 1 atmosphere do not show any separate LFERs, because these four cations are all hard Lewis' acids and there is no classification difference. With these LFERs, we can predict some undetermined stability constants or improve the reported values of stability constants by using the available constants of other complexes or ion pairs with the same ligands or same cations. The range for the estimated values is usually given, indicating the reliability of the estimation. The emphasis is mostly on the prediction of stability constants of carbonate and bicarbonate complexes and ion pairs. Most of them have been estimated from more than one LFER to increase the reliability of estimation. However, the estimation for stability constants of CoHCO_3^+ , NiHCO_3^+ , MnHCO_3^+ , FeHCO_3^{2+} , CrHCO_3^{2+} , CoCO_3° , NiCO_3° , MnCO_3° , FeCO_3^+ and CrCO_3^+ is just from the correlation of $\log K_{\text{MHCO}_3}^*$ with $\log K_{\text{MF}}^*$ or the correlation of $\log K_{\text{MCO}_3}^*$ with $\log K_{\text{MF}}^*$ at 0.7 ionic strength, because the stability data for Co^{2+} , Ni^{2+} , Mn^{2+} , Fe^{3+} and Cr^{3+} with other anions are lacking. The results by LFER estimation are listed in Tables 2.2 and 2.3 and the source figures from which the estimated values are obtained are also listed.

Besides the values presented in this work, one can also extend the estimation to other stability constants of complexes and ion pairs in the marine environment by making use of LFERs listed in Table 2.1. This procedure could lead to a more complete data file of stability constants for most complexes and ion pairs of geochemical and chemical oceanographic interest. Furthermore, it is significant to the speciation study of metal ions in seawater.

The effect of organic matter, like humic acid, is evaluated with corresponding LFERs between $\log K_{MHA}$ and $\log K_{MF}$ and $\log K_{MSO_4}$ at 25°, 1 atmosphere and zero ionic strength. The two correlations are shown in Fig. 2.27 and 2.28 respectively. The complexation between humic acid and Cu^{2+} and Pb^{2+} is much stronger than with other divalent metal ions such as Ni^{2+} , Zn^{2+} , Co^{2+} and Cd^{2+} . Conversely, the stabilities of CuF^+ , PbF^+ seem no different from other trace metal complexes with the ligand of fluoride, and this situation is in agreement with Lewis' theory, as they all belong to intermediate-type metal ions and divalent ion groups. The reason for the specific high stability of Cu^{2+} and Pb^{2+} complexes with humic acid is not yet understood. In this work, the effects of temperature and pressure on LFERs are not discussed, even though 1 atmosphere pressure and 25°C temperature are not able to stand for most of the marine situation.

The goals achieved in the present work were: (1) The evidence of LFERs in seawater in terms of the logarithms of stability constants at 25°C and 1 atmosphere is provided. The stability constants for complexes and ion pairs of geochemical and chemical oceanographic interest include two forms: thermodynamic stability constants and stoichiometric constants at 0.7 ionic strength. Both of them reflect the occurrence of LFER among the complexes and ion pairs discussed.

(2) The separate LFERs which are dependent on the classification of metal ions according to Lewis' hard and soft acid and base theory are analyzed. The appearance of separate LFER occurs only when $\log K_{MF}$ or $\log K_{MF}^*$ at 0.7 ionic strength are correlated, which reveals the different bonding between metal ions with fluoride and with other major ligands in seawater. (3) Adjusted stability constants with comparing them with reported values in the literature are supplied. (4) Unknown stability constants, mainly those of carbonate and bicarbonate complexes and ion pairs at zero and 0.7 ionic strength is given. In this case, different LFER are usually employed to make these estimations. (5) The effect of humic acid on the complexation between inorganic cations and anions is examined. In the correlations of $\log K_{MF}$ and $\log K_{MSO_4}$ with $\log K_{MHA}$, the complexes of Cu^{2+} and Pb^{2+} with humic acid show much stronger stability than the rest of divalent metal ions.

References

- Ahrland, S. (1973). The thermodynamics of stepwise formation of metal ion complex in aqueous solution. Structure and Bonding 15, 167-188.
- Ahrland, S., J. Chatt and N.R. Davies (1958). The relative affinities of ligand atoms for acceptor molecules and ions. Quarterly Review 12, 265-276.
- Atkinson, G., M.O. Dayhoff and D.W. Ebdon (1975). Computer modeling of ionic equilibria in seawater, in Marine Electrochemistry, Berkowitz, J.B. et al., eds., Electrochemical Society, Princeton, NJ, 124-138.
- Ball, J.W., D.K. Nordstrom and E.A. Jenne (1981). Additional and revised thermodynamic data and computer code for WATEQ2-A Computerized chemical model for trace and major element speciation and mineral equilibria of natural waters. U.S. Geological Survey, Water Resources Investigations WRI-78-116, pp. 109.
- Baes, C.F. and R.E. Mesmer (1976). The hydrolysis of cations. A critical review of hydrolytic species and their stability constants in aqueous solution, John Wiley & Sons, Inc., NY, pp. 489.
- Bassett, R.L. (1980). A critical evaluation of the thermodynamic data from boron ions, ion pairs, complexes, and polyamious in aqueous solution at 298.15c.c. and 1 bar. Geochimica et Cosmochimica Acta 44, 1151-1160.
- Berner, R.A. (1971). Principles of Chemical Sedimentology, Macgraw-Hill Press, NY, pp. 240.

- Butler, J.N. and R. Houston (1970a). Activity coefficient and ion pairs in the system sodium chloride-sodium bicarbonate-water and sodium chloride-sodium carbonate-water. Journal of Physical Chemistry 74, 2976-2983.
- Butler, J.N. and R. Houston (1970b). Potentiometric studies of multicomponent activity coefficient using the lanthamm fluoride membrane electrode. Analytical Chemistry 43, 1308-1311.
- Byrne, R.H., Jr. and D.R. Kester (1974). Inorganic species of boron in seawater. Journal of Marine Research 32, 119-127.
- Calderoni, G., T. Ferri, B. Giannetti and U. Masi (1985). The behavior of thallium during alteration of the K-alkaline rocks from the Roccamonfina volcano. Chemical Geology 48, 103-113.
- Chang, C.P., L.S. Liu and C.T.A. Chen (1983). Principle of least Σ and chemical model of seawater. Acta Oceanologia Sinica 5, 41-56 (in Chinese).
- Chlebek, R.W. and M.W. Lister (1966). Ion pair effects in the reaction between potassium ferrocyanide and potassium persulfate. Canadian Journal of Chemistry 44, 437-445.
- Clarke, E.C. and D.N. Glew (1966). Evaluation of thermodynamic functions from equilibrium constants. Transactions of the Faraday Society 62, 539-547.
- Constant, M.G.V. (1984). Speciation of boron with Cu^{2+} , Zn^{2+} , Cd^{2+} and Pb^{2+} in 0.7 in KNO_3 and in seawater. Geochimica et Cosmochimica Acta 48, 2613-2617.
- Dickson, A.G. and M. Whitfield (1981). An ion-association model for estimating acidity constants (at 25°C and 1 atm total pressure) in electrolyte mixtures related to seawater (ionic strength < 1 mol/kgH₂O). Marine Chemistry 10, 315-333.

- Divison, W. (1979). Soluble inorganic ferrous complexes in natural waters. Geochimica et Cosmochimica Acta 43, 1693-1696.
- Drago, R.S., C.V. Glenn and E.N. Terence (1971). A four-parameter equation for predicting enthalpies of adduct formation. Journal of the American Chemical Society 93, 6014-6026.
- Dyrssen, D. and M. Wedborg (1975). Equilibrium calculation of speciation of elements in seawater, in The Sea, Goldberg, E.D., ed., Vol. 5, John Wiley & Sons, Inc., NY, p. 181-195.
- Elgquist, B. (1970). Determination of the stability constants of MgF^+ and CaF^+ using a fluoride ion selective electrode. Journal of Inorganic and Nuclear Chemistry 32, 937-944.
- Elgquist, B. and M. Wedborg (1975). Stability of ion pairs from gypsum solubility. Marine Chemistry 3, 215-225.
- Elgquist, B. and M. Wedborg (1979). Stability of the calcium sulfate ion pair at the ionic strength of seawater by potentiometry. Marine Chemistry 7, 273-280.
- Ferri, D., I. Grenthe, S. Hietaner, E. Neber-Neumann and F. Salvatore (1985). Studies on metal carbonate equilibria 2: Zinc (II) carbonate complexes in acid solutions. Acta Chemica Scandinavia A39, 347-353.
- Fisher, F.H., J.M. Gieskes and C.C. Hsu (1982). $MgSO_4$ ion association in seawater. Marine Chemistry 11, 279-283.
- Fouillac and A. Criand (1984). Carbonate and bicarbonate trace metal complexes: Critical reevaluation of stability constants. Geochemical Journal 18, 297-303.
- Grasshoff, K., K. Ehrhardt and K. Kremling (1983). Methods of Seawater Analysis, 2nd ed., Verlag Chemie GmbH, D-6940, Weinheim, pp. 419.

- Hancock, R.D. and F. Marsicano (1978). Parametric correlation of formation constants in aqueous solution. 1. Ligands with small donor atoms. Inorganic Chemistry 17, 560-564.
- Hershey, J.P., M. Fernandez, P.J. Milne and F.J. Millero (1986). The ionization of boric acid in NaCl, Na-Ca-Cl and Na-Mg-Cl solutions at 25°C. Geochimica et Cosmochimica Acta 50, 143-148.
- Hirata, S. (1981). Stability constants for the complexes of transition metal ions with fulvic and humic acid in sediments measured by filtration, Talanta 28, 809-815.
- Johansson, O., I. Persson and M. Wedborg (1980). Calorimetric study of the thermodynamics of formation of $MgSO_4$ and $NaSO_4$ ion pairs at the ionic strength of seawater. Marine Chemistry 8, 191-198.
- Johnson, K.S. (1979). Ion association and activity coefficients in electrolyte solutions, Ph.D. thesis, Oregon State University, Corvallis, OR, pp. 320.
- Johnson, K.S. and R.M. Pytkowicz (1979). Ion association of chloride and sulfate with sodium, potassium, magnesium and calcium in seawater at 25°C. Marine Chemistry 8, 87-93.
- Kester, D.R. and R.M. Pytkowicz (1975). Theoretical model for the formation of ion pairs in seawater. Marine Chemistry 3, 365-374.
- Langmuir, D. (1979). Techniques of estimating thermodynamic properties for some aqueous complexes of geochemical interest, in Chemical Modeling in Aqueous Systems, Jenne, E.A., ed., Am. Chem. Soc. Symp. Ser. 93, 353-387.
- Mantoura, R.F.C., A. Dickson and J.P. Riley (1978). The complexation of metals with humic materials in natural water. Estuarine and Coastal Marine Science 6, 387-406.

- McGee, K.A. and P.B. Hostetler (1975). Studies in the system $\text{MgO-SO}_2\text{-CO}_2\text{-H}_2\text{O}$. 4. The stability of MgOH^+ from 10-90°C. American Journal of Science 275, 304-317.
- Millero, F.J. (1974). The physical chemistry of seawater. Annual Review of Earth and Planetary Sciences 2, 101-150.
- Millero, F.J. and D.R. Schreiber (1982). Use of the ionic pairing model to estimate activity coefficients of the ionic components of natural waters. American Journal of Science 282, 1508-1540.
- Morel, F.M.M. (1983). Principles of Aqueous Chemistry, John Wiley & Sons, Inc., NY, pp. 446.
- Palmer, D.A. and R.V. Eldik (1983). The chemistry of metal carbonate and carbon dioxide complexes. Chemistry Review 83, 651-731.
- Pearson, R.G. (1967). Hard and soft acids and bases. Chemistry in Britain 3, 103-107.
- Pearson, R.G. (1968). Hard and soft acids and bases, HSAB. Part 1. Journal of Chemical Education 45, 581-587.
- Pytkowicz, R.M. (1969). Use of apparent equilibrium constants in chemical oceanography, geochemistry, and biochemistry. Geochemical Journal 3, 181-184.
- Pytkowicz, R.M. (1979). Activity Coefficient in Electrolyte Solution, Vol. 2, CRC Press, Inc., FL, pp. 330.
- Pytkowicz, R.M. (1983). Equilibria, Nonequilibria, and Natural Waters, Vol. 1, John Wiley & Sons, Inc., NY, pp. 351.
- Pytkowicz, R.M. and J.E. Hawley (1974). Bicarbonate and carbonate ion-pairs and a model of seawater at 25°C. Limnology and Oceanography 19, 223-234.

- Pytkowicz, R.M. and D.R. Kester (1969). Harned's rule behavior of NaCl-Na₂SO₄ solutions explained by an ionic association model. American Journal of Science 267, 217-229.
- Reardon, E.J. (1975). Dissociation constants of some monovalent sulfate ion pairs at 25°C from stoichiometric activity coefficients. Journal of Physical Chemistry 79, 422-425.
- Reardon, E.J. (1976). Dissociation constants for alkali earth and sodium borate ion pairs from 10°-50°C. Chemical Geology 18, 309-325.
- Reardon, E.J. and D. Langmuir (1974). Thermodynamic properties of the ion pairs MgCO₃[°] and CaCO₃[°] from 10° to 50°C. American Journal of Science 274, 599-612.
- Reuter, J.H. and E.M. Perdue (1977). Importance of heavy metal-organic water interactions in natural water. Geochimica et Cosmochimica Acta 41, 325-334.
- Riesen, W., H. Gamsjager and P. Schindler (1977). Complex formation in the ternary system Mg(II)-CO₂-H₂O. Geochimica et Cosmochimica Acta 41, 1193-1200.
- Saar, R.A. and J.H. Weber (1979). Complexation of cadmium (II) with water and solid derived fulvic acid: effect of pH and fulvic acid concentration. Canadian Journal of Chemistry 57, 1263-1268.
- Schwarzenbach, G. (1961). The general selective and specific formation of complex by metallic cations. Advances in Inorganic and Radiochemistry 3, 265-271.
- Siebert, R.M. and P.B. Hostetler (1977). The stability of the magnesium bicarbonate ion pair from 10° to 90°C. American Journal of Science 277, 697-715.

- Sipos, L., B. Raspor, H.W. Hurnberg and R.M. Pytkowicz (1980).
Interaction of metal complexes with coulombic ion pairs in
aqueous media of high salinity. Marine Chemistry 9, 37-47.
- Smith, R.M. and A.E. Martell (1981). Critical Stability Constants,
Vol. 4, Plenum Press, NY, pp. 257.
- Spahiu, K. (1985). Studies on metal carbonate equilibria II. Ythrium
(IV) carbonate complex formation in aqueous perchlorate media of
various ionic strength. Acta Chimica Scandinavia A39, 34-45.
- Stevenson, F.J. (1976). Stability constants of Cu^{2+} , Pb^{2+} and Cd^{2+}
complexes with humic acid. Journal of Soil Science Society of
America 40, 665-672.
- Stumm, W. and J.J. Morgan (1981). Aquatic Chemistry, 2nd ed., John
Wiley & Sons, Inc., NY, pp. 780.
- Sverjensky, D.A. (1985). The distribution of divalent trace elements
between sulfides, oxides, silicates and hydrothermal solutions:
I. Thermodynamic basis. Geochimica et Cosmochimica Acta 49,
853-864.
- Turner, D.R., M. Whitfield and A.G. Dickson (1981). The equilibrium
speciation of dissolved components in fresh water and seawater at
25°C and 1 atm pressure. Geochimica et Cosmochimica Acta 45,
855-881.
- Van Luik, A.E. and J.J. Jurinake (1978). A chemical model of heavy
metals in the Great Salt Lake. Research Report 34, Utah
Agriculture Experiment Station, Utah State Univesity, pp. 155.
- Whitfield, M. (1979). Activity coefficients in natural water, in
Activity Coefficients in Electrolyte Solutions, Vol. 2,
Pytkowicz, R.M., ed., CRC Press, FL, 153-301.

Zirino, A. and S. Yamamoto (1972). A pH-dependent model for the chemical speciation of copper, zinc, cadmium and lead in seawater. Limnology and Oceanography 17, 661-671.

CHAPTER III

ANALYSIS OF THE CSS HUDSON WINTERTIME CARBONATE DATA IN THE NORTHERN
NORTH ATLANTIC OCEAN

Abstract

Excess CO₂ signals have been calculated for the Greenland and Norwegian Seas based on the wintertime carbonate data collected by the CSS HUDSON in 1982. The results suffer the least systematic error as compared with our previous efforts and indicate that the normalized surface alkalinity and total CO₂ correlate linearly with temperature; these two seas have been contaminated by anthropogenic CO₂ from surface to bottom; the Greenland Sea contains more excess CO₂ than the Norwegian Sea; the western basin is more contaminated than the eastern basin; and the excess CO₂ results are corroborated by the AOU and tritium data as linear correlations were found. Overall the Greenland and Norwegian Seas (between 65° and 80°N) contain $0.92 \pm 0.2 \times 10^{15}$ g excess CO₂.

ACKNOWLEDGMENTS

We thank J.H. Swift for providing hydrographic data; E.T. Drake for assistance. Funding was provided by the Department of Energy (19X-89608C under Martin Marietta Energy Systems, Inc., Contract DE-AC05-84 OR 21400).

Introduction

One of the greatest problems facing society today is the possible change of the global climate caused by human activity on the earth. The possibility of a significant global warming may be triggered by the increase in the atmosphere of a number of compounds, such as carbon dioxide (CO_2), methane, chlorofluorocarbons and nitrous oxide, released as a result of industrialization. These gases modify the radiation balance of the earth's surface. The difference between incoming and outgoing radiation causes the warming of the earth to a higher average temperature, known as the greenhouse effect. Among the compounds involved, the dominant one is CO_2 ; its increase in the atmosphere caused by the consumption of fossil fuels and deforestation has been extensively documented in the literature.

In the last 15 or more years, the scientific society and policy makers have promoted a great interest in this problem and much research has been generated to try to solve the problem and evaluate the effect of the increased CO_2 concentration on the global thermal regime and on life on earth. We know reasonably well that 40-60% of CO_2 produced by human activity, sometimes referred to as "excess CO_2 ," is now in the atmosphere, with the rest taken up by the oceans (Chen and Drake 1986; and references therein).

Although the world oceans play a paramount role in taking up excess CO_2 , the removal rate of CO_2 from the atmosphere and the transport mechanism for CO_2 in the oceans need to be clarified and monitored. Most investigations for excess CO_2 in the world ocean come either from surface water observations or studies of transient

tracers, such as tritium and C-14. Direct measurement of CO_2 is desired, however, in order to substantiate results obtained from modeling tracers.

The northern hemisphere sources of the densest of deep waters are the outflows to the North Atlantic from the Greenland and Norwegian Seas (Wust, 1935; Stefansson, 1968; Worthington, 1970, 1976, 1981; Reid and Lynn, 1971; Swift *et al.*, 1980; Swift and Aagaard, 1981; Swift, 1984; Livingston *et al.*, 1985). In this area, known as the formation region of the North Atlantic Deep Water is one of the regions with the highest effective thermocline diffusion coefficient (Hansen *et al.*, 1984). The surface water contains excess CO_2 as a result of air-sea exchange and sinks in winter because of cooling, thereby transmitting excess CO_2 to the deep oceans. Prior to the HUDSON winter cruise to the Norwegian and Greenland Seas, winter data were not available and this lack prevented us from accurately calculating the excess CO_2 in the North Atlantic.

The purpose of this chapter is to demonstrate the penetration of excess CO_2 in wintertime in the Norwegian and Greenland Seas, considered a main region of deep water formation in the world oceans. The carbonate data used in this thesis are based upon HUDSON CSS 82-001 cruise, from 60°N to almost 80°N in the northern North Atlantic, principally in the region between Jan Mayen and Spitsbergen. The cruise obtained the first comprehensive winter carbonate data in northern North Atlantic.

TTO (Transient Tracers of the Ocean) tritium data (Ostlund, 1983) are used in addition to the tritium data collected during the HUDSON cruise in order to study the movement of waters during the years since the bomb testing.

Source of Data

In this work, the chemical data and other standard oceanographic data are from HUDSON 82-001 (SIO reference, #84-14, 1984). The tritium data are also used in this work as a comparison with excess CO_2 results. They are from two sources - HUDSON 82-001 and Transient Tracers of the Ocean [North Atlantic study (TTO/NAS)] (Ostlund, 1983). The station locations are shown in Fig. 3.1, with solid lines indicating cross-sections discussed in the text. HUDSON 82-001 was carried out from February to April of 1982. The cruise covered stations throughout the Greenland Sea, extending northward and westward as far as the ice condition allowed. Two sections in the central Norwegian Sea were covered but no stations were located in the Denmark Strait. Sampling started with station 4 in the Iceland Sea and concluded with station 132. Heavy ice limited further northward and westward coverage.

Carbonate data, total CO_2 (TCO_2 , $\text{mmol}\cdot\text{kg}^{-1}$; $1\sigma = 8.1 \mu\text{mol}\cdot\text{kg}^{-1}$) and titration alkalinity (TA, $\text{meq}\cdot\text{kg}^{-1}$; $1\sigma = 5.6 \mu\text{eq}\cdot\text{kg}^{-1}$) were collected from 49 stations, whereas supporting data such as dissolved oxygen, depth, temperature, salinity, and nutrients were collected more extensively. Tritium data were reported for 15 stations. TTO/NAS carried out in July, 1981, for the Greenland and Norwegian Seas yielded tritium data for only nine stations.

Obvious experimental errors unfortunately exist in the reported TA and TCO_2 values. Some deletions or adjustments of the data were necessary at some stations. Deletion of data points was based on the assumption that TA (or TCO_2) vs depth or potential temperature (θ), TA vs TCO_2 and TCO_2 vs AOU should be smooth functions. In addition

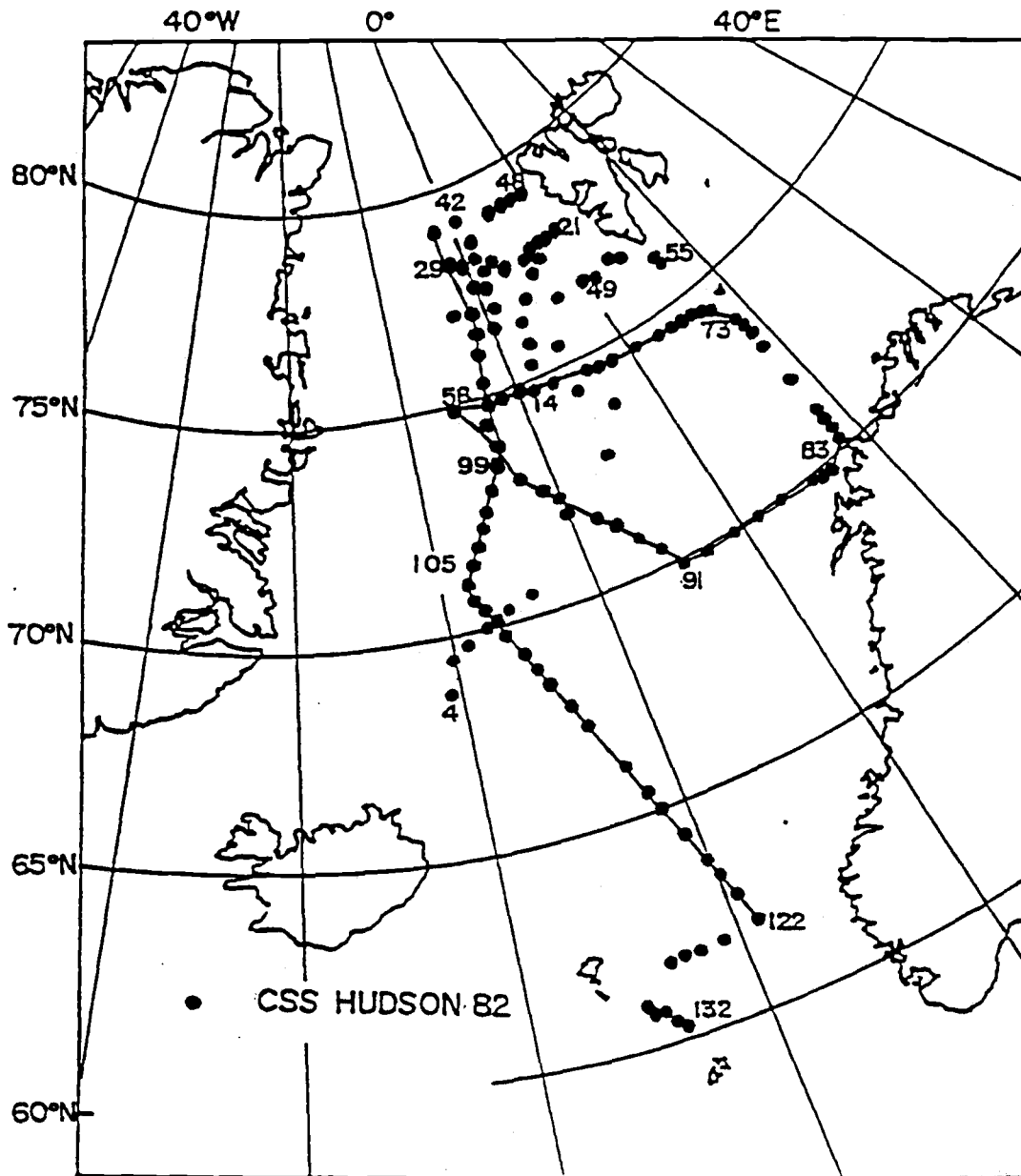


Fig. 3.1 CSS HUDSON 82-001 Cruise station locations and cruise track.

we assumed that deep-water TA or TCO_2 values in different parts of the same basin should have the same values when other physical and chemical parameters (salinity, temperature, oxygen and nutrients) were the same and remained constant. Values adjusted are given in Table 1. Most of these adjustments are smaller than 2σ .

TABLE 3.1. Adjustments to the measured alkalinity
and total CO₂ data.

Stations	NTCO ₂ ($\mu\text{mol}\cdot\text{kg}^{-1}$)	NTA ($\mu\text{eq}\cdot\text{kg}^{-1}$)
10	-15	-
18	-20	-5
20	- 8	-
23	- 5	-
29	Top 7 samples only, +10	-
32	Bottom 6 samples only, -20	-
33	-30	-5
34	-60	-5
41	+ 5	-
43	+10	-
98	+18	+8
100	+18	+8
102	+18	+8
106	+18	+8
110	+18	+8
113	+18	+8
116	+ 8	+8
118	+ 8	+8
120	+ 8	+8
122	+ 8	+8
124	+ 8	+8

Calculating Excess CO₂

The total concentration of CO₂ of a water mass after it leaves the surface is increased by the addition of dissolved CO₂ released from dissolution of inorganic calcium carbonate particles and decomposition of organic carbon. By subtracting these contributions from the measured TCO₂ values we obtain the preformed TCO₂ concentration (TCO₂[°]). The following relationship holds (Chen and Millero, 1979; Chen, 1984):

$$\text{NTCO}_2^\circ \text{ (preformed)} = \text{NTCO}_2 \text{ (measured)} + 0.5 [\text{NTA}^\circ \text{ (preformed)} - \text{NTA (measured)}] - 0.78 \text{ AOU}; \quad (1)$$

where NTCO₂[°] (preformed) denotes the normalized preformed TCO₂ for any seawater sample, NTCO₂ (measured) and NTA (measured) are the normalized measured NTCO₂ and NTA, NTA[°] (preformed) denotes the normalized preformed TA value, and AOU denotes the apparent oxygen utilization. All quantities except AOU in Eq. (1) are normalized to a salinity of 35.0.

The coefficient 0.5 in Eq. (1) is universally accepted but the use of the quantity 0.78 associated with AOU is somewhat uncertain because C/N/P/O ratios vary (Chen and Pytkowicz, 1979). Broecker et al. (1985) reported a "best correct estimate" of 0.72 ± 0.08 but used 0.80 for their calculations. Because the waters under discussion are all highly oxygenated with AOU less than $60 \mu\text{mol}\cdot\text{kg}^{-1}$, the difference in the coefficient gives an uncertainty of $4 \mu\text{mol}\cdot\text{kg}^{-1}$ or less in Eq. (1).

Because of the increase in NTCO_2° in the oceans due to input of excess CO_2 , the present-day NTCO_2° is higher than the NTCO_2° for a water formed some time earlier. As a result, the difference, $\Delta\text{TCO}_2^\circ = \text{NTCO}_2^\circ (\text{old}) - \text{NTCO}_2^\circ (\text{present})$, represents the effect due to excess CO_2 . ΔTCO_2° is closer to zero for a younger water and more negative for older waters.

Obviously NTCO_2° (present) and NTA° (present) are critical in calculating the excess CO_2 signal. Many investigations (Edmond, 1974; Chen and Millero, 1979; Chen and Pytkowicz, 1979; Chen, 1982a,b, 1984) have already revealed that the distribution of NTA° and NTCO_2° in surface waters seem to correlate linearly with temperature, especially in the temperate, subpolar, and polar regions, although temporal and spatial variations of these correlations certainly exist (Chen and Pytkowicz, 1979; Chen *et al.*, 1986). Broecker *et al.* (1985) could not find such correlations in the northern North Atlantic Ocean based on the TTO data (Takahashi and Chipman, 1982). However, the present NTCO_2° and NTA° in the Norwegian and Greenland Seas in winter seem to correlate linearly with temperature (Figs. 3.2 and 3.3) although there may be a slight break in slope for NTCO_2° at approximately -0.5°C . Heavy ice greatly reduces air-sea exchange and biological activity; NTCO_2° , therefore, may not change while temperature is reduced under ice. The best-fit NTCO_2° and NTA° equations are as follows:

$$\text{NTCO}_2^\circ (\mu\text{mol}\cdot\text{kg}^{-1}) = 2173 - 5.2 T, 1\sigma = 6.0 \mu\text{mol}\cdot\text{kg}^{-1} \quad (2)$$

$$\text{NTA}^\circ (\mu\text{eq}\cdot\text{kg}^{-1}) = 2317 - 0.18 T, 1\sigma = 3.7 \mu\text{eq}\cdot\text{kg}^{-1} \quad (3)$$

The standard deviations of the above empirical equations are comparable with the measurement error ($8.1 \mu\text{mol}\cdot\text{kg}^{-1}$ and $5.6 \mu\text{eq}\cdot\text{kg}^{-1}$ for TCO_2 and TA, respectively). The above three equations were combined to calculate ΔTCO_2° . The random error in ΔTCO_2° due to the measurement error in TA and TCO_2 is $8.4 \mu\text{mol}\cdot\text{kg}^{-1}$.

Results

Vertical Distribution of ΔTCO_2°

A typical ΔTCO_2° profile is given in Fig. 3.4 (crosses). The value is near zero near surface and becomes more negative with increasing depth because deeper waters contain less excess CO_2 than when formed. The ΔTCO_2° value reaches a minimum near 1500 m and starts to increase again with depth below 2000 m, suggesting that the bottom water has been in contact with the atmosphere at a more recent date than the water near 1500 m.

The maximum excess CO_2 signal of less than $-30 \mu\text{mol}\cdot\text{kg}^{-1}$ found here is about $10 \mu\text{mol}\cdot\text{kg}^{-1}$ smaller than that found in the South Atlantic (Chen and Millero, 1979; Chen, 1982a), Weddell Sea (Chen, 1984; Poisson and Chen, 1986), Southern Ocean (Chen, 1982a,c), Bering Sea (Chen et al., 1985) and in the Pacific Ocean (Chen and Pytkowicz, 1979; Chen, 1982b; Chen et al., 1982; 1986) where waters uncontaminated by excess CO_2 can be found. In other words, the entire water column at this station has been penetrated by the excess CO_2 . This is in agreement with the suggestion of Chen and Millero (1979) and Chen (1982a) that the entire water column north of approximately $15 \pm 10^\circ\text{N}$ has been contaminated by anthropogenic CO_2 .

Other chemical data (SIO reference #84-14, 1984) support the above conclusions. Nitrate, phosphate, silicate and AOU values show a broad maximum near 1800 m which may indicate that more time has elapsed for organic matter to decompose for waters at this depth. Consequently, it contains less excess CO_2 .

Tritium data (SIO reference #84-14, 1984) also show the same trend with a minimum near 1900 m, indicating older water at this depth (Fig. 3.4). Tritium throughout the water column indicates ventilation in the last thirty years. A TTO station nearby (Ostlund, 1983) also shows that tritium exists from surface to bottom (Fig. 3.4).

North-South Cross-Section

A cross-section extending from 78°N to 62°N is chosen for discussion here. A ridge separates the Greenland Sea to the north from the Norwegian Sea to the south. Portions of this cross-section were covered by ice. Temperature and salinity were both low immediately beneath the ice, and water here was not dense enough to sink to the bottom (Fig. 3.5). Consequently, the pool of cold water found in the Greenland Basin could not have been formed locally. This cold water also could not have originated from the north as bottom temperature is higher north of 76°N in the Greenland Sea (Fig. 3.5a) and even higher in the Arctic Ocean (Aagaard, 1980, 1981). The cold bottom water was probably advected here from the side. Temperature in the Norwegian Sea decreases monotonically with increasing depth.

Waters in the Norwegian Sea basin are slightly warmer and saltier than waters in the Greenland Sea basin (Fig. 3.5). Livingston *et al.* (1985) reported that three artificial radionuclides (tritium, Cs-137 and Sr-90) are strongly inversely correlated with salinity in the Denmark Strait overflow waters. The result suggests that fresher Greenland seawaters, which are cooler, have been ventilated more recently than the Norwegian seawaters. NTA and NTCO_2 of these two basins differ little but the Greenland Sea is slightly more oxygenated

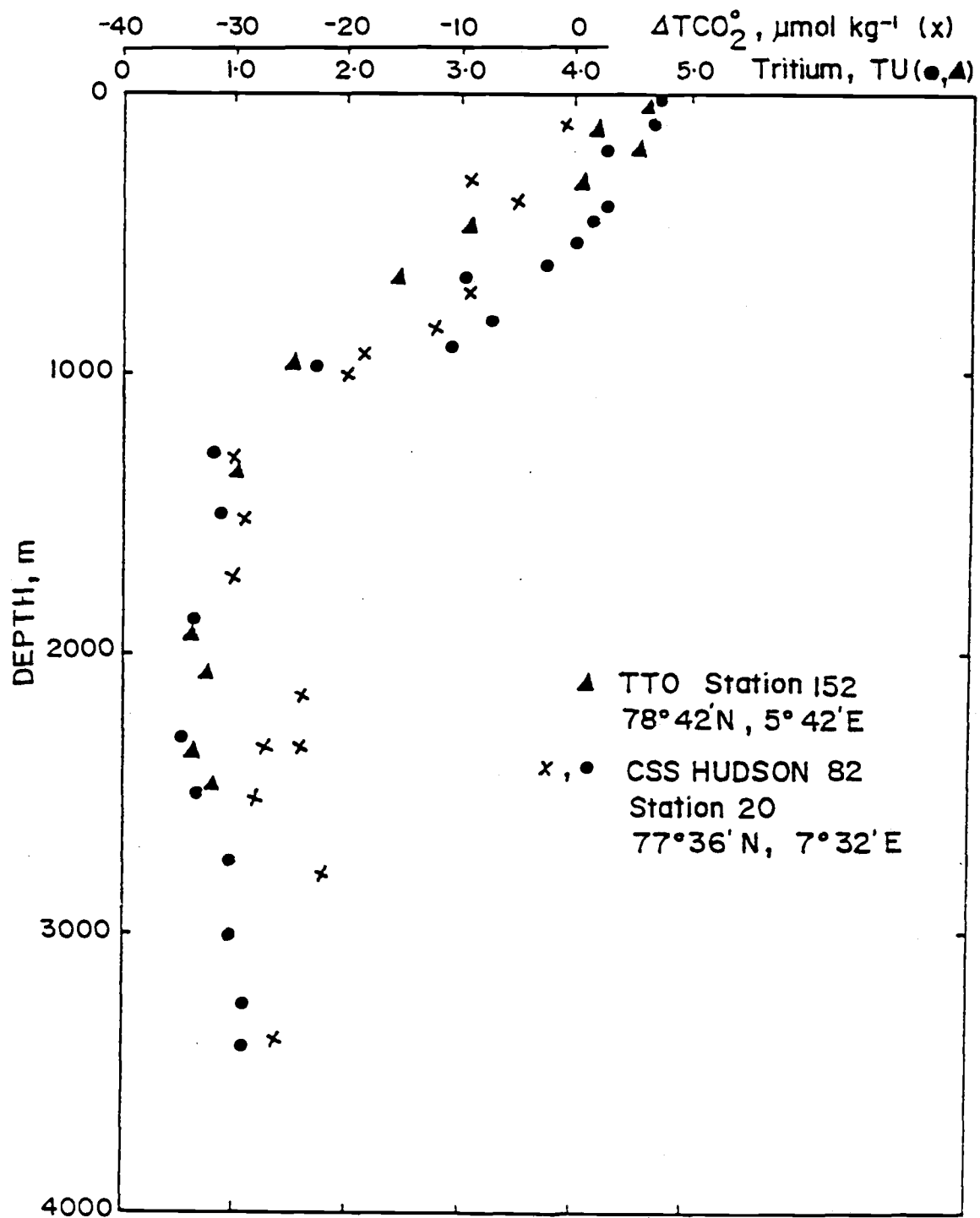


Fig. 3.4 Vertical distribution of ΔTCO_2° for HUDSON station 20 and TTO station 152.

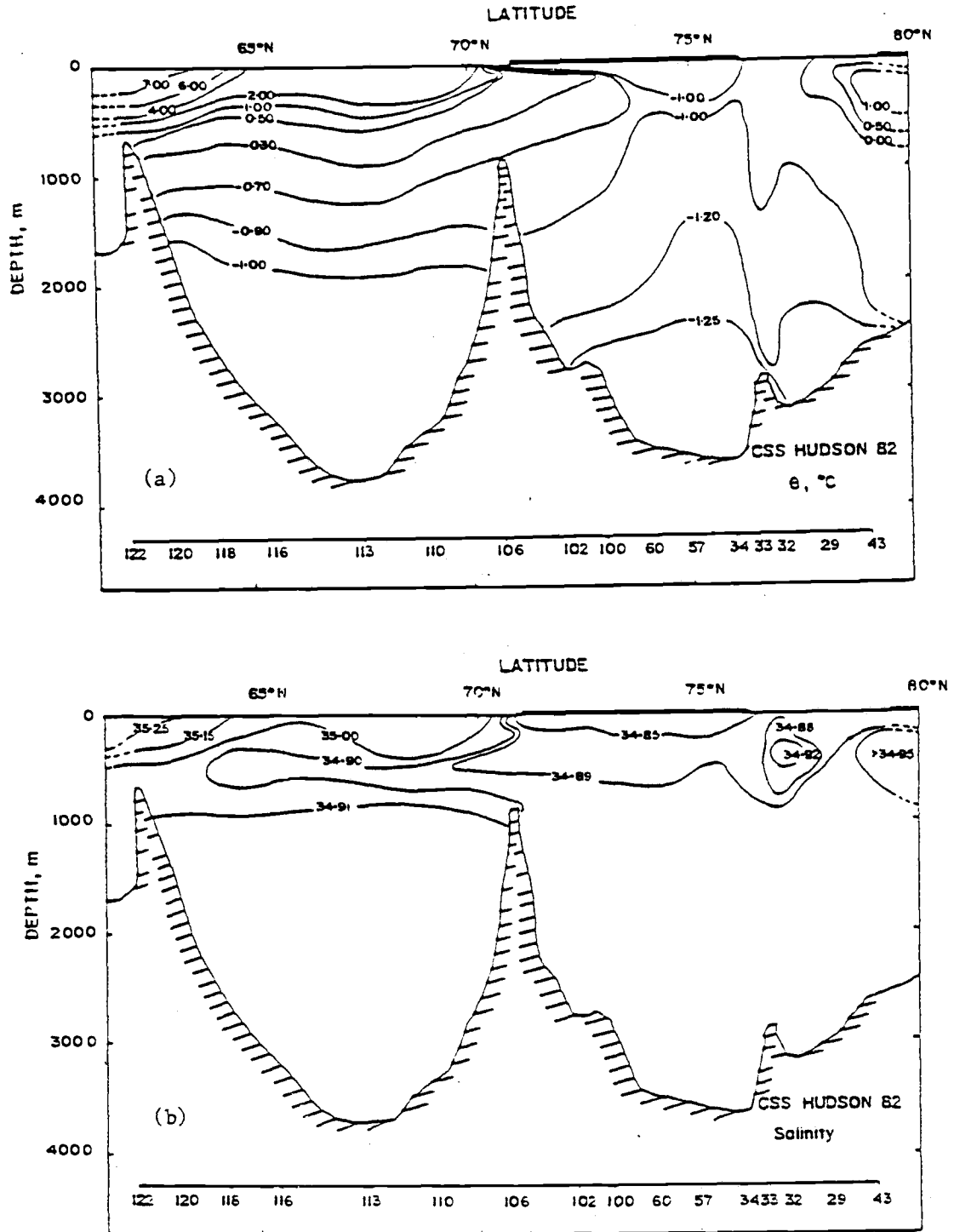


Fig. 3.5 North-South cross-section of (a) potential temperature and (b) salinity. The thick line at the surface represents sea ice.

but contains lower levels of nutrients (Figs. 3.6 and 3.7). Higher oxygen but lower nutrients also suggest more recent ventilation in the Greenland Sea basin.

The excess CO_2 seems to have come from the north with the more oxygenated Greenland Sea containing about $5 \mu\text{mol}\cdot\text{kg}^{-1}$ more excess CO_2 than waters in the Norwegian Sea (Fig. 3.8), in agreement again with the above suggestion that the Greenland Sea has been ventilated more recently. Although most excess CO_2 is still contained in waters above 1000 m, up to $10 \mu\text{mol}\cdot\text{kg}^{-1}$ does exist throughout the two basins if we assume that the maximum excess CO_2 signal is $40 \mu\text{mol}\cdot\text{kg}^{-1}$.

The high AOU but low ΔTCO_2° values immediately below the ice were the result of an artifact in calculation: waters below the ice could be cooled after ice formation but could not absorb oxygen quickly enough to reach a new equilibrium with the atmospheric oxygen. As a result, rather high AOU but low ΔTCO_2° were induced, similar to what was found in the Weddell Sea and the Bering Sea ice fields (Gordon *et al.*, 1984; Chen, 1984, 1985; Chen *et al.*, 1985; Poisson and Chen, 1986). Correcting this artifact below ice would make the surface ΔTCO_2° values approach zero (Chen, 1984; Poisson and Chen, 1986).

The Northern East-West Cross-Section

An east-west cross-section from 5°W to 18°E along roughly 75°N was studied to reveal the latitudinal contrast. On the western side the surface was covered by ice. The temperature of the surface water was low but the salinity was too low to form waters dense enough to sink to the bottom (Fig. 3.9). Thus the bottom water, colder than the intermediate water, was probably formed further to the west.

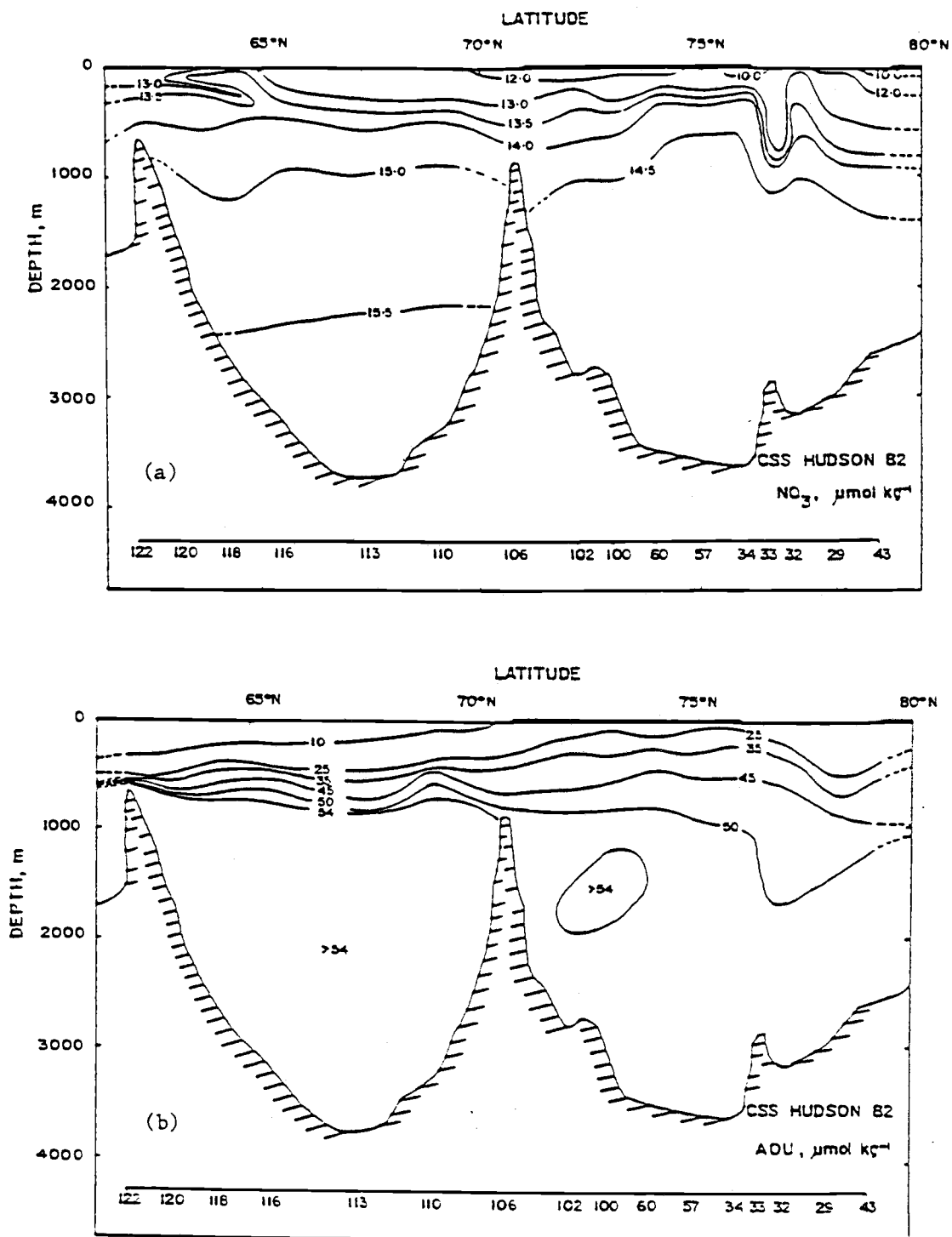


Fig. 3.6 North-South cross-section of (a) nitrate and (b) apparent oxygen utilization. The thick line at the surface represents sea ice.

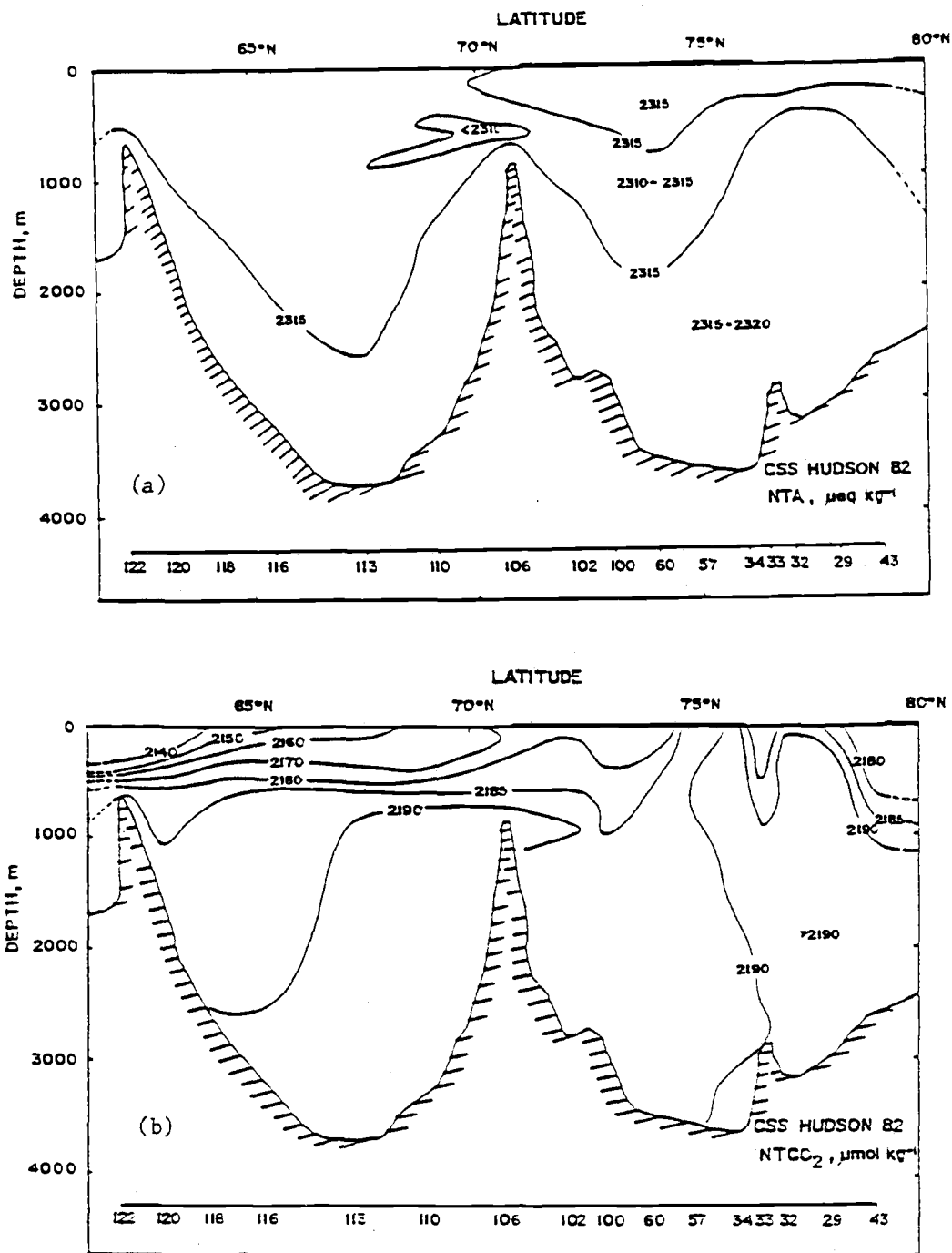


Fig. 3.7 North-South cross-section of (a) normalized alkalinity and (b) normalized total CO_2 . The thick line at the surface represents sea ice.

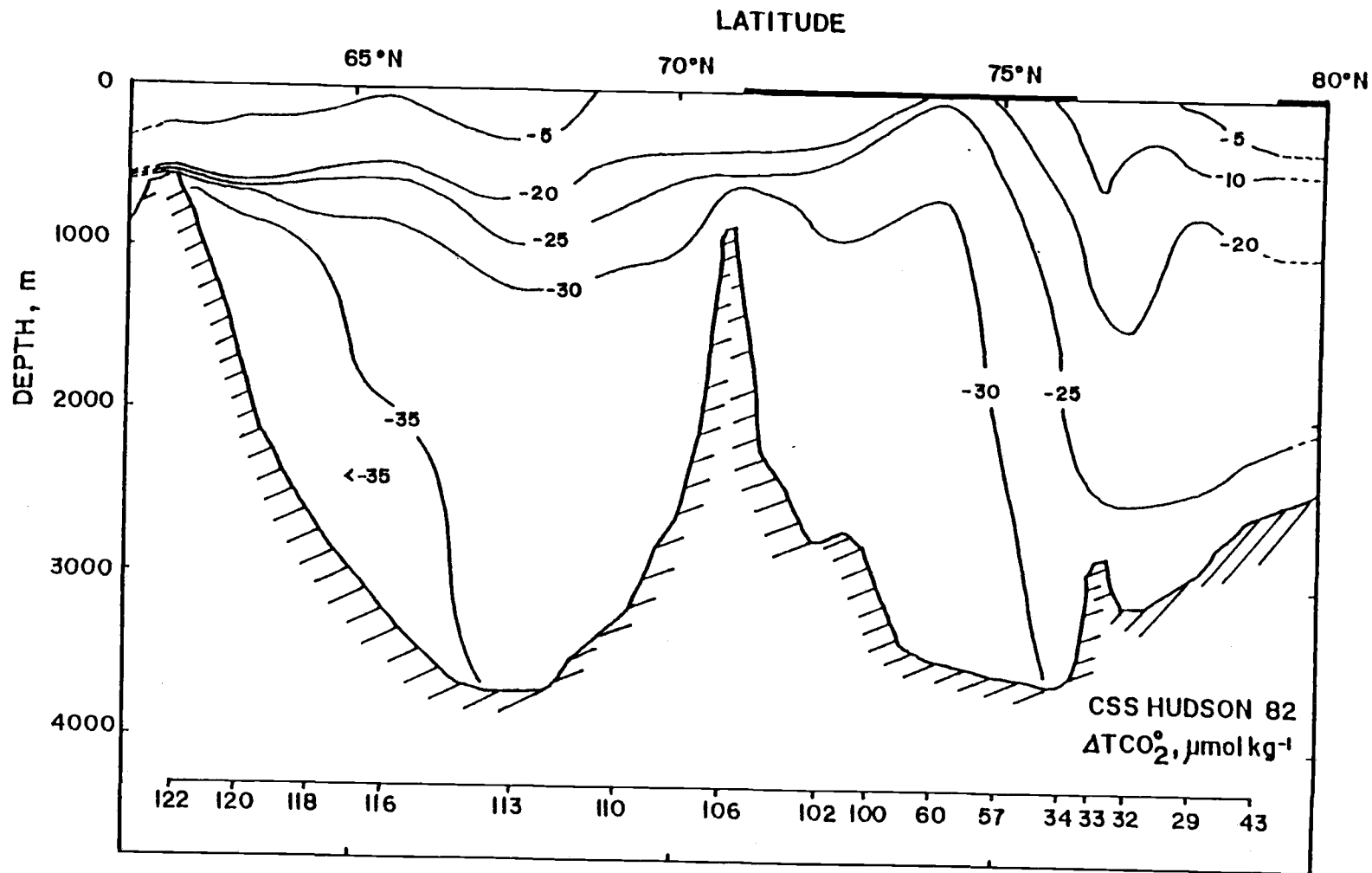


Fig. 3.8 North-South cross-section of ΔTCO_2 . The thick line at the surface represents sea ice.

The intermediate temperature maximum disappears in the eastern basin, where the water is warmer and saltier. Waters in the eastern basin also contain more nutrients, are higher in normalized alkalinity, total CO_2 and AOU (Figs. 3.9-3.11). These observations indicate that these waters are older than waters in the western basin. The excess CO_2 signal confirms this suggestion because the western basin contains a significant amount of excess CO_2 (probably more than $20 \mu\text{mol}\cdot\text{kg}^{-1}$) throughout the water column, whereas the bottom waters of the eastern basin contain about $10 \mu\text{mol}\cdot\text{kg}^{-1}$ less (Fig. 3.12).

The Southern East-West Cross-Section

A cross-section extending between zero to 5 degrees south of the cross-section discussed above is also examined, with similar results. The southern cross-section is slightly warmer, saltier, contains more nutrients and is higher in normalized alkalinity than the northern cross-section (Figs. 3.9-11, 3.13-15). NTCO_2 and AOU are also higher in the more southern cross-section except for a core of high AOU and NTCO_2 water centered around station 69 in the more northern cross-section (Figs. 3.11, 3.15). This information again suggests that the more northern waters are younger. The ΔTCO_2° results are similar within the precision of the data (Figs. 3.12, 3.16). The northern cross-section is less than $5 \mu\text{mol}\cdot\text{kg}^{-1}$ more enriched in excess CO_2 than the southern cross-section.

Little latitudinal difference exists for stations west of 5°E . The eastern stations are colder, fresher, contains less nutrients, NTA, NTCO_2 and is lower in AOU but these stations are also more northern (Figs. 3.13-15). These stations have been ventilated more recently and contain more excess CO_2 (Fig. 3.16).

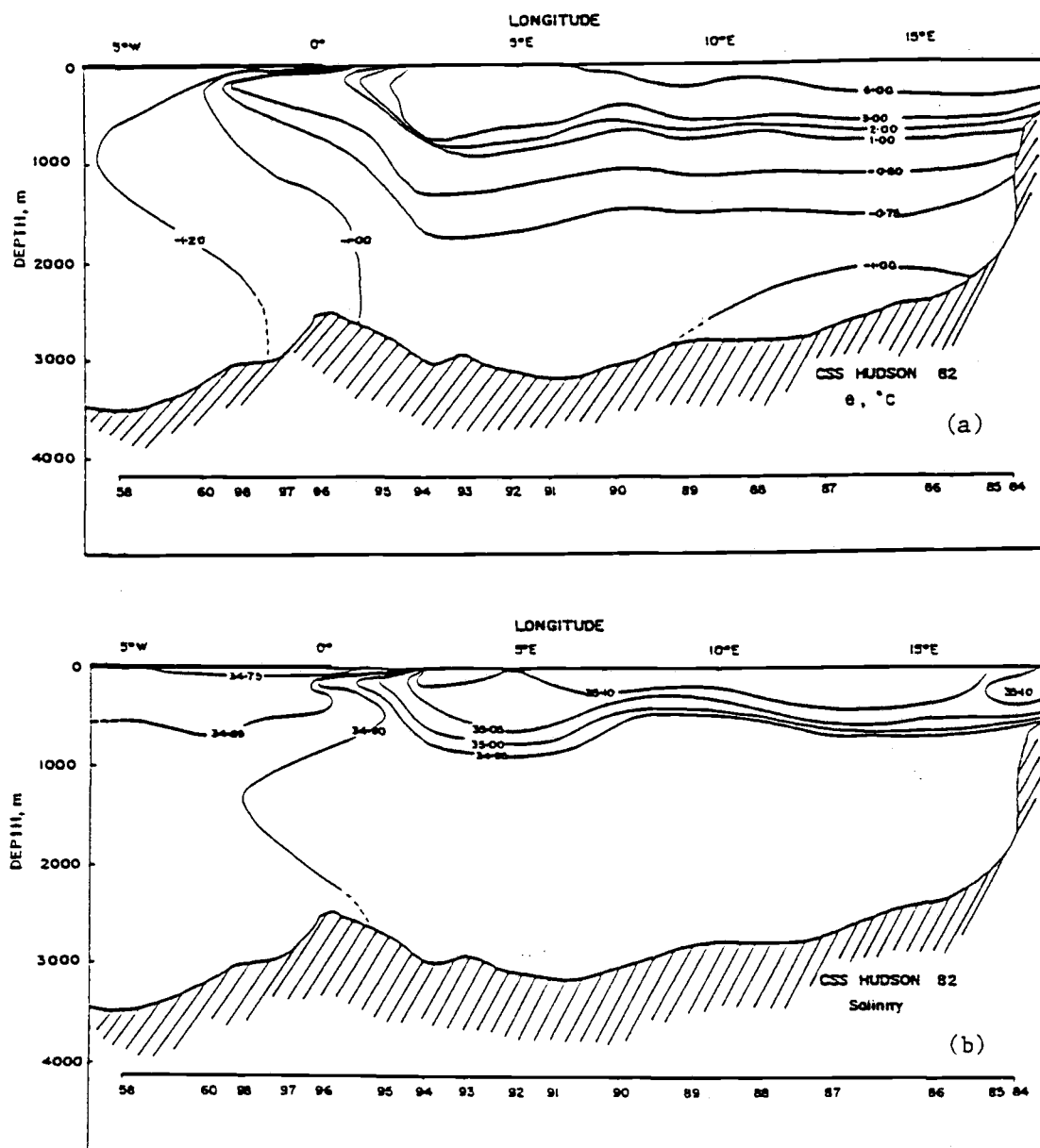


Fig. 3.9 Northern east-west cross-section of (a) potential temperature and (b) salinity. The thick line at the surface represents sea ice.

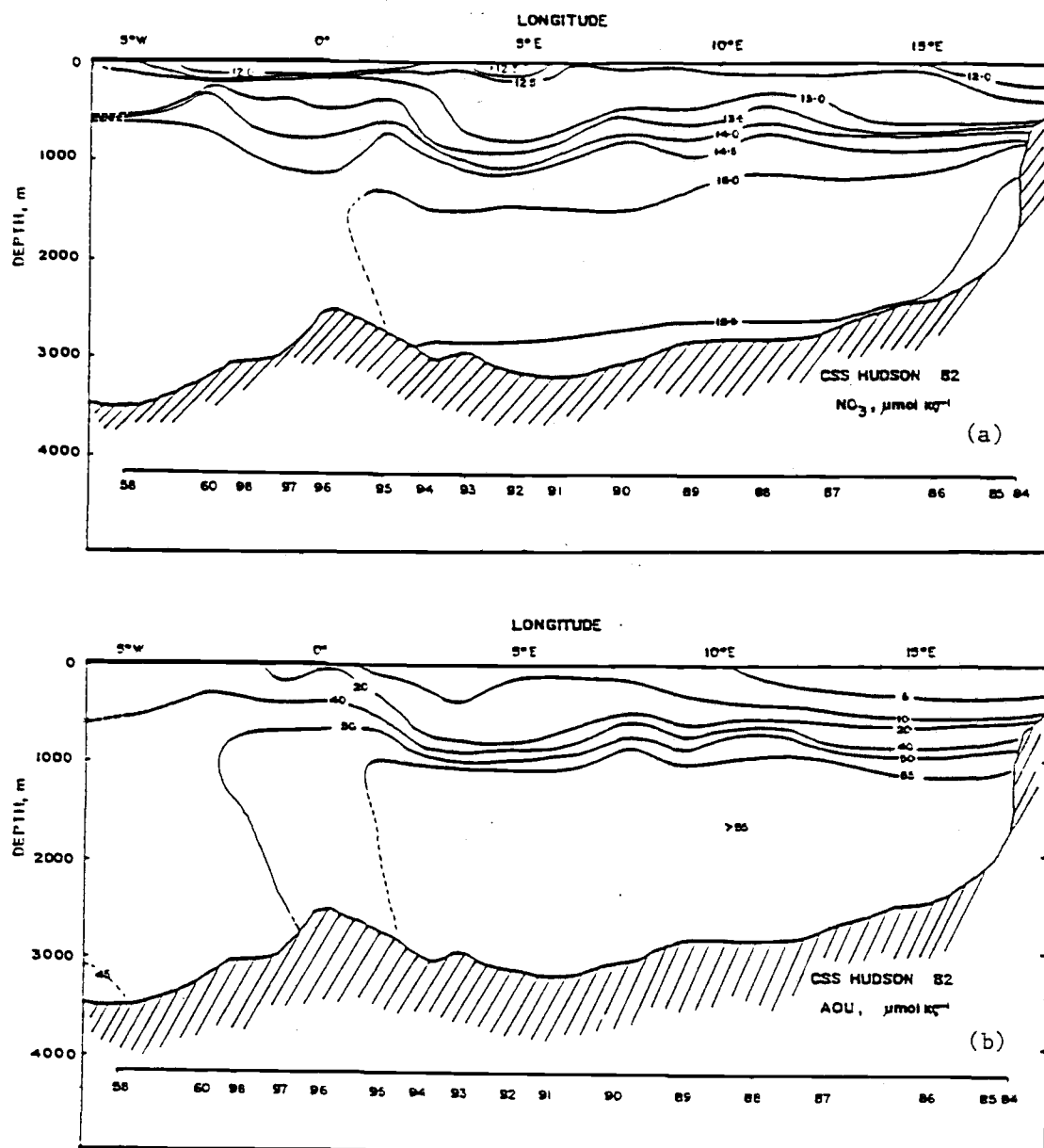


Fig. 3.10 Northern east-west cross-section of (a) nitrate and (b) apparent oxygen utilization. The thick line at the surface represents sea ice.

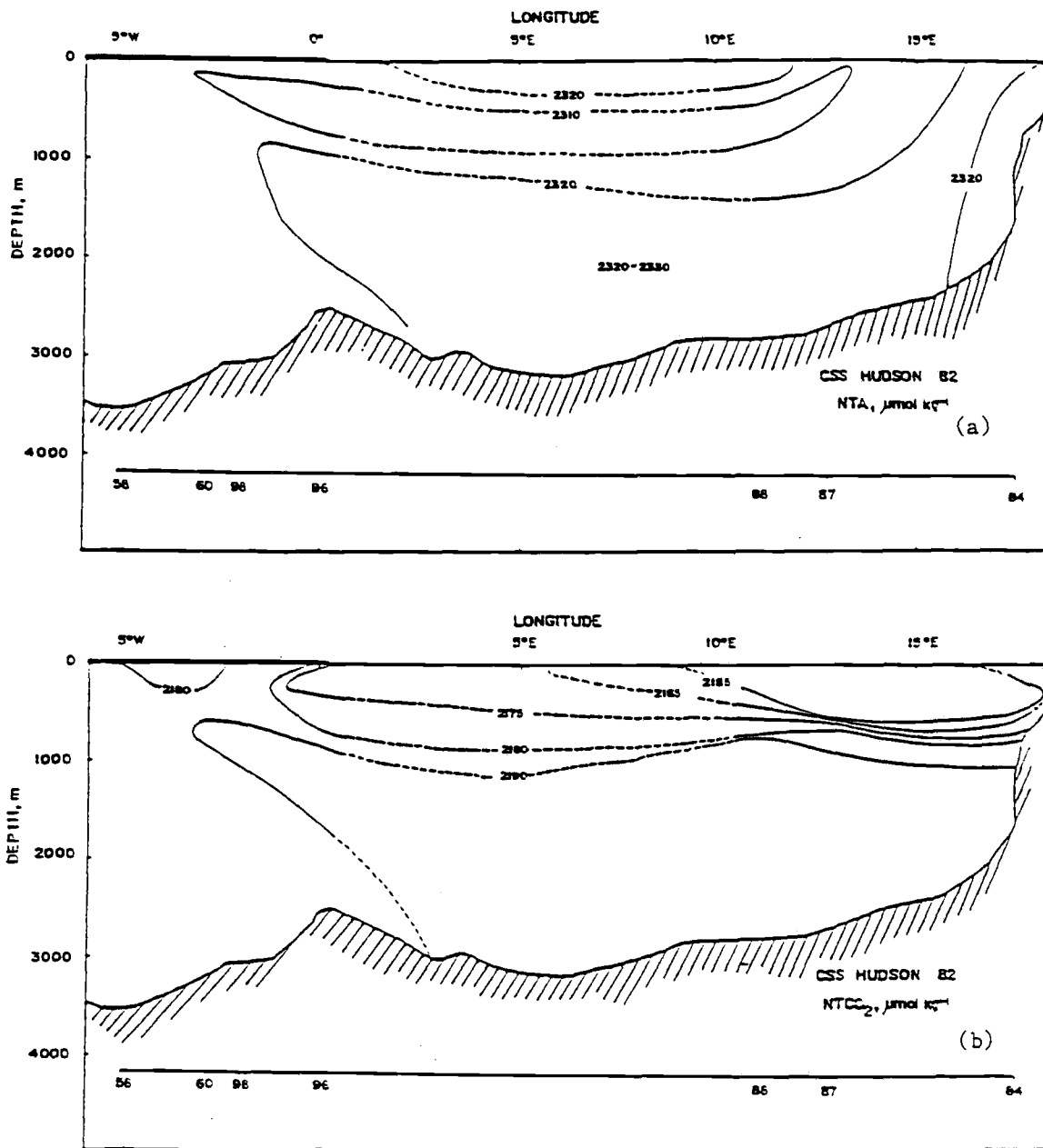


Fig. 3.11 Northern east-west cross-section of (a) normalized alkalinity and (b) normalized total CO_2 . The thick line at the surface represents sea ice.

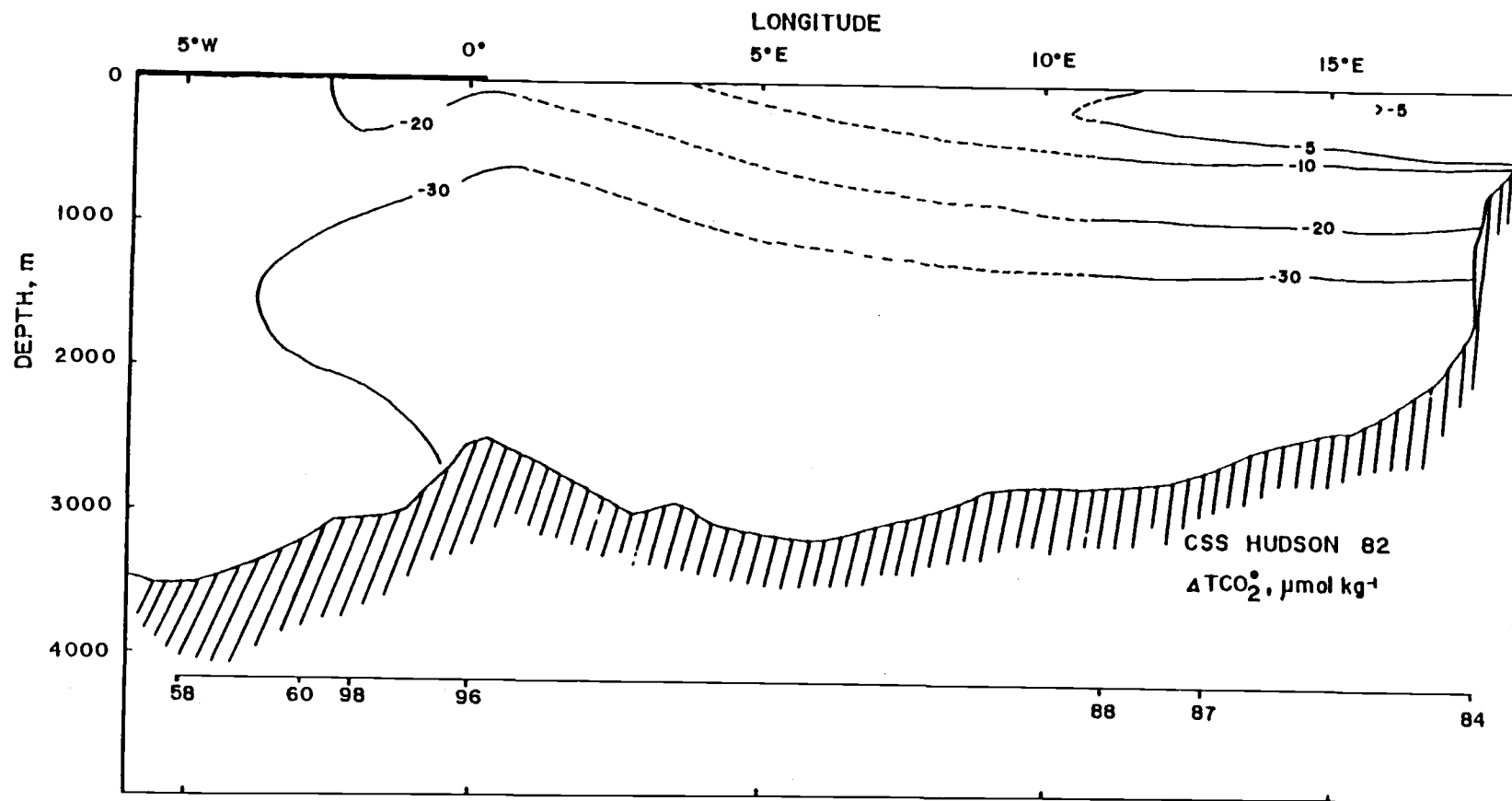


Fig. 3.12 Northern east-west cross-section of ΔTCO_2 . The thick line at the surface represents sea ice.

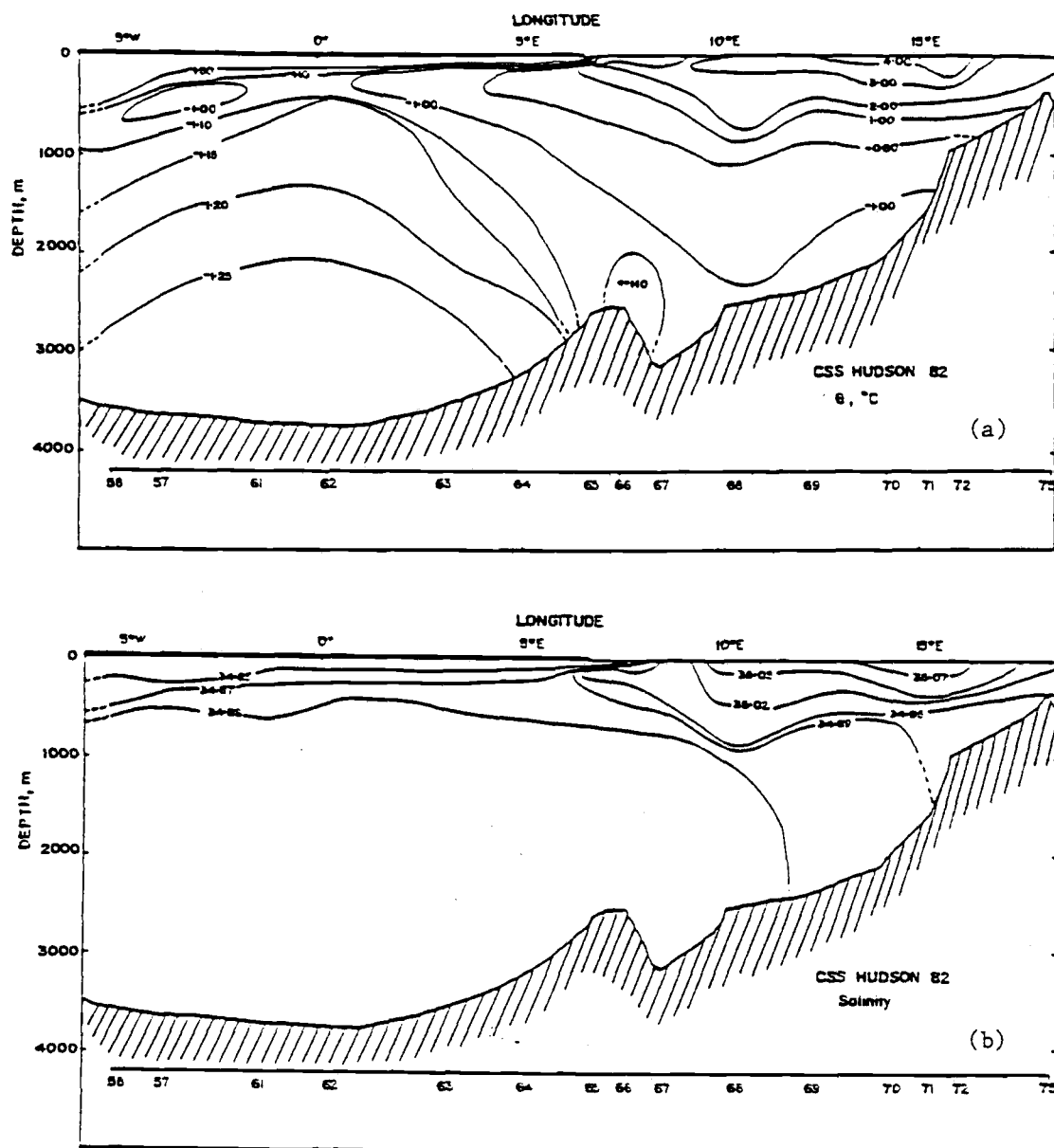


Fig. 3.13 Southern east-west cross-section of (a) potential temperature and (b) salinity. The thick line at the surface represents sea ice.

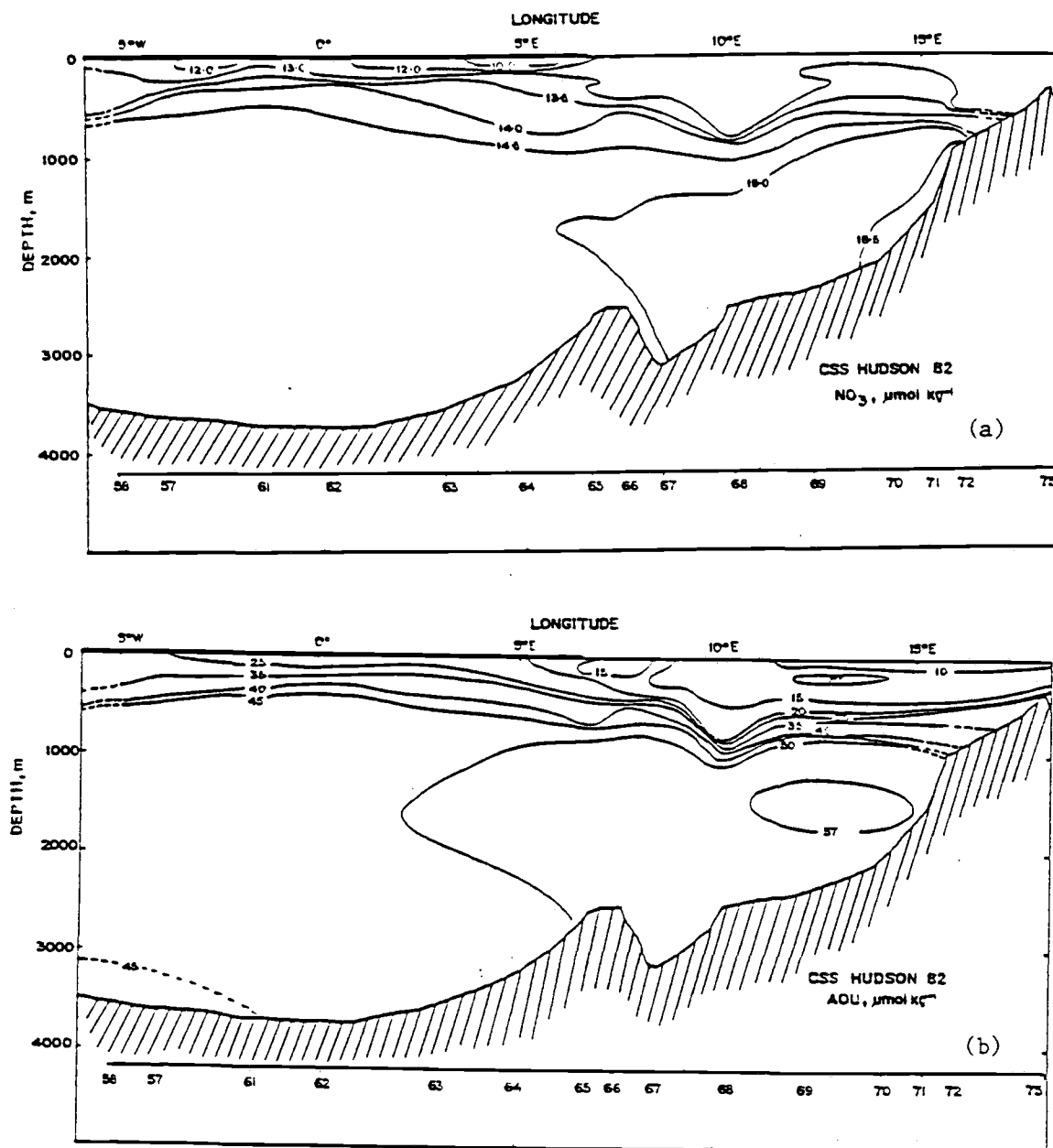


Fig. 3.14 Southern east-west cross-section of (a) nitrate and (b) apparent oxygen utilization. The thick line at the surface represents sea ice.

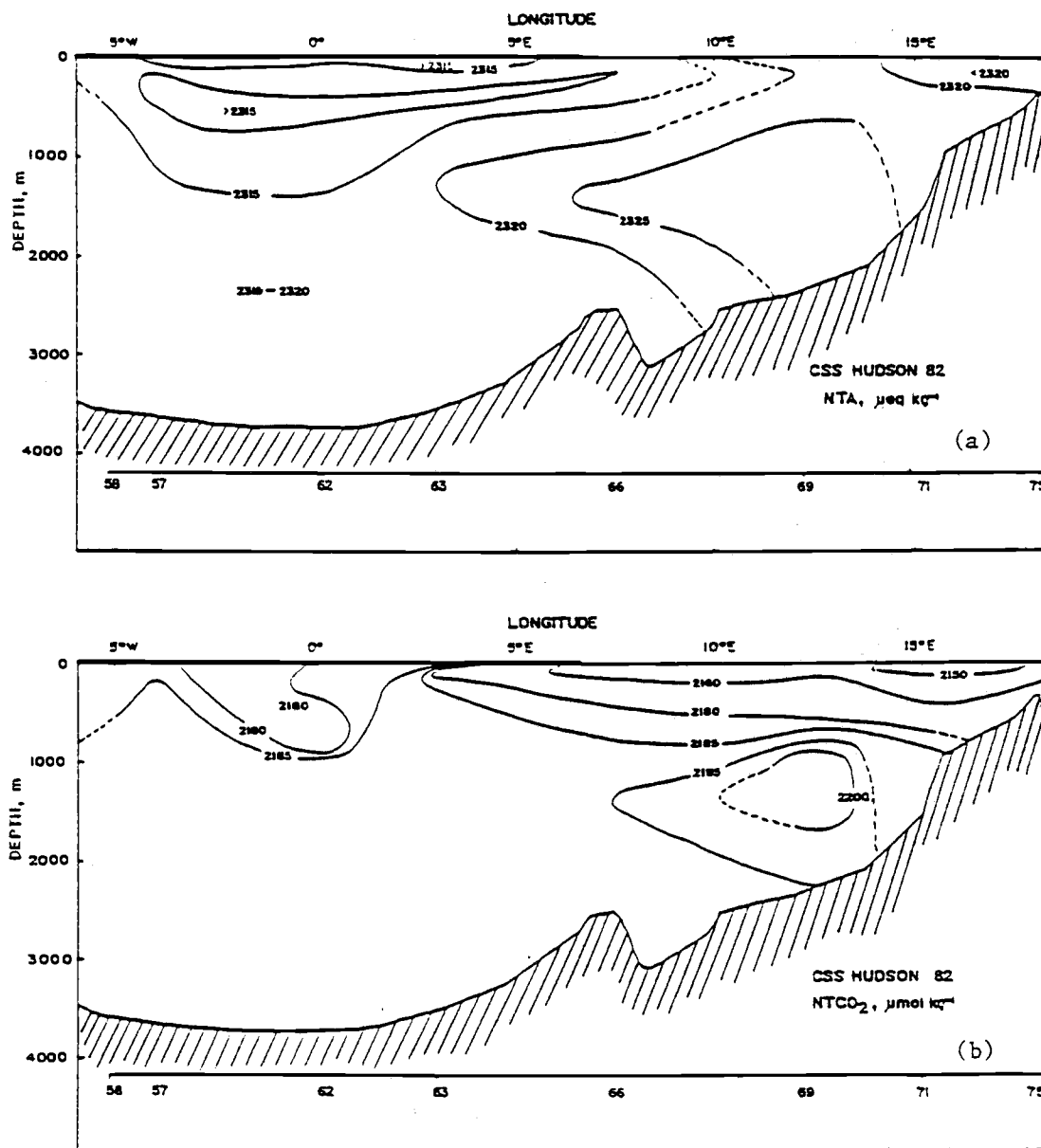


Fig. 3.15 Southern east-west cross-section of (a) normalized alkalinity and (b) normalized total CO_2 . The thick line at the surface represents sea ice.

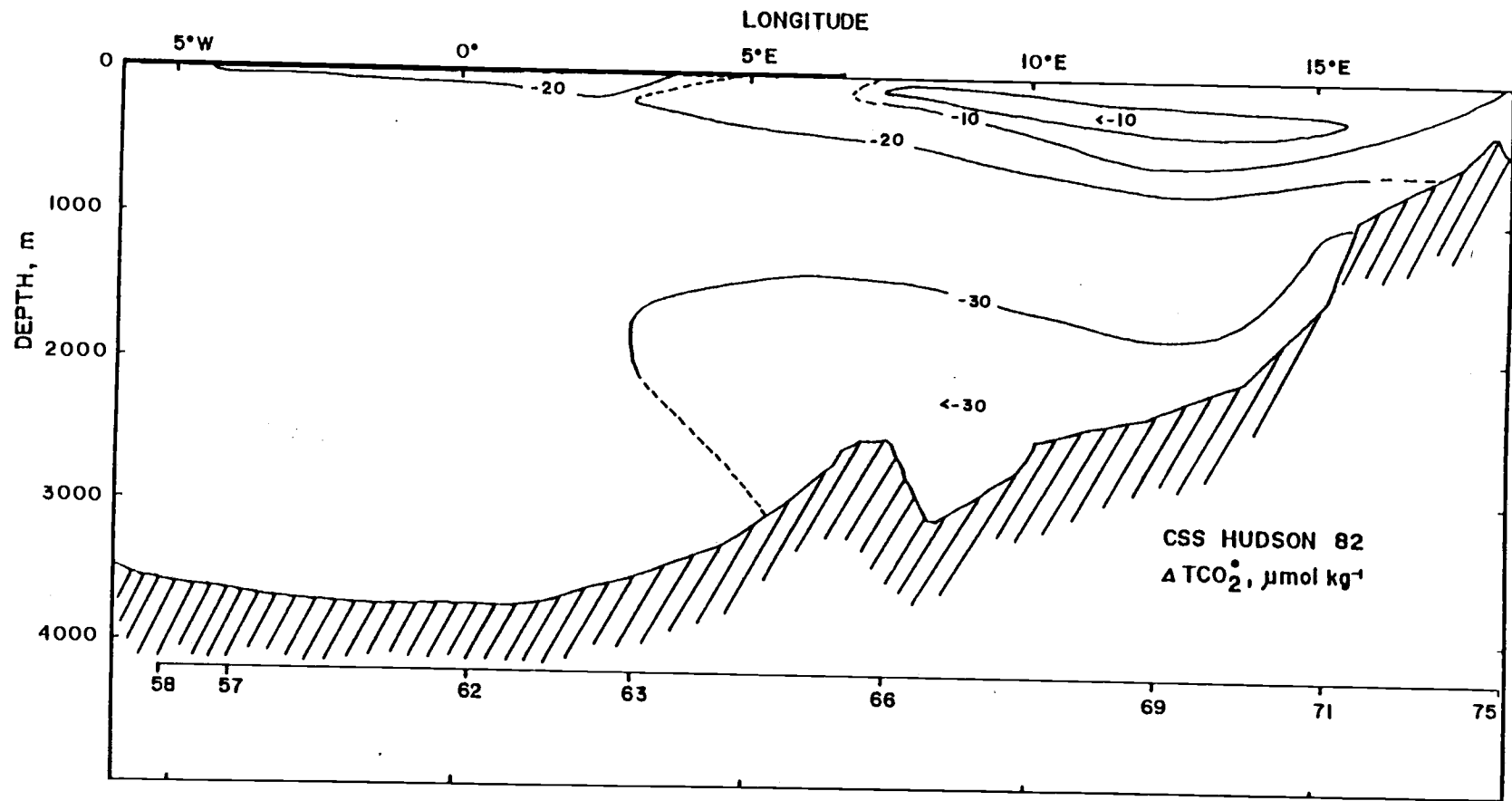


Fig. 3.16 Southern east-west cross-section of ΔTCO_2 . The thick line at the surface represents sea ice.

Overall, the Greenland and Norwegian Seas (between 65° and 80°N) contain $0.92 \pm 0.2 \times 10^{15}$ g excess carbon.

Discussion

Livingston et al (1985) observed an inverse correlation with salinity of three anthropogenic radionuclides, tritium, Cs-137 and Sr-90, in the Denmark Strait overflow water. For deep and bottom waters in the Greenland Sea, an inverse correlation also seems to exist, with higher salinity corresponding, though weakly, with a smaller excess CO_2 content (Fig. 3.17a), but no such correlation exists for the surface water. The excess CO_2 signal in the deep and bottom Norwegian seawaters does not show an inverse correlation with salinity (Fig. 3.17b). Higher salinity for near-surface waters there actually corresponds to more excess CO_2 .

No significant correlation between excess CO_2 signal and potential temperature can be detected for deep and bottom waters (Fig. 3.18). The near-surface waters contain more excess CO_2 because they are warmer (Fig. 3.18).

It is generally assumed that older waters have more organic matter decomposed in them thus more oxygen is utilized, hence they have higher AOU values. A water with an AOU near zero most likely received the full impact of excess CO_2 contamination (ΔTCO_2° near zero). On the other hand, an older water with higher AOU should contain less excess CO_2 (ΔTCO_2° more negative). In general, the HUDSON data show the expected trend (Fig. 3.19).

Because of the previously described near-surface artifacts in both quantities induced by temperature change without associated changes in chemical properties, samples above 100 m have not been included in the figure. Even so, there is still much scatter in the correlation caused by random error in the carbonate data. Besides,

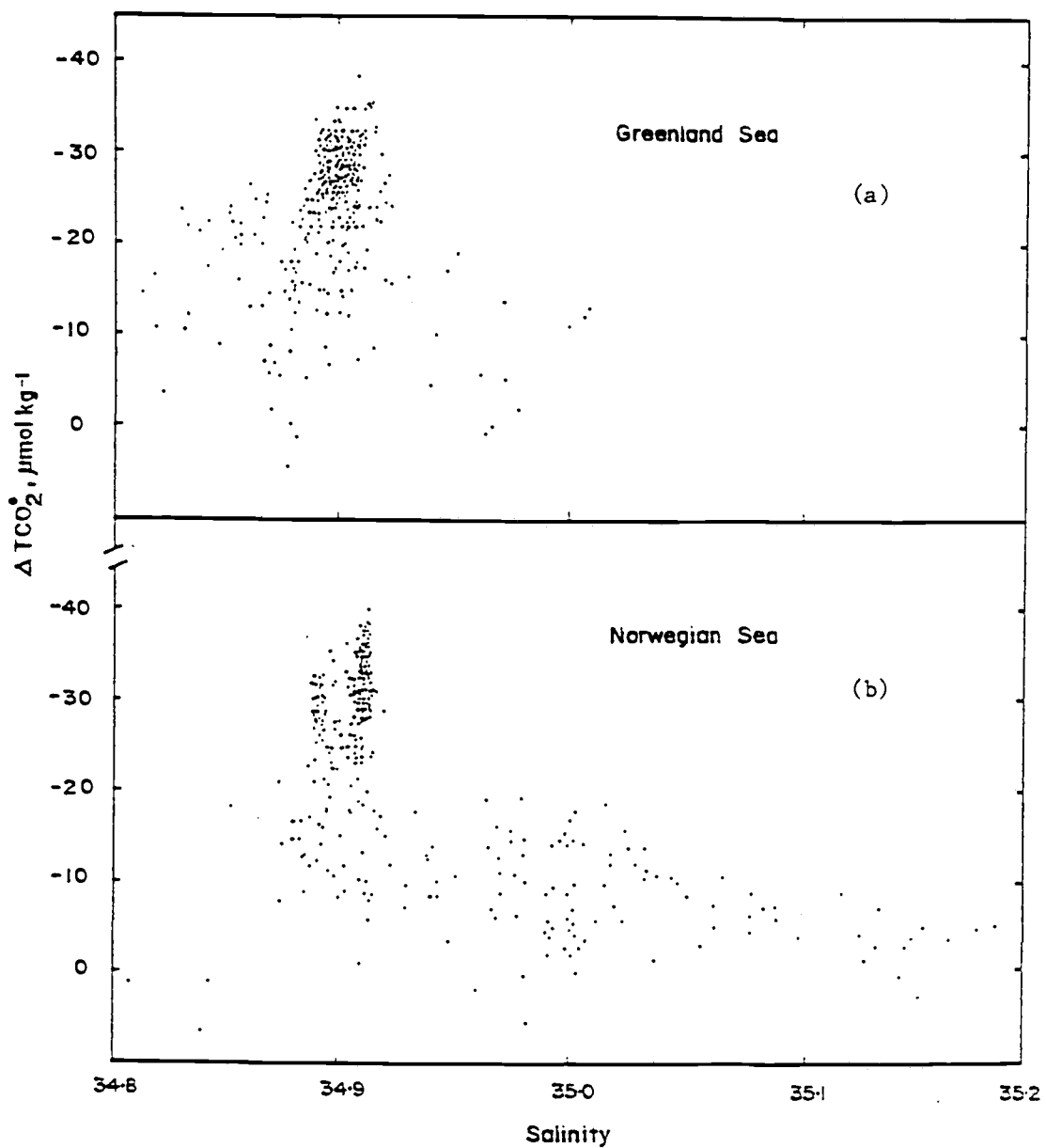


Fig. 3.17 Salinity plotted vs $\Delta \text{TCO}_2^\circ$ for all waters below 100 m in the
(a) Greenland and (b) Norwegian seas.

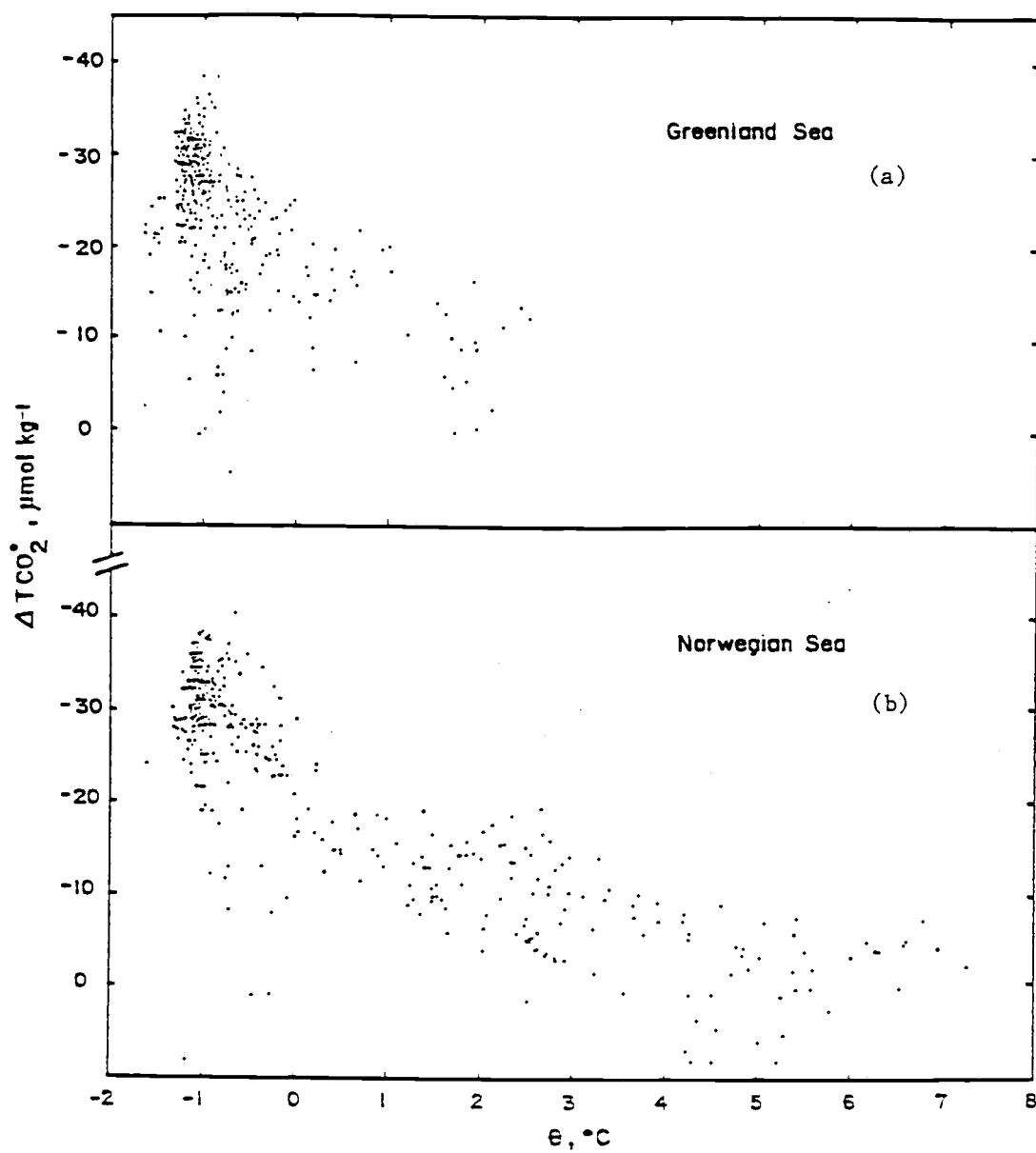


Fig. 3.18 Potential temperature vs ΔTCO_2° for all waters below 100 m in the (a) Greenland and (b) Norwegian seas.

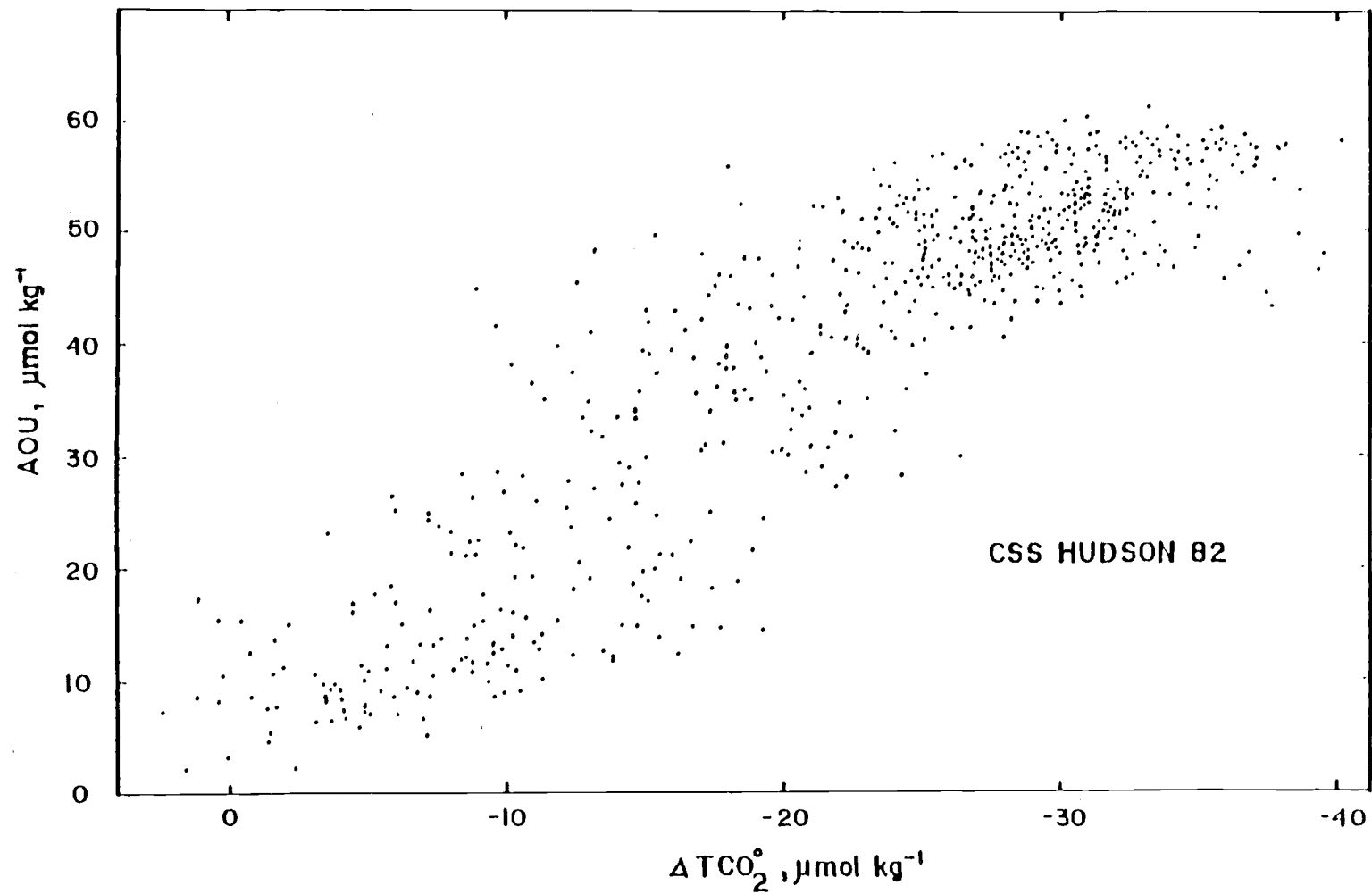


Fig. 3.19 Apparent oxygen utilization plotted vs ΔTCO_2^o for all waters below 100 m.

differences in primary productivity and the rates of sinking and decomposition of organic matter affect AOU regardless of the age (hence the concentration of excess CO_2) of the water. As a result, a tight correlation pattern probably should not be expected.

Tritium has been used to date water masses very successfully and it seems to correlate linearly with ΔTCO_2° (Fig. 3.20). Again, only samples below 100 m are included in Fig. 3.20, which shows that more excess CO_2 exists (less negative ΔTCO_2°) when tritium is high and vice versa. A linear extrapolation to zero tritium gives a ΔTCO_2° value of $-38 \pm 2.5 \mu\text{mol}\cdot\text{kg}^{-1}$. In other words, a water without tritium contained $38 \mu\text{mol}\cdot\text{kg}^{-1}$ less excess CO_2 when formed compared to its contemporary counterpart. Obviously $38 \mu\text{mol}\cdot\text{kg}^{-1}$ is a upper limit of the excess CO_2 signal because excess CO_2 had been produced long before the bomb testings which produced tritium. As a result, the preindustrial CO_2 level cannot be obtained from the HUDSON data.

These data, however, are extremely important and the resulting calculations probably suffer the least systematic error as compared with our previous efforts. The major factors that lead to uncertainties as reiterated by Chen and Millero (1979), Chen and Pytkowicz (1979), Shiller (1981, 1982), Chen (1982a,b, 1984), Chen et al. (1982, 1985), Broecker et al. (1985), Chen and Drake (1986) and Poisson and Chen (1986) are summarized as follows:

- (1) Summer data were used to model mainly winter-formed subsurface waters, inducing a possible error which is unknown without calibrating against field data collected in winter;
- (2) Uncertainties in estimating NTA° and NTCO_2° ;
- (3) Uncertainties in the C/N/P/O ratio;

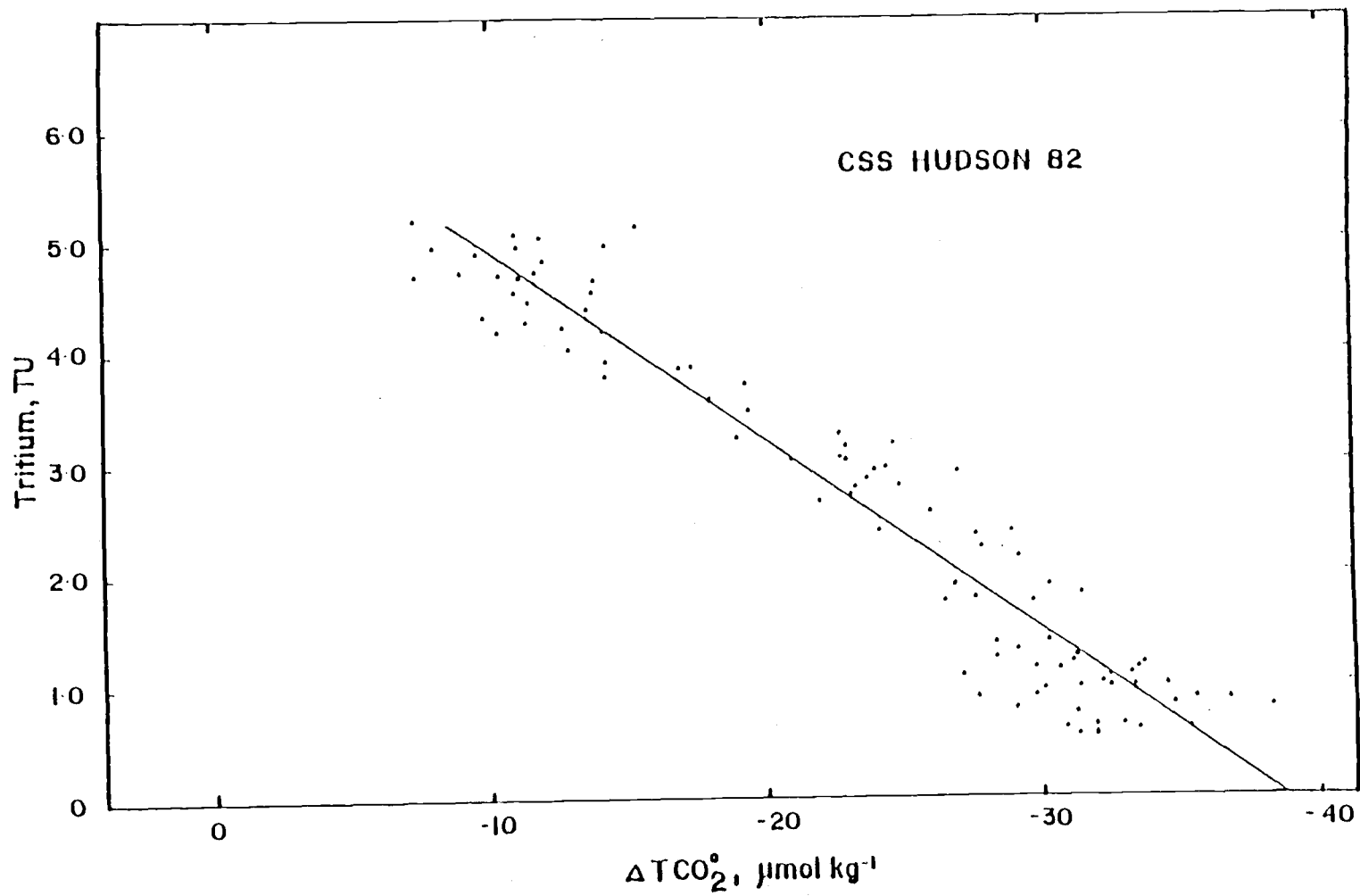


Fig. 3.20 Tritium plotted vs ΔTCO_2 for all waters below 100 m.

- (4) Preformed AOU is not zero;
- (5) and surface water may only show a partial response to the anthropogenic CO₂ impact.

The first factor has been minimized with the HUDSON data because winter data were collected near a major subsurface water formation region.

The second factor for uncertainty is small because Greenland and Norwegian seawaters come essentially from the same source. The NTA° and NTCO₂° values correlate essentially linearly with temperature (Figs. 3.2, 3.3) and can be estimated from potential temperatures. The resulting uncertainties are similar to the quality of the data.

The third factor is not important with the HUDSON data because AOU is less than 60. Whether we use Broecker *et al*'s. (1985) "best correct estimate" of 0.72, or the value 0.80 that they actually used for calculating ΔTCO₂°, the results agree with our results (based on an AOU coefficient of 0.78) to within 4 μmol·kg⁻¹. This systematic error is smaller than the random error (8.4 μmol·kg⁻¹) due to uncertainty in the TA and TCO₂ measurements.

The fourth and fifth concerns are critical for calculating the preindustrial CO₂ concentration. It is impossible to make such calculations with the HUDSON data because no really old waters exist in the Greenland and Norwegian Seas to form a baseline for obtaining the absolute excess CO₂ signal. The HUDSON data, however, give further insights on how preformed AOU and surface PCO₂ distribute in winter. This information will be combined with other data sets to estimate the preindustrial CO₂ level.

Conclusions

We have analyzed the data collected by the CSS HUDSON in 1982. They include the only wintertime carbonate data available in the Greenland and Norwegian Seas. These data have been used to calculate the excess CO₂ signal, and the results contain the least systematic error as compared with our previous efforts. The results indicate:

- * Surface alkalinity and total CO₂ correlate linearly with temperature when compared at the same salinity;
- * All HUDSON stations have been contaminated by excess CO₂ from surface to bottom;
- * The Greenland Sea contains more excess CO₂ than the Norwegian Sea, and the western basin is more contaminated than the eastern basin;
- * The excess CO₂ results are corroborated by the AOU and tritium data, as linear correlations were found;
- * Overall, the Greenland and Norwegian Seas (between 65° and 80°N) contain $0.92 \pm 0.2 \times 10^{15}$ g excess carbon.

References

- Aagaard, K. (1980). Report by the working group on physical oceanography of the Workshop on Eastern Arctic Science (Lyngby, Denmark, Jan. 1977), Commission for Scientific Work in Greenland, pp. 55-75.
- Aagaard, K. (1981). On the deep circulation in the Arctic Ocean. Deep-Sea Research 28, 251-268.
- Broecker, W.S., T. Takahashi and T.H. Peng (1985). Reconstruction of past atmospheric CO₂ contents from the chemistry of the contemporary ocean: an evaluation. DOE technical report, DOE/OR-857, 79 pp.
- Chen, C.T. (1982a). On the distribution of anthropogenic CO₂ in the Atlantic and Southern Oceans. Deep-Sea Research 29, 563-580.
- Chen, C.T. (1982b). Oceanic penetration of excess CO₂ in a cross-section between Alaska and Hawaii. Geophysical Research Letter 9, 117-119.
- Chen, C.T. (1982c). Carbonate chemistry during WEPOLEX-81. Antarctic Journal, 1982 Review, 102-103.
- Chen, C.T. (1984). Carbonate chemistry of the Weddell Sea. DOE technical report, DOE/EV/10611-4, 118 pp.
- Chen, C.T. (1985). Preliminary observation of oxygen and carbon dioxide of the wintertime Bering Sea marginal ice zone. Continental Shelf Research 4, 465-483.
- Chen, C.T. and F.J. Millero (1979). Gradual increase of oceanic carbon dioxide. Nature 277, 205-206.

- Chen, C.T. and R.M. Pytkowicz (1979). On the total CO₂-titration alkalinity-oxygen system in the Pacific Oceans. Nature 281, 362-365.
- Chen, C.T., F.J. Millero and R.M. Pytkowicz (1982). Comments on 'calculating the oceanic CO₂ increase: a need for caution,' by A.M. Shiller. Journal of Geophysical Research 87, 2083-2085.
- Chen, C.T. and E.T. Drake (1986). Carbon dioxide increase in the atmosphere and oceans and possible effects on climate. Annual Review of Earth and Planetary Sciences 14, 201-235.
- Chen, C.T., C.L. Wei and M.R. Rodman (1985). Carbonate chemistry of the Bering Sea. DOE technical report, DOE/EV/10611-5, 77 pp.
- Chen, C.T., A. Poisson and C. Goyet (1986). Preliminary data report for the INDIVAT 1 and INDIGO 1/INDIVAT 3 cruises in the Indian Ocean. DOE technical report, DOE/NBB-0074, 106 pp.
- Edmond, J.M. (1974). On the distribution of carbonate and silicate in the deep ocean. Deep-Sea Research 21, 455-480.
- Gordon, A.L., C.T. Chen and W.G. Metcalf (1984). Winter mixed layer entrainment of Weddell Sea water. Journal of Geophysical Research 89, 637-640.
- Hansen, J.A., L.D. Rind, G.R. Russell, P. Stone, I. Fung, R. Ruedy and J. Lerner (1984). Climate sensitivity: analysis of feedback mechanisms, in Climate Processes and Climate Sensitivity, J.E. Hansen and T. Takahashi, eds., American Geophysical Union, Washington, D.C., pp. 130-163.
- Livingston, H.D., J.H. Swift and H.G. Ostlund (1985). Artificial radionuclide tracer supply to the Denmark Strait overflow between 1972 and 1981. Journal of Geophysical Research 90, 6971-6982.

- Ostlund, H.G. (1983). TTO North Atlantic study: tritium and radiocarbon, Data Rel. 83-35, Tritium Lab., Rosenstiel Sch. Mar. Atmos. Sci., Univ. Miami, Fla.
- Poisson, A. and C.T. Chen (1986). Why is there little excess CO₂ in the Antarctic Bottom Water? Deep-Sea Research, submitted.
- Reid, J.L. and R. Lynn (1971). On the influence of the Norwegian-Greenland and Weddell seas upon the bottom waters of the Indian and Pacific oceans. Deep-Sea Research 18, 1063-1088.
- SIO reference #84-14 (1984). CSS HUDSON cruise 82-001, 14 February-6 April 1982, Vol. 1, Physical and Chemical Data, University of California, 305 pp.
- Shiller, A.M. (1981). Calculating the oceanic CO₂ increase: a need for caution. Journal of Geophysical Research 86, 11083-11088.
- Shiller, A.M. (1982). Reply to comments of Chen, Millero and Pytkowicz. Journal of Geophysical Research 87, 2086.
- Stefanssen, U. (1968). Dissolved nutrients, oxygen and water masses in the North Irminger Sea. Deep-Sea Research 15, 541-575.
- Swift, J.H. (1984). The circulation of the Denmark Strait and Iceland-Scotland overflow waters on the North Atlantic. Deep-Sea Research 29, 563-580.
- Swift, J.H., K. Aagaard and S.-A. Malmberg (1980). The contribution of the Denmark Strait overflow to the deep North Atlantic. Deep-Sea Research 27, 29-42.
- Swift, J.H. and K. Aagaard (1981). Seasonal transitions and water mass formation in the Iceland and Greenland seas. Deep-Sea Research 28, 1107-1129.

- Takahashi, T. and D. Chipman (1982). Measurements of the partial pressure of CO₂ in discrete water samples during the North Atlantic expedition, the Transient Tracers of Oceans project, NSF technical report, 9 pp. plus data listing.
- Worthington, L.V. (1970). The Norwegian Sea as a Mediterranean basin. Deep-Sea Research 17, 77-84.
- Worthington, L.V. (1976). On the North Atlantic circulation, The Johns Hopkins Oceanographic Studies 6, 110 pp.
- Worthington, L.V. (1981). The water masses in the World Ocean: some results of a fine-scale census, in Evaluation of Physical Oceanography, B.A. Warren and C. Wunsch, eds., MIT Press, Cambridge, MA, pp. 6-41.
- Wust, G. (1935). The stratosphere of the Atlantic Ocean, translated by W.J. Emery, Amerind Publishing Co., New Delhi, 1978, 112 pp.

BIBLIOGRAPHY

- Aagaard, K. (1980). Report by the working group on physical oceanography of the Workshop on Eastern Arctic Science (Lyngby, Denmark, Jan. 1977), Commission for Scientific Work in Greenland, pp. 55-75.
- Aagaard, K. (1981). On the deep circulation in the Arctic Ocean. Deep-Sea Research 28, 251-268.
- Ahrland, S. (1973). The thermodynamics of stepwise formation of metal ion complex in aqueous solution. Structure and Bonding 15, 167-188.
- Ahrland, S., J. Chatt and N.R. Davies (1958). The relative affinities of ligand atoms for acceptor molecules and ions. Quarterly Review 12, 265-276.
- Atkinson, G., M.O. Dayhoff and D.W. Ebdon (1975). Computer modeling of ionic equilibria in seawater, in Marine Electrochemistry, Berkowitz, J.B. et al., eds., Electrochemical Society, Princeton, NJ, 124-138.
- Ball, J.W., D.K. Nordstrom and E.A. Jenne (1981). Additional and revised thermodynamic data and computer code for WATEQ2-A Computerized chemical model for trace and major element speciation and mineral equilibria of natural waters. U.S. Geological Survey, Water Resources Investigations WRI-78-116, pp. 109.
- Baes, C.F. and R.E. Mesmer (1976). The hydrolysis of cations. A critical review of hydrolytic species and their stability constants in aqueous solution, John Wiley & Sons, Inc., NY, pp. 489.

- Bassett, R.L. (1980). A critical evaluation of the thermodynamic data from boron ions, ion pairs, complexes, and polyamions in aqueous solution at 298.15c.c. and 1 bar. Geochimica et Cosmochimica Acta 44, 1151-1160.
- Berner, R.A. (1971). Principles of Chemical Sedimentology, Macgraw-Hill Press, NY, pp. 240.
- Broecker, W.S., T. Takahashi and T.H. Peng (1985). Reconstruction of past atmospheric CO₂ contents from the chemistry of the contemporary ocean: an evaluation. DOE technical report, DOE/OR-857, 79 pp.
- Brönsted, L.N. and K.P. Pedersen (1924). The catalytic decomposition of nitramide and its physico-chemical applications. Z. Physik. Chem. (Leipzig) 108, 185-235.
- Butler, J.N. and R. Houston (1970a). Activity coefficient and ion pairs in the system sodium chloride-sodium bicarbonate-water and sodium chloride-sodium carbonate-water. Journal of Physical Chemistry 74, 2976-2983.
- Butler, J.N. and R. Houston (1970b). Potentiometric studies of multicomponent activity coefficient using the lanthamm fluoride membrane electrode. Analytical Chemistry 43, 1308-1311.
- Byrne, R.H., Jr. and D.R. Kester (1974). Inorganic species of boron in seawater. Journal of Marine Research 32, 119-127.
- Calderoni, G., T. Ferri, B. Giannetti and U. Masi (1985). The behavior of thallium during alteration of the K-alkaline rocks from the Roccamonfina volcano. Chemical Geology 48, 103-113.
- Chang, C.P., L.S. Liu and C.T.A. Chen (1983). Principle of least Σ and chemical model of seawater. Acta Oceanologia Sinica 5, 41-56 (in Chinese).

- Chen, C.T. (1982a). On the distribution of anthropogenic CO₂ in the Atlantic and Southern Oceans. Deep-Sea Research 29, 563-580.
- Chen, C.T. (1982b). Oceanic penetration of excess CO₂ in a cross-section between Alaska and Hawaii. Geophysical Research Letter 9, 117-119.
- Chen, C.T. (1982c). Carbonate chemistry during WEPOLLEX-81. Antarctic Journal, 1982 Review, 102-103.
- Chen, C.T. (1984). Marine chemistry in the People's Republic of China. Office of Naval Research (U.S. Government Printing Office, 1984 454 158 19338), 948 pp.
- Chen, C.T. (1984). Carbonate chemistry of the Weddell Sea. DOE technical report, DOE/EV/10611-4, 118 pp.
- Chen, C.T. (1985). Some personal observations on the status of marine sciences in the People's Republic of China. EOS Oceanographic Report, 66, 52.
- Chen, C.T. (1985). Preliminary observation of oxygen and carbon dioxide of the wintertime Bering Sea marginal ice zone. Continental Shelf Research 4, 465-483.
- Chen, C.T. and F.J. Millero (1979). Gradual increase of oceanic carbon dioxide. Nature 277, 205-206.
- Chen, C.T. and R.M. Pytkowicz (1979). On the total CO₂-titration alkalinity-oxygen system in the Pacific Oceans. Nature 281, 362-365.
- Chen, C.T., F.J. Millero and R.M. Pytkowicz (1982). Comments on 'calculating the oceanic CO₂ increase: a need for caution,' by A.M. Shiller. Journal of Geophysical Research 87, 2083-2085.
- Chen, C.T., C.L. Wei and M.R. Rodman (1985). Carbonate chemistry of the Bering Sea. DOE technical report, DOE/EV/10611-5, 77 pp.

- Chen, C.T. and E.T. Drake (1986). Carbon dioxide increase in the atmosphere and oceans and possible effects on climate. Annual Review of Earth and Planetary Sciences 14, 201-235.
- Chen, C.T., A. Poisson and C. Goyet (1986). Preliminary data report for the INDIVAT 1 and INDIGO 1/INDIVAT 3 cruises in the Indian Ocean. DOE technical report, DOE/NBB-0074, 106 pp.
- Chen, Y.T. (1961). Linear free energy relationship from stability of complex compounds and acid and base strength of ligands. Z. Physik. Chem. (Leipzig) 220, 231-239.
- Chlebek, R.W. and M.W. Lister (1966). Ion pair effects in the reaction between potassium ferrocyanide and potassium persulfate. Canadian Journal of Chemistry 44, 437-445.
- Clarke, E.C. and D.N. Glew (1966). Evaluation of thermodynamic functions from equilibrium constants. Transactions of the Faraday Society 62, 539-547.
- Constant, M.G.V. (1984). Speciation of boron with Cu^{2+} , Zn^{2+} , Cd^{2+} and Pb^{2+} in 0.7 in KNO_3 and in seawater. Geochimica et Cosmochimica Acta 48, 2613-2617.
- Dickson, A.G. and M. Whitfield (1981). An ion-association model for estimating acidity constants (at 25°C and 1 atm total pressure) in electrolyte mixtures related to seawater (ionic strength < 1 mol/kgH₂O). Marine Chemistry 10, 315-333.
- Divison, W. (1979). Soluble inorganic ferrous complexes in natural waters. Geochimica et Cosmochimica Acta 43, 1693-1696.
- Drago, R.S., C.V. Glenn and E.N. Terence (1971). A four-parameter equation for predicting enthalpies of adduct formation. Journal of the American Chemical Society 93, 6014-6026.

- Dyrssen, D. and M. Wedborg (1975). Equilibrium calculation of speciation of elements in seawater, in The Sea, Goldberg, E.D., ed., Vol. 5, John Wiley & Sons, Inc., NY, p. 181-195.
- Edmond, J.M. (1974). On the distribution of carbonate and silicate in the deep ocean. Deep-Sea Research 21, 455-480.
- Elgquist, B. (1970). Determination of the stability constants of MgF^+ and CaF^+ using a fluoride ion selective electrode. Journal of Inorganic and Nuclear Chemistry 32, 937-944.
- Elgquist, B. and M. Wedborg (1975). Stability of ion pairs from gypsum solubility. Marine Chemistry 3, 215-225.
- Elgquist, B. and M. Wedborg (1979). Stability of the calcium sulfate ion pair at the ionic strength of seawater by potentiometry. Marine Chemistry 7, 273-280.
- Ferri, D., I. Grenthe, S. Hietaner, E. Neber-Neumann and F. Salvatore (1985). Studies on metal carbonate equilibria 2: Zinc (II) carbonate complexes in acid solutions. Acta Chemica Scandinavica A39, 347-353.
- Fisher, F.H., J.M. Gieskes and C.C. Hsu (1982). $MgSO_4$ ion association in seawater. Marine Chemistry 11, 279-283.
- Fouillac and A. Criand (1984). Carbonate and bicarbonate trace metal complexes: Critical reevaluation of stability constants. Geochemical Journal 18, 297-303.
- Gordon, A.L., C.T. Chen and W.G. Metcalf (1984). Winter mixed layer entrainment of Weddell Sea water. Journal of Geophysical Research 89, 637-640.
- Grasshoff, K., K. Ehrhardt and K. Kremling (1983). Methods of Seawater Analysis, 2nd ed., Verlag Chemie GmbH, D-6940, Weinheim, pp. 419.

- Hammett, L.P. (1937). Solutions of electrolytes, with particular application to qualitative analysis. Journal of the American Chemical Society 59, 96-103.
- Hancock, R.D. and F. Marsicano (1978). Parametric correlation of formation constants in aqueous solution. 1. Ligands with small donor atoms. Inorganic Chemistry 17, 560-564.
- Hansen, J.A., L.D. Rind, G.R. Russell, P. Stone, I. Fung, R. Ruedy and J. Lerner (1984). Climate sensitivity: analysis of feedback mechanisms, in Climate Processes and Climate Sensitivity, J.E. Hansen and T. Takahashi, eds., American Geophysical Union, Washington, D.C., pp. 130-163.
- Hershey, J.P., M. Fernandez, P.J. Milne and F.J. Millero (1986). The ionization of boric acid in NaCl, Na-Ca-Cl and Na-Mg-Cl solutions at 25°C. Geochimica et Cosmochimica Acta 50, 143-148.
- Hirata, S. (1981). Stability constants for the complexes of transition metal ions with fulvic and humic acid in sediments measured by filtration, Talanta 28, 809-815.
- Johansson, O., I. Persson and M. Wedborg (1980). Calorimetric study of the thermodynamics of formation of $MgSO_4$ and $NaSO_4$ ion pairs at the ionic strength of seawater. Marine Chemistry 8, 191-198.
- Johnson, K.S. (1979). Ion association and activity coefficients in electrolyte solutions, Ph.D. thesis, Oregon State University, Corvallis, OR, pp. 320.
- Johnson, K.S. and R.M. Pytkowicz (1979). Ion association of chloride and sulfate with sodium, potassium, magnesium and calcium in seawater at 25°C. Marine Chemistry 8, 87-93.

- Kester, D.R. and R.M. Pytkowicz (1975). Theoretical model for the formation of ion pairs in seawater. Marine Chemistry 3, 365-374.
- Langmuir, D. (1979). Techniques of estimating thermodynamic properties for some aqueous complexes of geochemical interest, in Chemical Modeling in Aqueous Systems, Jenne, E.A., ed., Am. Chem. Soc. Symp. Ser. 93, 353-387.
- Livingston, H.D., J.H. Swift and H.G. Ostlund (1985). Artificial radionuclide tracer supply to the Denmark Strait overflow between 1972 and 1981. Journal of Geophysical Research 90, 6971-6982.
- Mantoura, R.F.C., A. Dickson and J.P. Riley (1978). The complexation of metals with humic materials in natural water. Estuarine and Coastal Marine Science 6, 387-406.
- McGee, K.A. and P.B. Hostetler (1975). Studies in the system $MgO-SO_2-CO_2-H_2O$. 4. The stability of $MgOH^+$ from 10-90°C. American Journal of Science 275, 304-317.
- Millero, F.J. (1974). The physical chemistry of seawater. Annual Review of Earth and Planetary Sciences 2, 101-150.
- Millero, F.J. and D.R. Schreiber (1982). Use of the ionic pairing model to estimate activity coefficients of the ionic components of natural waters. American Journal of Science 282, 1508-1540.
- Morel, F.M.M. (1983). Principles of Aqueous Chemistry, John Wiley & Sons, Inc., NY, pp. 446.
- National Academy of Sciences (1980). Oceanography in China. CSC PRC report 9, 106 pp.
- Ostlund, H.G. (1983). TTO North Atlantic study: tritium and radiocarbon, Data Rel. 83-35, Tritium Lab., Rosenstiel Sch. Mar. Atmos. Sci., Univ. Miami, Fla.

- Palmer, D.A. and R.V. Eldik (1983). The chemistry of metal carbonate and carbon dioxide complexes. Chemistry Review 83, 651-731.
- Pearson, R.G. (1967). Hard and soft acids and bases. Chemistry in Britain 3, 103-107.
- Pearson, R.G. (1968). Hard and soft acids and bases, HSAB. Part 1. Journal of Chemical Education 45, 581-587.
- Poisson, A. and C.T. Chen (1986). Why is there little excess CO₂ in the Antarctic Bottom Water? Deep-Sea Research, submitted.
- Pytkowicz, R.M. (1969). Use of apparent equilibrium constants in chemical oceanography, geochemistry, and biochemistry. Geochemical Journal 3, 181-184.
- Pytkowicz, R.M. (1979). Activity Coefficient in Electrolyte Solution, Vol. 2, CRC Press, Inc., FL, pp. 330.
- Pytkowicz, R.M. (1983). Equilibria, Nonequilibria, and Natural Waters, Vol. 1, John Wiley & Sons, Inc., NY, pp. 351.
- Pytkowicz, R.M. and J.E. Hawley (1974). Bicarbonate and carbonate ion-pairs and a model of seawater at 25°C. Limnology and Oceanography 19, 223-234.
- Pytkowicz, R.M. and D.R. Kester (1969). Harned's rule behavior of NaCl-Na₂SO₄ solutions explained by an ionic association model. American Journal of Science 267, 217-229.
- Reardon, E.J. (1975). Dissociation constants of some monovalent sulfate ion pairs at 25°C from stoichiometric activity coefficients. Journal of Physical Chemistry 79, 422-425.
- Reardon, E.J. (1976). Dissociation constants for alkali earth and sodium borate ion pairs from 10°-50°C. Chemical Geology 18, 309-325.

- Reardon, E.J. and D. Langmuir (1974). Thermodynamic properties of the ion pairs MgCO_3° and CaCO_3° from 10° to 50°C . American Journal of Science 274, 599-612.
- Reid, J.H. and R. Lynn (1971). On the influence of the Norwegian-Greenland and Weddell seas upon the bottom waters of Indian and Pacific Oceans. Deep-Sea Research 18, 1063-1088.
- Reuter, J.H. and E.M. Perdue (1977). Importance of heavy metal-organic water interactions in natural water. Geochimica et Cosmochimica Acta 41, 325-334.
- Riesen, W., H. Gamsjager and P. Schindler (1977). Complex formation in the ternary system $\text{Mg(II)-CO}_2\text{-H}_2\text{O}$. Geochimica et Cosmochimica Acta 41, 1193-1200.
- SIO reference #84-14 (1984). CSS HUDSON cruise 82-001, 14 February-6 April 1982, Vol. 1, Physical and Chemical Data, University of California, 305 pp.
- Saar, R.A. and J.H. Weber (1979). Complexation of cadmium (II) with water and solid derived fulvic acid: effect of pH and fulvic acid concentration. Canadian Journal of Chemistry 57, 1263-1268.
- Schwarzenbach, G. (1961). The general selective and specific formation of complex by metallic cations. Advances in Inorganic and Radiochemistry 3, 265-271.
- Shiller, A.M. (1981). Calculating the oceanic CO_2 increase: a need for caution. Journal of Geophysical Research 86, 11083-11088.
- Shiller, A.M. (1982). Reply to comments of Chen, Millero and Pytkowicz. Journal of Geophysical Research 87, 2086.

- Siebert, R.M. and P.B. Hostetler (1977). The stability of the magnesium bicarbonate ion pair from 10° to 90°C. American Journal of Science 277, 697-715.
- Sipos, L., B. Raspor, H.W. Hurnberg and R.M. Pytkowicz (1980). Interaction of metal complexes with coulombic ion pairs in aqueous media of high salinity. Marine Chemistry 9, 37-47.
- Smith, R.M. and A.E. Martell (1981). Critical Stability Constants, Vol. 4, Plenum Press, NY, pp. 257.
- Spahiu, K. (1985). Studies on metal carbonate equilibria II. Ythrium (IV) carbonate complex formation in aqueous perchlorate media of various ionic strength. Acta Chimica Scandinavia A39, 34-45.
- Stefanssen, U. (1968). Dissolved nutrients, oxygen and water masses in the North Irminger Sea. Deep-Sea Research 15, 541-545.
- Stevenson, F.J. (1976). Stability constants of Cu^{2+} , Pb^{2+} and Cd^{2+} complexes with humic acid. Journal of Soil Science Society of America 40, 665-672.
- Stumm, W. and J.J. Morgan (1981). Aquatic Chemistry, 2nd ed., John Wiley & Sons, Inc., NY, pp. 780.
- Sverjensky, D.A. (1985). The distribution of divalent trace elements between sulfides, oxides, silicates and hydrothermal solutions: I. Thermodynamic basis. Geochimica et Cosmochimica Acta 49, 853-864.
- Swift, J.H. (1984). The circulation of the Denmark Strait and Iceland-Scotland overflow waters on the North Atlantic. Deep-Sea Research 29, 563-580.
- Swift, J.H., K. Aagaard and S.-A. Malmberg (1980). The contribution of the Denmark Strait overflow to the deep North Atlantic. Deep-Sea Research 27, 29-42.

- Swift, J.H. and K. Aagaard (1981). Seasonal transitions and water mass formation in the Iceland and Greenland seas. Deep-Sea Research 28, 1107-1129.
- Takahashi, T. and D. Chipman (1982). Measurements of the partial pressure of CO₂ in discrete water samples during the North Atlantic expedition, the Transient Tracers of Oceans project, NSF technical report, 9 pp. plus data listing.
- Tardy, Y. and R.M. Garrels (1976). Prediction of Gibbs energies of formation, Part I: Relationships among Gibbs energies of formation of hydroxides, oxides and aqueous ions. Geochimica et Cosmochimica Acta 40, 1051-1056.
- Tardy, Y. and P. Vieillard (1977). Relationship among Gibbs free energies and enthalpies of formation of phosphates, oxides and aqueous ions. Contribution to Mineralogy and Petrology 63, 75-88.
- Tardy, Y. and L. Gartner (1977). Relationship among Gibbs free energies of formation of sulphate, nitrates, carbonates, oxides and aqueous ions. Contribution to Mineralogy and Petrology 63, 89-102.
- Tardy, Y. and R.M. Garrels (1977). Prediction of Gibbs energies of formation, Part I. Relationships among Gibbs energies of silicates, oxides, and aqueous ions. Geochimica et Cosmochimica Acta 41, 87-92.
- Turner, D.R., M. Whitfield and A.G. Dickson (1981). The equilibrium speciation of dissolved components in fresh water and seawater at 25°C and 1 atm pressure. Geochimica et Cosmochimica Acta 45, 855-881.

- Van Luik, A.E. and J.J. Jurinake (1978). A chemical model of heavy metals in the Great Salt Lake. Research Report 34, Utah Agriculture Experiment Station, Utah State University, pp. 155.
- Whitfield, M. (1979). Activity coefficients in natural water, in Activity Coefficients in Electrolyte Solutions, Vol. 2, Pytkowicz, R.M., ed., CRC Press, FL, 153-301.
- Worthington, L.V. (1970). The Norwegian Sea as a Mediterranean basin. Deep-Sea Research 17, 77-84.
- Worthington, L.V. (1976). On the North Atlantic circulation. The Johns Hopkins Oceanographic Studies 6, 110 pp.
- Worthington, L.V. (1981). The water masses in the World Ocean: Some results of a fine-scale census, in Evaluation of Physical Oceanography, B.A. Warren and C. Wunsch, eds., MIT Press, Cambridge, MA, pp. 6-41.
- Wust, G. (1935). The stratosphere of the Atlantic Ocean, translated by W.J. Emery, American Publishing Co., New Dehli, 1978, 112 pp.
- Zirino, A. and S. Yamamoto (1972). A pH-dependent model for the chemical speciation of copper, zinc, cadmium and lead in seawater. Limnology and Oceanography 17, 661-671.

APPENDIX

Appendix 1. Cited stability constants of MCl

Cations	LogK(I=0)	LogK* (I=0.7)	Cations	LogK(I=0)	LogK* (I=0.7)
Li ⁺	-0.48(4) ⁺		Fe ³⁺	2.48(4)(5)(37) ⁺	
Na ⁺	-0.24(26)	-0.45(26)	Dy ³⁺	0.8(5)	
K ⁺	-0.7(4)	-0.32(7)	Er ³⁺	0.8(5)	
Rb ⁺	-0.55(4)		Eu ³⁺	0.8(5)	
Cs ⁺	-0.39(4)(5)		Gd ³⁺	0.8(5)	
Be ²⁺	0.32(5)	-0.3(5)	Ho ³⁺	0.8(5)	
Mg ²⁺	0.29(26)	-0.32(25)	In ³⁺	3.26(5)	
Ca ²⁺	0.45(26)	0.08(25) 0.37(26)	La ³⁺	0.8(5)	
Ba ²⁺	-0.13(5)		Lu ³⁺	0.5(5)	
Cd ²⁺	1.97(5) 1.98(4)(37)	1.36(17) 1.6(7)	Ng ³⁺	0.8(5)	
Pb ²⁺	1.58(5) 1.59(4) 1.6(37)	1.01(7) 1.02(17)	Pr ³⁺	0.8(5)	
Mn ²⁺	0.61(37) 0.66(5)(15)		Sc ³⁺	0.92(5)	
Cu ²⁺	0.40(4)(5) 0.43(37)	0.7(17)	Sm ³⁺	0.8(5)	
Zn ²⁺	0.43(4)(37) 0.49(5)	-0.18(17)	Tb ³⁺	0.8(5)	
Ni ²⁺	0.4(37) 0.72(5)		Tm ³⁺	0.8(5)	
Co ²⁺	0.57(5)		Tl ³⁺	7.73(5)	7.72(40)
Fe ²⁺	0.32(27)		Y ³⁺	0.8(5)	
Hg ²⁺	7.43(5)	6.74(17)	Yb ³⁺	0.7(5)	
Ag ⁺	3.27(5)		Tl ⁺	0.49(40)	
Cr ³⁺	0.62(5)		UO ₂ ²⁺	0.21(5)	
			Hf ⁴⁺	1.65(5)	
			Th ⁴⁺	1.39(5)	
			Zr ⁴⁺	1.57(5)	

⁺ Numbers in parenthesis denote the references given at the end of the Appendix

Appendix 2. Cited stability constants of MF

Cations	LogK(I=0)	LogK* (I=0.7)	Cations	LogK(I=0)	LogK* (I=0.7)
Na ⁺	-0.26(12) -0.64(2)	-1.34(13) -1.0(2) -0.8(20)(19)	Ni ²⁺	1.1(3) 1.12(5) 1.26(45) 1.3(37)	0.6(4)*
Be ²⁺	5.61(5)	4.8(4)*	Co ²⁺	1.0(3) 1.02(5) 1.33(45)	0.5(4)*
Mg ²⁺	1.8(4)(3) 1.82(45)	1.28(13) 1.29(2) 1.3(39) 1.4(21)	Fe ²⁺	1.4(3)(45)	
Ca ²⁺	1.1(3)(4) (45) 1.31(2) 0.94(37)	0.65(13) 0.46(7) 0.62(21) 1.04(12)	Hg ²⁺	1.5(45) 1.6(3)	1.01(17)
Sr ²⁺	0.55(12) 1.04(2)(24)	0.1(4)	Ag ⁺	0.4(3)(5) 0.36(37) 0.37(45)	
Ba ²⁺	0.32(5) 1.04(2)	-0.2(4)*	Cr ³⁺	5.15(45) 5.2(5)(4) 5.21(3)	4.2(4)*
Cd ²⁺	1.0(3) 1.08(5) 1.06(45) 1.1(37)	0.46(4)(5)	Fe ³⁺	6.0(3)(5) 6.07(45) 6.2(37)	1.2(4)*
Pb ²⁺	1.25(37) 2.0(3) 2.06(5) 2.08(45)	1.5(7)(4)*	Bi ³⁺	2.28(5) 5.84(45)	
Mn ²⁺	0.85(37) 1.32(5) 1.4(45) 1.9(3)	0.8(4)*	Ce ³⁺	4.0(5)(4)	
Cu ²⁺	1.23(4) 1.26(37) 1.27(45) 1.5(3) 1.52(5)	0.7(17) 0.8(4)*	Gd ³⁺	4.3(4)	
Zn ²⁺	1.15(4)(5) (37) 1.2(3) 1.26(45)	0.7(17) 0.8(4)*	Dy ³⁺	4.36(5)	
			Er ³⁺	4.44(4)	
			Eu ³⁺	4.09(4)	
			Pr ³⁺	3.91(5)	
			Sc ³⁺	7.03(5) 7.1(4)	
			Sm ³⁺	4.02(5)	
			Tb ³⁺	4.32(5)	

Appendix 2. (continued)

Cations	LogK(I=0)	LogK* (I=0.7)
Tm ³⁺	4.46(5)	
Y ³⁺	4.80(5)(4)	
Yb ³⁺	4.48(5)	
Zr ⁴⁺	9.80(5)	
Hf ⁴⁺	10.23(4)	
Th ⁴⁺	8.45	
UO ₂ ²⁺	5.16(5)	
Ho ³⁺	4.42(4)	
In ³⁺	4.6(4)(45)	
La ³⁺	3.6(4)(5)	
Lu ³⁺	4.51(5)	
Nd ³⁺	3.99(5)	

Appendix 3. Cited stability constants of MOH

Cations	LogK(I=0)	LogK* (I=0.7)	Cations	LogK(I=0)	LogK* (I=0.7)
Li ⁺	-0.36(4)		Ni ²⁺	4.1(3)(4)(45)	
Na ⁺	-0.57(24) -0.2(4) -0.18(2)	-0.43(4)	Co ²⁺	3.9(45) 4.3(3)(4)	
K ⁺	-0.5(4)		Fe ²⁺	3.7(45) 4.5(3)	
Be ²⁺	8.6(4)		Ag ⁺	2.0(3) 3.32(45)	
Mg ²⁺	2.2(2)(37) 2.21(14) 2.56(3) 2.58(4)(45) 2.60(30)	1.70(2)	Hg ²⁺	10.6(3) 11.51(45)	10.1(17)
Ca ²⁺	1.15(12) 1.3(2)(4) 1.4(45)	0.25(23) 0.74(2)	Cr ³⁺	10.0(3) 10.05(45)	
Sr ²⁺	0.71(12) 0.8±0.1(4) 0.82(2)	0.25(2)	Fe ³⁺	11.8(45)(6)(3)	
Ba ²⁺	0.6(4)	0.01(2)	Sc ³⁺	9.7(4)	9.4(45)
Cd ²⁺	3.9(4)(6) 4.59(30) 5.2(45)	4.3(17)	Y ³⁺	6.3(4)	
Pb ²⁺	6.3(3)(6) (45) 6.9(7) 7.83(30)	5.63(17)	La ³⁺	5.5(4)	
Mn ²⁺	3.4(3)(4) 3.41(45)		Nd ³⁺	6.0(4)	
Cu ²⁺	6.0(30) 6.3(4) 6.5(5) 6.66(45)	5.73(18) 6.1(17) 6.4(17)	Pu ³⁺	7.0(4)	
Zn ²⁺	4.52(30) 4.6(45) 5.0(3)(6)	4.8(17)	Pa ⁴⁺	14.8(4)	
			Np ⁴⁺	12.5(4)	
			Hf ⁴⁺	13.7(4)	
			In ³⁺	10.0(4)	12.0(45)
			Tl ³⁺	13.4(4)(40)	12.8(45)
			Tl ⁺	0.79(4)(37)	
			UO ₂ ²⁺	8.2(4)	

Appendix 4. Cited stability constants of MHCO_3

Cations	LogK(I=0)	LogK* (I=0.7)	Cations	LogK(I=0)	LogK* (I=0.7)
Na^+	-0.3(10)	-0.55(2)	Co^{2+}	2.20(31)	
	-0.25(12)	-0.51(10)			
	-0.19(2)		Fe^{2+}	1.25(9)	
	-0.08(10)			2.17(31)	
	0.15(4)				
Mg^{2+}	0.69(38)	0.21(4)	Hg^{2+}		5.6(17)
	0.93(30)	0.28(2)	Fe^{3+}	1.5(4)	
	0.95(4)(2)				
	1.07(12)		Y^{3+}	1.29(28)	
	1.08(46)				
1.21(24)					
Ca^{2+}	1.0(2)(9)	0.02(2)			
	1.10(12)	0.29(11)			
	1.26(30)	0.33(2)			
		0.68(22)			
Sr^{2+}	1.0(2)				
	1.24(12)(24)				
	1.25(4)				
Ba^{2+}	1.0(2)				
	1.52(17)				
Cd^{2+}	2.00(31)	0.25(7)			
	2.1(37)	1.2(17)			
Pb^{2+}	1.9(31)	2.2(17)			
	2.9(9)				
Mn^{2+}	1.27(37)				
	1.95(9)(31)				
Cu^{2+}	2.08(9)	1.5(17)			
	2.2(31)				
	2.7(37)				
Zn^{2+}	0.8±2(36)	1.0(17)			
	2.1(4)(37)				
	2.2(31)				
Ni^{2+}	2.14(37)				
	2.22(31)				

Appendix 5. Cited stability constants of MNO_3

Cations	LogK(I=0)	LogK* (I=0.7)
Li^+	-1.1(4)	
Na^+	-0.6(2)(5) -0.5(4) -0.25(30)	-1.09(2)
K^+	-0.16(16) -0.15(4) -0.12(5) 0.078(44) 0.08(2)	-0.43(2)
Ca^{2+}	0.28(2) 0.7(4)(5)	-0.51(2)
Sr^{2+}	0.8(4) 0.82(2)	0.02(2)
Ba^{2+}	0.9(4)	
Cd^{2+}	0.1-0.5(4) 0.4(37)	
Pb^{2+}	1.17(4)(37)	
Mn^{2+}	0.2(4)	
Cu^{2+}	0.5(4)	
Zn^{2+}	0.4(4)	
Ni^{2+}	0.4(4)	
Co^{2+}	0.2(4)	
Ag^+	-0.29(37) 2.0(4)	
Fe^{3+}	1.00(4)	
Eu^{3+}	1.23(4)	
Tb^{3+}	0.88(4)	
Pu^{4+}	1.8(4)	

Appendix 6. Cited stability constants of MB(OH)_4

Cations	LogK(I=0)	LogK* (I=0.7)
Na^+	0.22(2) 0.33(43) -0.24(41)	
Mg^{2+}	1.62(2) 1.63(42) 1.45(47) 0.90(41)	0.72(25)
Ca^{2+}	1.11(2)(41) 1.72(47) 1.8(2)(42)	0.72(25)
Sr^{2+}	1.55(2)(42)	
Ba^{2+}	1.49(42) 1.5(2)	
Cd^{2+}		1.42(48)
Pb^{2+}	5.2 ^a (43)	2.20(48)
Cu^{2+}		3.48(48)
Zn^{2+}		0.9(48)
Ag^+	1.20(43)	

^a 22°C

Appendix 7. Cited stability constants of MCO_3

Cations	LogK(I=0)	LogK*(I=0.7)	Cations	LogK(I=0)	LogK*(I=0.7)
Na^+	0.55(2) 0.77(39) 1.02(2) 1.27(30)	0.63(2) 0.2(2) 0.42(2)	Zn^{2+}	4.1(18) 4.8(31) 5.1(36) 5.3(9)(37)	3.3(17)
K^+	0.7(12)	0.38(25)	Ni^{2+}	4.83(31) 5.37(5) 6.87(9)	
Be^{2+}	5.13(10)		Co^{2+}	4.41(31) 4.91(5)	
Mg^{2+}	2.85(38) 2.88(8) 2.9(2) 3.40(3)	2.51(2)(25) 1.94(2) 2.05(4)	Fe^{2+}	4.73(5)	
Ca^{2+}	3.15(4)(9) (8) 3.2(2)	1.51(2) 2.21(9)	Ag^+	3.40(5)	
Sr^{2+}	3.8(4) 3.92(2)(9)		Fe^{3+}	9.72(5)	
Ba^{2+}	2.78(5)(9) 2.8(3)		Gd^{3+}	7.29(5)	
Cd^{2+}	4.35(5) 5.4(4)(37)	3.2(17) 3.5(7)	Dy^{3+}	7.17(5)	
Pb^{2+}	5.34(5) 5.59(9) 6.3(6) 7.24(37)	5.36(4)(9) 6.2(7)	Eu^{3+}	6.83(5)	
Mn^{2+}	4.10(5) 4.28(5) 4.32(32) 4.9(4)		Ho^{3+}	7.23(5)	
Cu^{2+}	6.73(31) 6.75(4)(5) 6.77(30)(39) 6.78(9)	5.6(17)	In^{3+}	7.60(5)	
			La^{3+}	6.16(5)	
			Pr^{3+}	6.62(5)	
			Sc^{3+}	10.10(5)	
			Nd^{3+}	6.72(5)	
			Ga^{3+}	8.79(5)	
			Y^{3+}	6.02(28)	
			UO_2^{2+}	7.5(5)	

Appendix 8. Cited stability constants of MSO_4

Cations	LogK(I=0)	LogK* (I=0.7)	Cations	LogK(I=0)	LogK* (I=0.7)
Li^+	0.77(2) 0.64(5)	0.26(2)(43)	Mn^{2+}	2.26(37)(4)(5) 2.3(3)	
Na^+	0.65(33) 0.7(37) 0.82(35) 0.94(44) 0.992(7) 1.00(3)	-0.03(22) 0.08(25) 0.09(2) 0.31(1) 0.26(29)	Cu^{2+}	2.31(37) 2.36(4)(5)	0.95(4)
K^+	0.82(2) 0.85(35)(37) 0.88(44) 0.96(2)	0.26(2)	Zn^{2+}	2.1(3) 2.36(5) 2.37(37) 2.38(4)	0.89(4)
Rb^+	0.6(2)	-0.09(2)	Ni^{2+}	2.29(4) 2.30(3) 2.32(4)	0.57(4)
Cs^+	0.33(2)	-0.41(2)	Co^{2+}	2.36(4)(5) 2.40(3)	
Be^{2+}	1.95(4) 2.04(5)		Fe^{2+}	2.2(3) 2.25(37)	
Mg^{2+}	2.16(5) 2.21(2) 2.23(33) 2.25(12) 2.33(34)	0.66(5) 1.01(2) 1.08(33) 1.09(25) 1.62(44)	Hg^{2+}	2.5(3) 2.66(5)	
Ca^{2+}	2.28(2) 2.31(3)(4) (12)	0.99(22) 1.03(4) 1.40(29) 1.49(25)	Ag^+	1.3(3)	
Sr^{2+}	2.31(2) 2.55(4) 2.60(3)	0.85(2) 2.10(2)	Cr^{3+}	3.0(3) 4.61(5)	
Ba^{2+}	2.3(2) 2.7(3)(4)	0.66(4)(5) 0.98(2)	Fe^{3+}	3.92(37) 4.4(6)	
Cd^{2+}	2.30(3) 2.46(4)(37)	1.88(7)	Gd^{3+}	3.66(5)	
Pb^{2+}	2.75(4)(5) 2.80(3)	0.95(4)	Dy^{3+}	3.62(5)	
			Er^{3+}	3.59(5)	
			Ho^{3+}	3.59(5)	
			In^{3+}	3.86(5)	
			Nd^{3+}	3.99(5)	
			Pr^{3+}	3.62(5)	

Appendix 8. (continued)

Cations	LogK(I=0)	LogK* (I=0.7)
Sc ³⁺	4.40(5)	
Sm ³⁺	3.67(5)	
Tb ³⁺	3.64(5)	
Tm ³⁺	3.59(5)	
Y ³⁺	3.47(5)	
Yb ³⁺	3.58(5)	
Tl ³⁺	4.38(5)	
Tl ⁺	1.37(40)	
Zr ⁴⁺	7.79(5)	
Hf	7.16(5)	
UO ₂ ²⁺	2.95(5)	

Appendix 9. Cited stability constants of MHSO_4

Cations	LogK(I=0)
---------	-----------

Na^+	-0.7(12)
---------------	----------

Mg^{2+}	0.4(12)
------------------	---------

Ca^{2+}	0.3(12)
------------------	---------

Sr^{2+}	0.5(12)
------------------	---------

Appendix 10. Cited stability constants of MH_2PO_4

Cations	LogK(I=0)
Na^+	-0.043(2)
Mg^{2+}	1.12(2)
Ca^{2+}	1.0(2) 0.06-1.4(4)
Pb^{2+}	1.5(4)
Fe^{2+}	2.7(4)
Fe^{3+}	4.17(32)
Al^{3+}	3.1(32)
Y^{3+}	2.65(4)
Ce^{3+}	2.33(4)
Pb^{3+}	2.51(4)
Am^{3+}	2.51(4)

Appendix 11. Cited stability constants of MH_3SiO_4

Cations	LogK(I=0)
Mg^{2+}	1.26(5)
Ca^{2+}	1.01(5)

Appendix 12. Cited stability constants of MH_2SiO_4

Cations	LogK(I=0)
Mg^{2+}	5.67(5)
Ca^{2+}	4.59(5)

Appendix 13. Cited stability constants of MHPO_4

Cations	LogK(I=0)
Na^+	0.29(37) 0.8(2)
K^+	0.29(37) 1.05(5)
Mg^{2+}	2.85(2) 2.91(4)
Ca^{2+}	2.66(2) 2.74-0.06(4)
Pb^{2+}	3.1(4)
Zn^{2+}	3.2(32)
Ni^{2+}	2.9(32)
Co^{2+}	3.0(32)
Fe^{2+}	3.6(4)
Fe^{3+}	9.92(32) 5.43(37)

Appendix 14. Cited stability constants of MPO_4

Cations	LogK(I=0)
Na^+	1.6(2)
Mg^{2+}	5.78(2)
Ca^{2+}	6.46(4)
	6.47(2)

Appendix 15. Cited stability constants of MHA

Cations	LogK(I=0)
Zn ²⁺	5.73(5)
Cd ²⁺	5.23(5)
Mn ²⁺	5.0(5)
Co ²⁺	5.2(5)
Ni ²⁺	5.78(5)
Cu ²⁺	9.84(5)
Pb ²⁺	8.7(5)

(1) Pytkowicz (1969), (2) Millero and Schreiber (1982), (3) Morel (1983), (4) Smith and Martell (1981), (5) Turner et al. (1981), (6) Pytkowicz (1979), (7) Sipos et al. (1980), (8) Reardon and Langmuir (1974), (9) Palmer and Eldik (1983), (10) Butler and Houston (1970a), (11) Pytkowicz and Hawley (1974), (12) Dickson and Whitfield (1982), (13) Kester and Pytkowicz (1975), (14) McGee and Hostetter (1975), (15) Baes and Mesmer (1976), (16) Chlebek and Lister (1966), (17) Whitfield (1979), (18) Zirino and Yamamoto (1972), (19) Millero (1974), (20) Butler and Houston (1970b), (21) Elgquist (1970), (22) Berner (1971), (23) Dyrssen and Wedborg (1975), (24) Atkinson et al. (1975), (25) Elgquist and Wedborg (1975), (26) Johnson (1979), (27) Divison (1979), (28) Spahiu (1985), (29) Elgquist and Wedborg (1979), (30) Van Liuk and Jurinake (1978), (31) Fouillac and Griand (1984), (32) Langmuir (1979), (33) Johansson (1980), (34) Fisher et al. (1982), (35) Reardon (1975), (36) Ferri et al. (1985), (37) Ball et al. (1981), (38) Riesen et al. (1977), (39) Stumm and Morgan (1981), (40) Calderoni (1985), (41) Byrne and Kester (1974), (42) Reardon (1976), (43) Bassett (1980), (44) Johnson and Pytkowicz (1979), (45) Hancock and Marsicano (1978), (46) Siebert and Hostetter (1977), (47) Hershey et al. (1986), (48) Constant (1984), (4)* Obtained graphically from Smith and Martell (1981).